Quantitative spectral and orientational analysis in surface sum frequency generation vibrational spectroscopy (SFG-VS)

Article *in* International Reviews in Physical Chemistry · April 2005

DOI: 10.1080/01442350500225894

CITATIONS
341

READS
294

5 authors, including:

Hong-fei Wang
Pacific Northwest National Laboratory
69 PUBLICATIONS **2,154** CITATIONS
SEE PROFILE

Wei Gan
Harbin Institute of Technology Shenzhen Gra…
45 PUBLICATIONS **1,570** CITATIONS
SEE PROFILE

Yi Rao
Temple University
38 PUBLICATIONS **1,111** CITATIONS
SEE PROFILE

International Reviews in Physical Chemistry,
Vol. 24, No. 2, April–June 2005, 191–256

Taylor & Francis
Taylor & Francis Group

Quantitative spectral and orientational analysis in surface sum frequency generation vibrational spectroscopy (SFG-VS)

HONG-FEI WANG*, WEI GAN†‡, RONG LU†‡§,
YI RAO†‡¶ and BAO-HUA WU†

State Key Laboratory of Molecular Reaction Dynamics, Institute of Chemistry,
The Chinese Academy of Sciences, ZhongGuanCun, Beijing, PR China 100080

(*Received 6 March 2005; in final form 20 May 2005*)

Sum frequency generation vibrational spectroscopy (SFG-VS) has been proven to be a uniquely effective spectroscopic technique in the investigation of molecular structure and conformations, as well as the dynamics of molecular interfaces. However, the ability to apply SFG-VS to complex molecular interfaces has been limited by the ability to abstract quantitative information from SFG-VS experiments. In this review, we try to make assessments of the limitations, issues and techniques as well as methodologies in quantitative orientational and spectral analysis with SFG-VS. Based on these assessments, we also try to summarize recent developments in methodologies on quantitative orientational and spectral analysis in SFG-VS, and their applications to detailed analysis of SFG-VS data of various vapour/neat liquid interfaces. A rigorous formulation of the polarization null angle (PNA) method is given for accurate determination of the orientational parameter $D = \langle\cos\theta\rangle/\langle\cos^3\theta\rangle$, and comparison between the PNA method with the commonly used polarization intensity ratio (PIR) method is discussed. The polarization and incident angle dependencies of the SFG-VS intensity are also reviewed, in the light of how experimental arrangements can be optimized to effectively abstract crucial information from the SFG-VS experiments. The values and models of the local field factors in the molecular layers are discussed. In order to examine the validity and limitations of the bond polarizability derivative model, the general expressions for molecular hyperpolarizability tensors and their expression with the bond polarizability derivative model for C_{3v}, C_{2v} and $C_{\infty v}$ molecular groups are given in the two appendixes. We show that the bond polarizability derivative model can quantitatively describe many aspects of the intensities observed in the SFG-VS spectrum of the vapour/neat liquid interfaces in different polarizations. Using the polarization analysis in SFG-VS, polarization selection rules or guidelines are developed for assignment of the SFG-VS spectrum. Using the selection rules, SFG-VS spectra of vapour/diol, and vapour/*n*-normal alcohol ($n \sim 1$–8) interfaces are assigned, and some of the ambiguity and confusion, as well as their implications in previous IR and Raman assignment, are duly discussed. The ability to assign a SFG-VS spectrum using the polarization selection rules makes SFG-VS not only an effective and useful vibrational spectroscopy technique for interface studies, but also a complementary vibrational spectroscopy method in general

*Corresponding author. Email: hongfei@iccas.ac.cn
†Graduate Students of Graduate School of the Chinese Academy of Sciences.
‡In alphabetical order. These three authors contributed equally.
§Current address: Reaction and Excitation Dynamics Group, Materials Engineering Laboratory, National Institute for Material Science, Sengen, Tsukuba, Japan.
¶Current address: Department of Chemistry, Columbia University, New York, NY 10025, U.S.A.

International Reviews in Physical Chemistry
ISSN 0144–235X print/ISSN 1366–591X online
http://www.tandf.co.uk/journals
DOI: 10.1080/01442350500225894

condensed phase studies. These developments will put quantitative orientational and spectral analysis in SFG-VS on a more solid foundation. The formulations, concepts and issues discussed in this review are expected to find broad applications for investigations on molecular interfaces in the future.

Contents

1. Scope of this review

This review is intended to report on recent developments in sum frequency generation vibrational spectroscopy (SFG-VS) as a quantitative vibrational spectroscopic method for understanding the detailed spectroscopy, structure and energetics of the vapour/liquid interface. These developments can be used for the investigation of interfaces beyond vapour/liquid interfaces, and knowledge of the vapour/liquid interfaces at the detailed molecular level can be used for an understanding of other kinds of molecular interfaces as well.

There was an excellent review in this journal on aqueous interfaces studied with SFG-VS by Schultz *et al.* in the year of 2000 [1]. In the past 20 years, it has been an ever-growing field to employ second-order non-linear optical methods, namely, second harmonic generation (SHG) and sum frequency generation vibrational spectroscopy (SFG-VS), for studies on various surfaces and interfaces in order to gain an understanding of their basic physical chemistry, and to find important applications and implications in material sciences, as well as in the biological sciences. There have been many comprehensive reviews on detailed SHG and SFG-VS interface studies [1–20], and many are on the investigation of various liquid interfaces, especially aqueous solution interfaces [1–9]. These developments suggest that SFG-VS is a uniquely effective experimental technique among many modern techniques for understanding molecular interfaces [20, 21].

This review is not going to repeat the successful stories of the SFG-VS techniques in this growing field of current research. We would rather like to add to the arsenal of interface SFG-VS with more quantitative aspects of vibrational spectral analysis and molecular orientational analysis, which may enable more detailed understanding of the interactions, structure and energetics of the molecular interfaces. These developments rely on careful analysis of the coherent nature and polarization dependence of the effective macroscopic second-order susceptibility $\chi^{(2)}_{\text{eff}}$, which contains all microscopic information about the spectroscopic responses and orientation of the molecular groups at the interface. With quantitative analysis of the key parameters, such as polarization configuration, the local field factor in the interface layers, and the molecular symmetry and susceptibility tensorial relationships, SFG-VS has already provided rich information about the molecular interface [22]. Based on such pioneering successes, we can still sharpen our tools and go further for broader applications to more complex molecular interfaces.

In this review, two novel aspects of SFG-VS are particularly discussed.

The first aspect is the use of the polarization null angle (PNA) method for more accurate determination of the molecular orientational parameter $D = \langle \cos\theta \rangle / \langle \cos^3\theta \rangle$. With accurate D values, not only can the orientational angle of the molecular groups at the interface be deduced, but small changes of molecular orientational angle or orientational distribution can be discerned [23–25]. Therefore, accurate determination of the D value can be particularly important in terms of investigating changes of the complex interfaces with subtle influences of the various environmental parameters, such as concentration, pH, temperature, pressure, etc. We shall show that in order to be able to accurately obtain D values, issues on the polarization configuration, incident angle geometry, local field factors in the interface layer,

molecular symmetry and hyperpolarizability tensor ratios, have to be systematically examined.

The second aspect is the use of vibrational spectral polarization selection rules based on the molecular symmetry analysis for accurate vibrational spectral assignment [26]. Since the interface is always with some orientational order, SFG-VS is intrinsically a coherent and polarization spectroscopy, and surface SFG-VS spectra usually exhibit narrower spectral peaks; therefore, SFG-VS is an ideal tool for determining molecular symmetry and discerning complex vibrational modes. Traditionally, SFG-VS studies relied on the spectral assignments of vibrational bands from IR and Raman studies. This has in some ways prevented SFG-VS from studying complex interfaces, where the molecular vibrational spectrum can be complicated due to the complex chemical environments and interactions. The polarization selection rules can thus be used to assign vibrational modes not clearly observed in the IR or Raman spectra, and to clarify confusions in SFG-VS spectral assignments, as well as in previous IR and Raman assignments.

With the development of commercial SFG-VS spectrometers in the past few years [27], as well as the development of the broadband SFG-VS technique for fast acquisition of the SFG-VS spectrum [28, 29], SFG-VS measurement of interface vibrational spectroscopy has become much easier and more reliable for ordinary chemists and material scientists in more and more research and development laboratories. The methodology of choosing a proper SFG-VS experimental configuration for a specific problem, and the methodology to perform quantitative analysis on SFG-VS spectral data are two key limiting factors for broader applications of SFG-VS as a surface and interface diagnostic technique. We hope that what is discussed here can help break these limitations to some extent.

2. Background

2.1. *Understanding molecular interfaces*

Interfaces are ubiquitous in nature. Chemical properties and processes at molecular interfaces, especially material interfaces and biological interfaces, are among the central themes in modern chemical research [30]. Historically, the application of interfacial science, including colloid science, has often been more of an art than a science. Greater knowledge about various interfacial phenomena at the atomic and molecular level as guiding principles for further application is in great demand. This is where physical chemistry studies come into play.

The physical chemist's interests in interface studies are the understanding and prediction of interfacial thermodynamic properties, e.g. population or density, surface free energy, equilibrium constants, polarity, phase distribution and phase transitions; kinetic properties, e.g. diffusivity and viscosity; structural properties, e.g. chemical composition, molecular orientation, hydrogen bonding and other interaction forces; and molecular dynamic properties, e.g. chemical reaction dynamics, rotational, vibrational and other relaxation dynamics. All these properties and processes at interfaces

are usually very different from those in the bulk phase, due to the unique nature of the interfaces [30].

The interface is the boundary separating and connecting any two bulk phases. All the chemical and physical processes involving exchange of energy and mass or interactions between two bulk media must involve molecules crossing the interface. This makes interface science not only fundamentally but also technologically important. The interface is a region with a thickness of only one or several molecular layers. The distinct properties of the interface in comparison to those of the bulk originate not only from the difference of chemical compositions but also from the asymmetry of the forces that molecules and atoms experience at the interface. The asymmetry of the forces and discontinuity of electric fields across the interface region orient molecules, affect their structure and change their dynamic properties by perturbing the potential surfaces governing these motions. The discontinuity and asymmetry determine the interfacial dielectric properties, e.g. polarity, and transport properties, e.g. viscosity. Interface equilibrium and dynamic behaviour, which depend on these interfacial properties, markedly differ from those in bulk media.

Despite the very scientific and practical importance of interface studies, our understanding of the chemistry and physics at an interface is still primitive, especially for liquid and aqueous interfaces. This arises from the fact that the interface region is such a small entity. Not only is it difficult to characterize well by conventional experimental methods, but it is also very easily contaminated with a small level of impurities from the bulk medium. Therefore, until the 1950s, studies of surfaces and interfaces were mostly on the macroscopic level. This unavoidably hindered the development of surface studies. With the development of modern techniques of purification and analysis, a great number of advances in surface and colloid science and technology have been achieved [21]. However, even now the sensitivity and complexity of surfaces and colloids causes difficulties in developing a comprehensive understanding of many phenomena of academic and practical importance [31]. New techniques need to be developed to tackle those problems.

With the advance of modern high-vacuum technology, laser technology, sensitive and fast electronics in the past 50 years or so, a large number of techniques and instrumentation have been developed to study various interface properties at the atomic and molecular level [21]. Most of these techniques are based on the scattering, absorption, or emission of photons, X-rays, neutrons, electrons, atoms and ions. Many of these techniques can only be applied to flat surfaces in a high-vacuum environment, which have brought great advances to our understanding, on the atomic level, of metal, semiconductor and oxide model surfaces with great applications in the semiconductor industry. However, microscopic study of surfaces under high pressure and temperature, and molecular interfaces which are common in material and biological systems, have been mostly left behind.

Gas/liquid interfaces, along with buried interfaces, i.e. liquid/liquid, liquid/solid and solid/solid interfaces, are mostly inaccessible by the techniques mentioned above. However, most interesting and important natural chemical and physical processes on Earth occur at these interfaces under ambient conditions. These include equilibria and reactions in environmental and life systems with both fundamental

and practical importance. Because these interfaces are buried and cannot be studied with invasive techniques, optical techniques are desirable for experimental studies of these systems. Because the molecular interface is usually one or a few molecules thick, the ideal optical technique has to be interface specific or selective, and must have submonolayer sensitivity to probe changes of composition, orientation and structure of the interface layer. In order to distinguish different chemical species at the molecular interface, such an optical technique also has to have chemical selectivity, or spectroscopic selectivity.

Fortunately, such an optical technique does exist. Since the early 1980s, Ron Shen and his colleagues have firmly established that second-order non-linear optical methods, namely second harmonic generation (SHG) and sum frequency generation vibrational spectroscopy (SFG-VS), are ideal interface probing optical techniques with interface selectivity, submonolayer sensitivity, spectroscopic selectivity, and are also non-invasive [32]. SHG and SFG are called second-order non-linear optical processes because in such processes two photons of certain frequencies interact simultaneously with an atom or molecule to instantaneously produce a new photon with the sum of the two frequencies. If the two frequencies are the same, the process is called SHG; otherwise, SFG. The interfacial selectivity of SHG and SFG comes from the fact that coherent second-order optical processes are symmetrically forbidden in media having a centre of inversion. This centrosymmetry is naturally broken at the interface layer, but it is conserved for the isotropic bulk, and consequently SHG and SFG become intrinsically interface specific [33].

In SFG-VS, tunable IR laser light and visible light at fixed frequency are used to obtain the vibrational spectrum at the sum frequency of the molecular groups at a molecular interface. As we know, with the vibrational spectrum of the interfacial molecular species, interfacial chemistry can be studied in unprecedented molecular detail. Since the first SFG-VS experiment by Shen *et al.* in 1987 [34, 35], SFG-VS has been proven to be a uniquely powerful technique in studying surface chemistry. Along with the development of laser technology in the past decade, broad applications of SFG-VS have been found to more complex molecular interface systems in various technologically important fields, such as catalysis, chemical vapour deposition, electrochemistry, and liquid interfaces, as well as interfaces related to environmental problems and life sciences [7, 15].

Application of SFG-VS lies in its capability of obtaining quantitative information. The major obstacles for SFG-VS at the moment are that its ability for effective spectral assignment has been limited by IR and Raman studies, and that the quantitative analysis of molecular orientation is limited by the complications in quantitative assessment of the experimental and molecular parameters. Great effort has been dedicated to addressing these issues in the past [13, 22, 36–41], but the general consensus in the field so far is that these are still 'qualitative or semi-quantitative accomplishments' [13, 15, 39, 42]. This review of progress mainly in our research group aims to shed some new lights on these issues regarding the ability for quantitative analysis with SFG-VS [23–26, 43], and we hope that these efforts can help advance the capability of SFG-VS for effective spectral assignment and analysis, as well as accurate orientational and polarization analysis towards better understanding of interface phenomena.

2.2. *Interface sum frequency generation vibrational spectroscopy (SFG-VS)*

Here we shall follow the descriptions in the literature [22, 23, 26] and briefly present the mathematical formulation of SFG-VS in the reflection geometry from a rotationally isotropic achiral interface ($C_{\infty v}$). Then we will discuss the issues in quantitative analysis in SFG-VS applications [13, 15, 22, 39].

2.2.1. General formulation of SFG-VS. The SFG intensity is proportional to the two incident laser intensities and the square of the absolute value of the effective sum frequency susceptibility $\chi^{(2)}_{\text{eff}}$, which contains all the measurable information on the response of the molecular system to the incident optical fields at the sum frequency ω [22]:

$$I(\omega) = \frac{8\pi^3\omega^2\sec^2\beta}{c_0^3 n_1(\omega)n_1(\omega_1)n_1(\omega_2)}\left|\chi^{(2)}_{\text{eff}}\right|^2 I(\omega_1)I(\omega_2) \tag{1}$$

with

$$\chi^{(2)}_{\text{eff}} = [\hat{e}(\omega)\cdot\mathbf{L}(\omega)]\cdot\chi^{(2)}_{ijk} : [\mathbf{L}(\omega_1)\cdot\hat{e}(\omega_1)][\mathbf{L}(\omega_2)\cdot\hat{e}(\omega_2)]. \tag{2}$$

Here ω, ω_1 and ω_2 are the frequencies of the SF signal, visible and IR laser beams, respectively. $n_m(\omega_i)$ is the refractive index of the bulk medium m ($m = 1, 2, '$) at frequency ω_i ($i = 0, 1, 2$); β_i is the incident or reflection angle from the interface normal to the beam with frequency ω_i; $I(\omega_i)$ is the intensity of the SFG signal or the input laser beams, respectively; $\hat{e}(\omega_i)$ is the unit electric field vector for the light beam at frequency ω_i at the interface. We defined the xy plane in the laboratory coordinates system $\lambda(x, y, z)$ as the plane of the interface with z axis as the surface normal; all the light beams propagate in the xz plane; p denotes the polarization of the optical field in the xz plane, while s is the polarization perpendicular to the xz plane [22, 26]. Among the total of 27 macroscopic susceptibility tensors $\chi^{(2)}_{ijk}$ ($(i,j,k) = (x, y, z)$), there are seven non-zero terms for an achiral rotationally isotropic interface ($C_{\infty v}$ symmetry), namely, $\chi^{(2)}_{xxz} = \chi^{(2)}_{yyz}$, $\chi^{(2)}_{xzx} = \chi^{(2)}_{yzy}$, $\chi^{(2)}_{zxx} = \chi^{(2)}_{zyy}$, $\chi^{(2)}_{zzz}$ [22, 26]. Therefore, for the co-propagation geometry with which the visible and IR beams are incident within the same quarter in the xz plane, we have

$$\begin{aligned}
\chi^{(2)}_{\text{eff}} = {} & \sin\Omega\sin\Omega_1\cos\Omega_2 L_{yy}(\omega)L_{yy}(\omega_1)L_{zz}(\omega_2)\sin\beta_2\chi_{yyz} \\
& + \sin\Omega\cos\Omega_1\sin\Omega_2 L_{yy}(\omega)L_{zz}(\omega_1)L_{yy}(\omega_2)\sin\beta_1\chi_{yzy} \\
& + \cos\Omega\sin\Omega_1\sin\Omega_2 L_{zz}(\omega)L_{yy}(\omega_1)L_{yy}(\omega_2)\sin\beta\chi_{zyy} \\
& - \cos\Omega\cos\Omega_1\cos\Omega_2 L_{xx}(\omega)L_{xx}(\omega_1)L_{zz}(\omega_2)\cos\beta\cos\beta_1\sin\beta_2\chi_{xxz} \\
& - \cos\Omega\cos\Omega_1\cos\Omega_2 L_{xx}(\omega)L_{zz}(\omega_1)L_{xx}(\omega_2)\cos\beta\sin\beta_1\cos\beta_2\chi_{xzx} \\
& + \cos\Omega\cos\Omega_1\cos\Omega_2 L_{zz}(\omega)L_{xx}(\omega_1)L_{xx}(\omega_2)\sin\beta\cos\beta_1\cos\beta_2\chi_{zxx} \\
& + \cos\Omega\cos\Omega_1\cos\Omega_2 L_{zz}(\omega)L_{zz}(\omega_1)L_{zz}(\omega_2)\sin\beta\sin\beta_1\sin\beta_2\chi_{zzz}
\end{aligned} \tag{3}$$

and

$$\omega \sin \beta = \omega_1 \sin \beta_1 + \omega_2 \sin \beta_2. \tag{4}$$

The parameters Ω, Ω_1 and Ω_2 are the polarization angles of the SFG signal, visible and IR laser beam, respectively. Equation (4), which is from the conservation of momentum in the x direction, determines the outgoing angle β of the SFG signal [44]. Equation (4) represents the case for IR and visible beams co-propagating and the SFG signal in the reflection direction. Because $\omega_1 \gg \omega_2$ and $\omega = \omega_1 + \omega_2$, $\beta \simeq \beta_1$. If it is the case for counter-propagation in the reflection geometry, the '+' sign and the '−' sign of the fifth and sixth terms in equation (3) are interchanged; and the '+' sign becomes a '−' sign in equation (4). Therefore, β will be significantly different from β_1. Sign interchange also occurs between the second and third terms in equation (9) for a counter-propagating geometry. This difference in β can have a significant influence on the polarization analysis in SFG-VS. We shall come back to this point in section 3.2. Since the interface layer is molecularly thin and much less than the wavelength, the three-layer model for the interface SFG-VS is valid, and $L_{ii}(\omega_i)$ is the tensorial Fresnel factor at frequency ω_i as shown below [22, 40, 45]:

$$\begin{aligned} L_{xx}(\omega_i) &= \frac{2n_1(\omega_i)\cos\gamma_i}{n_1(\omega_i)\cos\gamma_i + n_2(\omega_i)\cos\beta_i} \\ L_{yy}(\omega_i) &= \frac{2n_1(\omega_i)\cos\beta_i}{n_1(\omega_i)\cos\beta_i + n_2(\omega_i)\cos\gamma_i} \\ L_{zz}(\omega_i) &= \frac{2n_2(\omega_i)\cos\beta_i}{n_1(\omega_i)\cos\gamma_i + n_2(\omega_i)\cos\beta_i}\left(\frac{n_1(\omega_i)}{n'(\omega_i)}\right)^2 \end{aligned} \tag{5}$$

in which γ_i is the refractive angle into medium 2 defined by $n_1(\omega_i)\sin\beta_i = n_2(\omega_i)\sin\gamma_i$. $n'(\omega_i)$ is the effective refractive index parameter of the interface layer. The definition and physical meaning of $n'(\omega_i)$ was elucidated by Shen *et al.* a few years ago [22, 40]. One can see that the term $n'(\omega_i)$ goes only into the expression of $L_{zz}(\omega_i)$, and $n'(\omega_i)$ is the only unknown parameter in the calculation of the Fresnel factor $L_{ii}(\omega_i)$. $n'(\omega_i)$ value may be different from the refractive indices of the bulk medium at the corresponding frequencies, respectively. The value of $n'(\omega_i)$ and its effect on quantitative analysis in SFG will be discussed in detail in section 3.3.

$\chi^{(2)}_{\text{eff}}$ depends on the experimental polarization and geometry, and there are an infinite number of combinations of experimental configurations which can give different $\chi^{(2)}_{\text{eff}}$. $\chi^{(2)}_{\text{eff}}$ is also a linear combination of the four most commonly used independent experimental polarization combinations in the SFG literature, namely, *ssp*, *sps*, *pss* and *ppp*, as shown in the following:

$$\chi^{(2)}_{\text{eff},ssp} = L_{yy}(\omega)L_{yy}(\omega_1)L_{zz}(\omega_2)\sin\beta_2\chi_{yyz} \tag{6}$$

$$\chi^{(2)}_{\text{eff},sps} = L_{yy}(\omega)L_{zz}(\omega_1)L_{yy}(\omega_2)\sin\beta_1\chi_{yzy} \tag{7}$$

$$\chi^{(2)}_{\mathrm{eff},pss} = L_{zz}(\omega)L_{yy}(\omega_1)L_{yy}(\omega_2)\sin\beta\chi_{zyy} \tag{8}$$

$$\begin{aligned}\chi^{(2)}_{\mathrm{eff},ppp} = &-L_{xx}(\omega)L_{xx}(\omega_1)L_{zz}(\omega_2)\cos\beta\cos\beta_1\sin\beta_2\chi_{xxz}\\ &- L_{xx}(\omega)L_{zz}(\omega_1)L_{xx}(\omega_2)\cos\beta\sin\beta_1\cos\beta_2\chi_{xzx}\\ &+ L_{zz}(\omega)L_{xx}(\omega_1)L_{xx}(\omega_2)\sin\beta\cos\beta_1\cos\beta_2\chi_{zxx}\\ &+ L_{zz}(\omega)L_{zz}(\omega_1)L_{zz}(\omega_2)\sin\beta\sin\beta_1\sin\beta_2\chi_{zzz}.\end{aligned} \tag{9}$$

Furthermore, the macroscopic sum frequency susceptibility tensors $\chi^{(2)}_{ijk}$ are related to the microscopic hyperpolarizability tensor elements $\beta^{(2)}_{i'j'k'}$ in the molecular coordinates system $\lambda'(a,b,c)$ through the ensemble average, denoted by $\langle\ \rangle$, over all possible molecular orientations [22]:

$$\chi^{(2)}_{ijk} = N_s \sum_{i'j'k'} \langle R_{ii'} R_{jj'} R_{kk'} \rangle \beta^{(2)}_{i'j'k'}. \tag{10}$$

Here N_s is the number density of the interface moiety under investigation; $R_{\lambda\lambda'}$ is an element of the rotational transformation matrix from the molecular coordination $\lambda'(a,b,c)$ to the laboratory coordination $\lambda(x,y,z)$ [46, 47], as shown in equation (25) in Appendix A. All the mathematical expressions connecting the 27 $\chi^{(2)}_{ijk}$ and 27 $\beta^{(2)}_{i'j'k'}$ have been meticulously worked out by Hirose *et al*. through transformation of all the three angles (θ,ϕ,ψ) [46]. In any application, one needs to make appropriate symmetry considerations and angular averages to obtain the expressions of the non-vanishing $\chi^{(2)}_{ijk}$ elements as a linear combination of the non-vanishing $\beta^{(2)}_{i'j'k'}$ elements. It has to be noted that in equation (10) the microscopic local field factors are not incorporated. Zhuang, Wei and Shen *et al*. discussed this issue in great detail [22, 40]. It was shown that by properly altering the expression of the Fresnel factor $L_{ii}(\omega_i)$, the expressions for $\chi^{(2)}_{ijk}$ in these two cases differ only by a common factor [22, 40].

In SFG-VS, the IR frequency is near resonance to molecular vibrational transitions, and the second-order molecular polarizability is

$$\beta^{(2)} = \beta^{(2)}_{\mathrm{NR}} + \sum_q \frac{\beta^q}{\omega_{\mathrm{IR}} - \omega_q + i\Gamma_q} \tag{11}$$

where the first term $\beta^{(2)}_{\mathrm{NR}}$ represents non-resonant contributions; β^q, ω_q and Γ_q are the sum frequency strength factor tensor, resonant frequency and damping constant of the qth molecular vibrational mode, respectively. In general, $\beta^{(2)}_{\mathrm{NR}}$ should be small and real when the substrate is not in resonance with either of the three ω_i frequencies. This is generally true for the dielectric interfaces not in electronic resonance. However, for metal or semiconductor substrate interfaces, $\beta^{(2)}_{\mathrm{NR}}$ is generally complex and not small at all. In actual spectral fittings, the simple assumption of a Lorentzian line profile in equation (11) has been successful for most purposes, especially for dielectric interfaces [15]. However, for metal or semiconductor interfaces, incorporation of inhomogeneous effects on the line shape can be considered [39, 48–50].

In the theory of SFG-VS with a single resonance with IR frequencies, the tensor elements of β^q are related to the IR and Raman properties of the vibrational mode [40, 51],

$$\beta^q_{i'j'k'} = -\frac{1}{2\epsilon_0\omega_q}\frac{\partial\alpha^{(1)}_{i'j'}}{\partial Q_q}\frac{\partial\mu_{k'}}{\partial Q_q} \tag{12}$$

in which $\partial\alpha^{(1)}_{i'j'}/\partial Q_q = \alpha'_{i'j'}$ and $\partial\mu_{k'}/\partial Q_q = \mu'_{k'}$ are the partial derivatives of the Raman polarizability tensor and the IR transition dipole moment of the qth vibrational mode; and Q_q is the normal coordinate of the same mode [40]. It is important to know that the squares of $\alpha'_{i'j'}$ and $\mu'_{k'}$ are directly proportional to the intensities of the Raman and IR transition of the qth vibrational mode. Therefore, any non-zero sum frequency vibrational mode has to be both IR and Raman active. This is the transition selection rule for SFG-VS.

Molecular symmetry determines the non-zero elements of the molecular polarizability tensor $\beta^q_{i'j'k'}$ for the qth vibrational mode. The non-zero elements of $\beta_{i'j'k'}$ for different modes with common symmetries, i.e. C_{3v}, C_{2v} and $C_{\infty v}$, as well as the expression for the corresponding macroscopic susceptibility tensors in equation (10) are given in Appendix A. For stretching vibrational modes of the aromatics, the expressions can be found in the literature [39, 52].

From equations (1)–(12), the experimentally measured SFG-VS intensity can be directly related to the microscopic molecular polarizability tensor $\beta^q_{i'j'k'}$ through the orientational average. If all the parameters and the values of $\beta^q_{i'j'k'}$ are known, the whole problem can be treated quantitatively. Combining both SFG-VS and SHG techniques, Zhuang and Shen *et al.* [22] pedagogically demonstrated the analysis methodology with detailed study on the molecular orientation and conformation of the –CN, $–CH_3$ and the $–(C_6H_4)_3–$ terphenyl groups of the 4″-*n*-pentyl-4-cyano-*p*-terphenyl [5CT, $CH_3(CH_2)_4(C_6H_4)_3CN$] molecule in the Langmuir monolayer at the air/water interface. It is a great example and very educational on what could be done with SFG-VS and SHG for interface studies. However, Professor Shen himself sometimes considered it still a 'qualitative or semi-quantitative accomplishment' [42]. Indeed, some issues discussed in this work still call for further examination.

Before we go further, we shall present the following formulations of equations (1)–(12) into simpler expressions, which can be useful for quantitative analysis in SFG-VS and SHG with simple physical pictures of molecular orientational analysis, and for developing new quantitative techniques in SFG-VS and SHG [23–26, 53].

2.2.2. Some simple formulations of SHG and SFG-VS for interface studies. As we have shown previously [23], for SHG and SFG-VS the $\chi^{(2)}_{\text{eff}}$ in equation (3) can be generally simplified by integration over the Euler angles ψ and ϕ into the following expression:

$$\chi^{(2)}_{\text{eff}} = N_s d(\langle\cos\theta\rangle - c\langle\cos^3\theta\rangle) = N_s\, d\, r(\theta). \tag{13}$$

Here $r(\theta)$ is the *orientational field functional*, which contains all orientational information at a given SFG experimental configuration. The dimensionless parameter c is called the *general orientational parameter*, which determines the orientational response $r(\theta)$ to the molecular orientation angle θ; and d is the susceptibility strength factor, which is a constant in a certain experimental configuration with a given molecular system. It is easy to show that the d and c values are both functions of the related Fresnel coefficients, including the refractive index of the interface and the bulk phases, and the experimental geometry. d is proportional to the hyperpolarizability values. Therefore, d measures the strength of the non-linearity, while c is only related to the relative ratios between the hyperpolarizability tensor elements. Therefore, c measures order and anisotropy, i.e. molecular orientation. The expressions in equation (13) can be explicitly derived for both SHG and SFG from the rotationally isotropic monolayer or ordered molecular films, because in equation (10) (see Appendix A) there are only linear combinations of $\langle\cos\theta\rangle$ and $\langle\cos^3\theta\rangle$ terms [23]. For some cases ψ and ϕ cannot be integrated in an ordered molecular system; then the expressions for d and c will contain terms with ψ and ϕ.

This formulation has certain advantages in terms of quantitative orientational and polarization analysis in SHG and SFG experiments [23]. In order to compare SFG-VS experiments in different polarizations and experimental geometry conditions, the SFG intensity of any SFG experimental configuration can be expressed as [23],

$$I(\omega) = A\, d^2\, R(\theta) N_s^2\, I(\omega_1) I(\omega_2) \tag{14}$$

$$R(\theta) = \left|r(\theta)\right|^2 = \left|\langle\cos\theta\rangle - c\,\langle\cos^3\theta\rangle\right|^2 \tag{15}$$

in which A is the experimental constant, including the pre-factors in equation (1) times the instrumental response constant, and $R(\theta)$ is called the *orientational functional*. As we have shown elsewhere [23], the *general orientational parameter* c controls the orientational behaviour of $I(\omega)$ through the function $R(\theta)$. By changing experimental incident angles and polarizations, the c value can be changed from $-\infty$ to $+\infty$ [23]. The rich behaviour of $R(\theta)$ has been carefully analysed, and the case for a δ-distribution function is illustrated in figure 1. For example, there are orientationally very sensitive regions on the $c = 2.25$ and $c = 4$ curves, as well as orientationally insensitive regions on the $c = 0.5$ and $c = 1$ curves. In comparison, linear polarization spectroscopy can only measure the orientation parameter $K = \langle\cos^2\theta\rangle$, which varies only slowly with the tilt angle θ [23].

For a non δ-distribution of θ, the behaviour of $R(\theta)$ becomes more complicated as fully discussed elsewhere [23]. However, in such cases the formulation with the *general orientational parameter* c can help disentangle the complicated behaviour of $R(\theta)$ [23]. It is clear that with different c values, orientationally sensitive and insensitive SFG or SHG measurements of the monolayer or ordered molecular films can be achieved. Orientationally insensitive measurements in SHG were first discussed by Simpson and Rowlen [54, 55]. With the concept of the *general orientational parameter* c, the proper condition for effective orientationally insensitive measurements can be explicitly determined by reading the behaviour of $R(\theta)$ for different c values. Generally, the relatively flat region on the $R(\theta)$ curve for a particular c can be used for orientationally

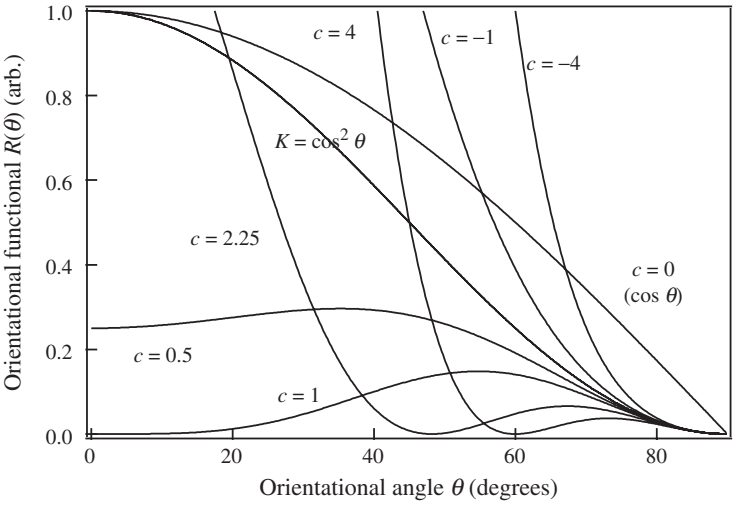

Figure 1. Orientational functional $R(\theta)$ versus orientational angle θ at $c = -4, -1, 0, 1, 0.5, 1, 2.25, 4$ and $K = \langle\cos^2\theta\rangle$ versus θ, assuming a δ-distribution function for θ [23].

insensitive measurements. The experimental configurations corresponding to these c values can be used for such measurements.

The orientational parameter $D = \langle\cos\theta\rangle/\langle\cos^3\theta\rangle$ is the crucial parameter to be determined from SFG-VS and SHG experiments. The behaviour of D in terms of the orientational angle θ and the distribution function $f(\theta)$ has been carefully studied, especially by Rowlen and Simpson *et al.* [23, 56, 57]. It has been shown that the D value alone cannot uniquely provide information on both θ and $f(\theta)$. However, the formulation of $R(\theta)$ not only allows using SHG and SFG measurements at different c values (polarization or experimental geometry) to uniquely determine θ and $f(\theta)$ in many cases [23], but also allows explicit and accurate determination of D values [23–25].

D values can be accurately determined through the polarization null angle (PNA) method. The null signal of $I(\omega)$ gives $R(\theta) = 0$, then $c_0 = D = \langle\cos\theta\rangle/\langle\cos^3\theta\rangle$. Compared with the commonly used polarization intensity ratio (PIR) method in the SFG and SHG literature, the PNA method not only has much higher intrinsic accuracy, but also has the ability to obtain accurate D values for interface systems where the PIR method fails [23–25]. Even though both the PNA and PIR methods use exactly the same set of parameters in analysis, it has been explicitly shown that the PIR method is simply a less accurate equivalent method to calculate the orientational parameter D [23–25]. However, the PIR method has been commonly used in the SFG-VS literature for orientational analysis [23, 34]. In practice in many SFG-VS works, the intensity ratio was directly modelled without explicitly obtaining the D value [58]. In this way, the elegance in the analysis [23, 56, 57] of the behaviour of the orientational parameter D on molecular orientation and its distribution is generally lost. The fact is that with more accurately determined D values through the PNA method, the sensitivity of the unknown parameters in the treatment of SFG-VS data can be more effectively assessed. The PNA method is central to the quantitative applications of SFG-VS, and we shall come back to it in detail in section 3.

With the accurate determination of D, the first- and third-order orientational order parameters of the interface layer or ordered molecular films, i.e. $S_1 = \langle\cos\theta\rangle$ and $S_3 = (5\langle\cos^3\theta\rangle - 3\langle\cos\theta\rangle)/2$, can be explicitly connected to SHG and SFG-VS measurements as in the following [23, 53]:

$$r(\theta) = \left(1 - \frac{c}{c_0}\right)\langle\cos\theta\rangle = \left(1 - \frac{c}{c_0}\right)S_1$$
$$= (c_0 - c)\langle\cos^3\theta\rangle = \frac{1}{5}(c_0 - c)(2S_3 + 3S_1). \quad (16)$$

These orientational order parameters are important in understanding the orientational order and phase transition behaviour of molecular layers as well as molecular films. Various spectroscopic methods, such as polarized Raman and fluorescent emission spectroscopies, have been formulated to obtain orientational parameters of liquid crystal molecular films [59–61]. In these studies, $S_2 = (3\langle\cos^2\theta\rangle - 1)/2$ and $S_4 = (35\langle\cos^4\theta\rangle - 30\langle\cos^2\theta\rangle + 3)/8$ parameters were obtained. Simple formulation can demonstrate the advantages of coherent non-linear spectroscopy, such as SFG, SHG, CARS, Stimulated Raman, over incoherent spectroscopic methods, such as Raman and fluorescent emission, in experimental measurements of the orientational order parameters [53].

The above formulation provides new physical pictures and techniques for SFG-VS and SHG interface studies [24–26]. The PNA method will be discussed in section 3, with more examples of its applications.

2.2.3. General issues in application of SFG-VS. Even though SFG-VS is an interface specific spectroscopic technique, the total SFG-VS signal observed may not come only from the interface species [62–64]. If the contribution from the interfacial molecules cannot be separated from contributions from other sources, quantitative and polarization analysis of the SFG-VS signal is more complicated or in question. The good thing is that it has been consistently shown that for SFG-VS studies on the vapour/liquid and most dielectric interfaces in reflection geometry, the SFG-VS signal comes dominantly from the contribution of the interfacial species [62–65].

Techniques of quantitative treatment in SFG-VS have been developed [22–26, 34, 36–39, 66], and important issues have also been intensively reviewed [13, 15, 22, 23, 39]. The interfaces studied with SFG-VS were also carefully compiled and reviewed in the literature [7, 15]. In terms of SFG-VS and SHG interface studies of molecular structure and dynamics, the schematics in figure 2, following the review of the subject summarized by C. D. Bain [13], illustrates the scope of the problems and issues in SFG-VS and SHG interface studies.

The purpose of studies with SFG-VS and SHG is to obtain detailed molecular level information on the population, orientation, conformation, and properties of the molecular hyperpolarizability, and their changes under different chemical environments, as well as their time dependent behaviour. The results from the analysis of the SFG-VS and SHG experimental data can be compared with the molecular dynamics (MD) and Monte Carlo molecular simulations, as well as *ab initio* calculations of the

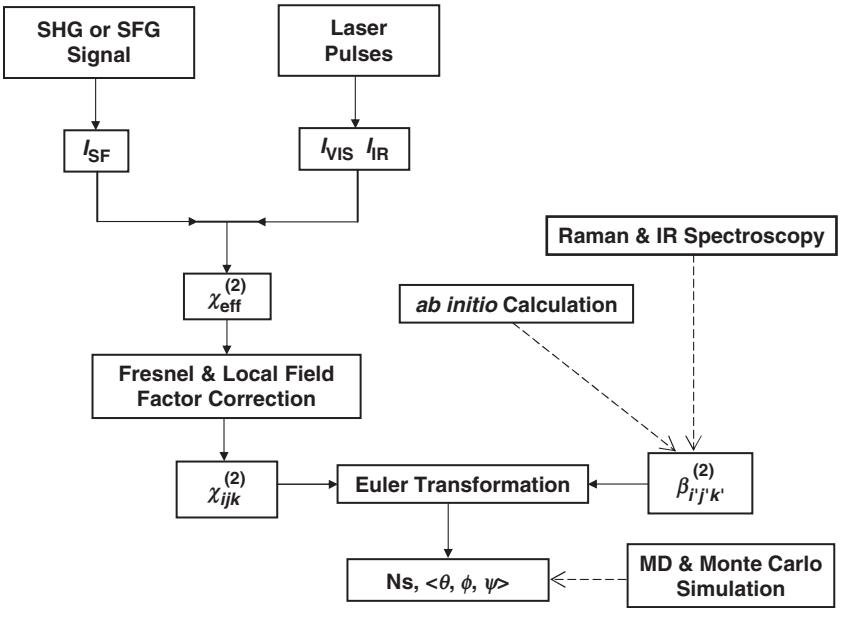

Figure 2. Schematic illustration of SFG-VS quantitative analysis. Adapted with permission from J. Chem. Soc. Faraday Trans. 1995, **91** 1281–1296. Copyright (1995) the Royal Society of Chemistry [13].

interfacial structure and dynamics. Some general considerations for the advantages and limitations of the treatment of SFG experimental data are as follows.

(a) From the known SFG-VS or SHG signal, and from the knowledge on the incoming laser beams, the $\chi^{(2)}_{\text{eff}}$ of the interface layer or molecular film can be directly measured.

(b) With quantitative correction of the Fresnel factors and local field factors, the macroscopic SFG-VS or SHG susceptibility tensor elements $\chi^{(2)}_{ijk}$ can be obtained. In this case, the values and the influences of the local field factors in the interface layer are generally not known. They are the major uncertain parameters for quantitative treatment of the SFG-VS and SHG data. Since there are only four independent $\chi^{(2)}_{ijk}$ for a rotationally isotropic interface, measurements in four different polarization combinations, i.e. *ssp*, *sps*, *pss*, and *ppp*, are usually needed.

(c) Through transformation of the Euler angle, the $\chi^{(2)}_{ijk}$ elements are directly connected to the microscopic (molecular) hyperpolarizability tensors, $\beta^{(2)}_{i'j'k'}$. This connection is generally mathematical, and can be straightforwardly worked out [46, 67]. Since there are 12 different ways to do the Euler angle transformation [47], it is tedious to derive and to check these relationships. Simplification comes when only a few non-zero elements of $\chi^{(2)}_{ijk}$ and $\beta^{(2)}_{i'j'k'}$ are allowed because of macroscopic and microscopic (molecular) symmetry requirements. Such symmetry allowed terms can be identified in the literature [16, 33, 68].

(d) Knowledge of the spectral response of $\beta^{(2)}_{i'j'k'}$ from Raman and IR spectroscopy, and also from *ab initio* calculations, is very important in terms of spectral assignment and spectral fitting [13]. Spectral assignment in SFG-VS has been basically dependent on the spectral assignment with knowledge from Raman and IR studies. Only until very recently, efforts have been made to develop a methodology for spectral assignment with polarization analysis of SFG-VS [26].

(e) For quantitative orientational analysis, the relative ratios between the $\beta^{(2)}_{i'j'k'}$ elements can be obtained from the Raman depolarization measurement, combining with the bond polarizability derivative model, as well as comparison with *ab initio* calculations [22, 34, 36–39, 66]. As shown in Appendices A and B, with these ratios known, all the $\beta^{(2)}_{i'j'k'}$ elements can be expressed in a single $\beta^{(2)}_{i'j'k'}$ element and a few known ratio values. Therefore, since there are several independent measurements in different polarizations, the absolute value of $\beta^{(2)}_{i'j'k'}$ is not necessary for obtaining structural and dynamical information in the interface layer. However, the approaches for determining these ratios and the effectiveness of the bond polarizability derivative model has been generally questioned [39], and has been rarely practiced [22, 36, 37, 39, 40].

It is then clear that the key issues on the applications of quantitative analysis of SFG-VS and SHG techniques lie mainly in steps (b), (d), and (e). In short, they are the values for the local field factors in the interface layer, the explicit spectral assignment, and the values of the hyperpolarizability ratios. If these issues are not better addressed and formulated on solid foundations, the understanding of SFG-VS spectral data, and the calculation of the orientation and orientational distribution of the molecular groups, cannot be substantiated, and is subject to misinterpretations and large error bars. Consequently, SFG-VS remains a mostly qualitative, rather than a quantitative, spectroscopic and analytical technique.

In the next two sections, we shall try to discuss how these issues can be addressed or avoided in SFG-VS analysis, and to present recent progress in these regards.

3. Quantitative orientational and polarization analysis with SFG-VS

Here we try to give a solid formulation of the polarization null angle (PNA) method and to demonstrate its advantages over the commonly used polarization intensity ratio (PIR) method, on orientational analysis in SFG-VS.

Since all spectral, orientational and polarization information in SFG-VS is contained in the $\chi^{(2)}_{\text{eff}}$ as defined in equation (3), quantitative analysis with SFG-VS is to obtain molecular information from experimental measurement of $\chi^{(2)}_{\text{eff}}$ in specifically chosen experimental conditions and configurations. As we discussed in section 2.2.3, the primary concerns in this analysis of $\chi^{(2)}_{\text{eff}}$ are its dependence on experimental configurations, namely, on polarization configurations and light incident angles; on molecular hyperpolarizability tensors, namely, the hyperpolarizability tensor ratios; and on the local field factor values. We shall discuss these relationships, and based on these discussions we shall discuss how the PNA method can be used for accurate molecular orientation studies of molecular interfaces. Examples of simple vapour/liquid interfaces are used to illustrate the improvement of the quantitative analysis in SFG-VS, for their

SFG-VS spectra have clear and simple features. The same principles can be generally applied to complex molecular interfaces.

3.1. *Experimental configuration: the polarization null angle (PNA) method*

In previous SFG-VS studies, experimental configuration analysis is certainly one of the neglected dimensions. From our recent quantitative analysis with SHG [23], we have noticed the importance of this missing dimension in the SFG-VS technique.

In order to better discuss issues in quantitative analysis of $\chi^{(2)}_{\text{eff}}$, equation (3) can be rewritten as the following expressions from equations (6)–(9):

$$\begin{aligned}\chi^{(2)}_{\text{eff}} = &\sin\Omega\sin\Omega_1\cos\Omega_2\chi^{(2)}_{\text{eff},ssp}\\ &+\sin\Omega\cos\Omega_1\sin\Omega_2\chi^{(2)}_{\text{eff},sps}\\ &+\cos\Omega\sin\Omega_1\sin\Omega_2\chi^{(2)}_{\text{eff},pss}\\ &+\cos\Omega\cos\Omega_1\cos\Omega_2\chi^{(2)}_{\text{eff},ppp}.\end{aligned} \tag{17}$$

Equation (17) explicitly underlines the idea that $\chi^{(2)}_{\text{eff}}$ is just a linear combination of $\chi^{(2)}_{\text{eff}}$ in four independently measurable experimental configurations, i.e. *ssp*, *sps*, *pss*, and *ppp* polarization configurations. In SFG-VS studies, measurements were done either with all these four experimental configurations; or one, usually with *ssp* or *ppp*; or two, usually with *ssp* and *ppp*; or three, usually with *ssp*, *ppp*, and *sps*, of the four configurations.

However, since in SFG-VS experiments the measured quantity is $|\chi^{(2)}_{\text{eff}}|^2$, instead of $\chi^{(2)}_{\text{eff}}$, the information of $\chi^{(2)}_{\text{eff}}$ cannot be completely recovered from the independently measured *ssp*, *sps*, *pss*, and *ppp* SFG-VS intensities. Recent reports on the PNA method [23–25], polarization selection rules in SFG vibrational spectral assignment [26], and the polarization mapping method [69] in SFG-VS have signified this point. In this subsection we shall discuss the PNA method first, and the polarization selection rules for vibrational spectral assignment in SFG-VS are discussed in section 4.

In the PNA method, a specific polarization set $(\Omega^{\text{null}}, \Omega_1^{\text{null}}, \Omega_2^{\text{null}})$ exists to make the SFG signal become zero (null), thus through $R(\theta) = 0$ with equation (26), the orientational parameter D can be determined. In practice, the problem can be greatly simplified by letting $\Omega_2 = 0$ and $\Omega_1 = -45^\circ$ [24, 25]. Then

$$0 = \chi^{(2)}_{\text{eff}} = -\frac{\sqrt{2}}{2}\sin\Omega^{\text{null}}\chi^{(2)}_{\text{eff},ssp} + \frac{\sqrt{2}}{2}\cos\Omega^{\text{null}}\chi^{(2)}_{\text{eff},ppp} \tag{18}$$

and

$$\tan\Omega^{\text{null}} = \sin\Omega^{\text{null}}/\cos\Omega^{\text{null}} = \chi^{(2)}_{\text{eff},ppp}/\chi^{(2)}_{\text{eff},ssp}. \tag{19}$$

The right side of equation (19) is the polarization intensity ratio $\chi^{(2)}_{\text{eff},ppp}/\chi^{(2)}_{\text{eff},ssp}$, which can directly lead to the determination of the orientational parameter D, as in the

well established and commonly used PIR method, which calculates the D value from either $\chi^{(2)}_{\text{eff},ppp}/\chi^{(2)}_{\text{eff},ssp}$ or $\chi^{(2)}_{\text{eff},sps}/\chi^{(2)}_{\text{eff},ssp}$ ratios [22, 34].

There are two common disadvantages with the PIR method. Firstly, when either $\chi^{(2)}_{\text{eff},ppp}$ or $\chi^{(2)}_{\text{eff},ssp}$ is small, i.e. close to the noise level, the intensity ratio cannot be very accurately determined from direct SFG intensity measurements. Especially for the vapour/methanol [65], vapour/acetone [70], as well as vapour/acetonitrile [71] interfaces, only *ssp* polarization has a significant SFG signal observed above the noise level in the CH_3 stretching vibrational spectral region. So the PIR method cannot provide a good measurement of the orientational parameter D of the CH_3 groups for these interfaces [65]. Generally, peaks strong in one of the four standard polarizations are small in other polarizations; this is how the polarization selection rule works [26], and this is discussed in section 4. Because one of the two intensities is usually small, this undoubtedly introduces difficulties and uncertainties into the PIR method. Therefore, the PIR method produces the desired measurement of the molecular orientation only for a small number of interfaces [22]. Secondly, since the SFG intensities in different polarizations are measured in the PIR method, the relative sign between the two $\chi^{(2)}_{\text{eff}}$s has to be independently determined [65].

The expression in equation (19) gives explicit reasons why the PNA method is more advantageous than the commonly used PIR method. Firstly, because the polarization angle Ω^{null} is the polarization when the SFG signal goes to zero (null), it can easily be determined with an accuracy of about 1 degree, or much less. Thus, the $\chi^{(2)}_{\text{eff},ppp}/\chi^{(2)}_{\text{eff},ssp}$ ratio in equation (19) can be obtained with an accuracy determined by the error bar of the null angle Ω^{null}, instead of by the error bar of the SFG intensity. Apart from the accuracy, there is no relative sign problem in the PNA method [23]. After the $\chi^{(2)}_{\text{eff},ppp}/\chi^{(2)}_{\text{eff},ssp}$ ratio is accurately determined, PNA uses exactly the same set of parameters as PIR to calculate the orientational parameter D. Therefore, the PNA method is not simply an alternative method for the PIR method. It overcomes the major disadvantages of the PIR method.

In the PIR method, if there is no spectral interference, the intensity ratio at the peak position gives the same orientational parameter from the ratio of the oscillator strength fitted from the SFG spectra. If there is spectral interference, the only reliable way is to use the ratio between the fitted oscillator strengths from spectra of different polarizations.

Similarly, there are two ways to obtain the null angle. The first is to directly fit the SFG intensities measured at the peak position in different polarizations of the SF signal, if there is no spectral interference. The second is to measure the SFG spectra in different SF signal polarization angles and fit the spectra for the oscillator strength values, which are then used to fit for the null angle value. The latter method is useful when there are spectral interferences present. For the cases of vapour/acetone and vapour/methanol interfaces, the CH_3 symmetric stretch mode is a fairly isolated peak in their SFG-VS spectrum, and experimental data have shown that both approaches in the PNA method gave the same null angle values within the experimental error.

Using the same parameters for the vapour/methanol interfaces, measurement with the PNA method gave $D = 0.97 \pm 0.04$ [24, 25], while the PIR method gave $D < 1.8$ [65]. Because the SFG intensity in both the *ppp* and *sps* polarization configurations are very small and at the noise level, the PIR method can only give an upper limit

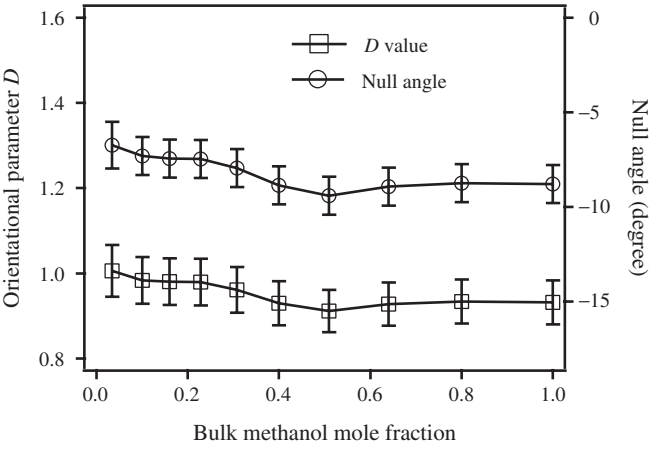

Figure 3. Null angle and D values for vapour/methanol–water mixture interfaces for different bulk methanol mole fractions [77].

on the D value. This has left room for speculations on the orientational order at the vapour/methanol interface [65, 72–75]. Such a significant improvement of the accuracy of the orientational parameter D with the PNA method now provides new opportunities in orientational analysis of the molecular interfaces. The most important aspect of applications with the PNA method may lie with the ability to measure small changes of the orientational order of a given molecular interface.

Figure 3 exemplifies one such application. The null angle of the symmetric stretching SFG-VS spectral peak of the CH_3 group at the vapour/methanol–water mixture interface is measured at different bulk methanol concentrations. The error bar for the null angle is about 1.5°, and the error bar for the D value is about 0.06. Because the D value is very close to unity, the interfacial CH_3 group is well ordered and its symmetry axis points up close to the surface normal. The dependence of D on θ and its distribution $f(\theta)$, shown in figure 6, has been elegantly discussed by Simpson and Rowlen [23, 56, 57]. It is clear from figure 3 that the orientational order of the methanol CH_3 group at the vapour/methanol–water mixture interface changes very little throughout the whole range of the bulk methanol concentration; and it is clear that the CH_3 is getting slightly more ordered as the bulk methanol concentration increases. These results provide strikingly detailed knowledge of the structure and energetics of this very important and benchmark interface [65, 72–77]. With such knowledge of the molecular orientation, a double layered structure of the vapour/methanol–water mixture interface is determined, and the adsorption free energies for the first and second layers of methanol molecules were also determined [77, 78].

PNA measurements on the vapour/acetone–water mixture [79, 80], vapour/acetonitrile–water mixture, vapour/DMSO-water mixture as well as vapour/tert-butanol–water mixture interfaces [81] have also been conducted. These results are fully consistent with these for the vapour/methanol–water mixture and vapour/neat methanol interfaces, and some new features of the PNA method can also be developed for studies on complex molecular interfaces. These aspects are discussed in section 3.5 using vapour/acetone and vapour/DMSO interfaces as examples.

The PNA method should find unprecedented applications in molecular interface studies. To our knowledge, the null angle measurement has been mentioned only once [38] in previous SFG-VS studies, prior to our recent work [23–25]. Even though the principle of null angle measurement in surface SHG was first demonstrated for the determination of molecular orientation at silica surfaces some 20 years ago [82], and the null angle method in SHG was further elaborated in 1990 [83], the practice has been scarce in the SHG interface studies [23–25].

It is to be noted that even though the determination of Ω^{null} is straightforward and accurate, in order to calculate D, parameters like the hyperpolarizability ratio and the local field factors in the interface layer, whose values are subject to uncertainties, have to be employed. In the following sections, we shall discuss these parameters and show that their value can be determined with fair accuracy. We shall also discuss the implications of the accurately determined D values for understanding of the orientational order of complex interfaces. Nevertheless, the relatively small changes of the orientational order of a given molecular interface can always be measured with the PNA method. This will bring many new applications to molecular interfaces studies.

In any case, even though PNA and PIR use different methods to obtain the $\chi^{(2)}_{\text{eff}}$ ratio, they use the same set of parameters to calculate the D value. PNA measurement is not only much more accurate than PIR, it can also make accurate measurement when PIR fails. We shall see that there are many more advantages for the PNA method in terms of quantitative polarization and orientational analysis, when we discuss the incident angle dependence of the SFG-VS intensities below.

3.2. *Experimental configuration: the incident angles*

Here we discuss how incident angle geometry can be optimized for SFG-VS measurement and for obtaining accurate D values free from complications of the unknown IR refractive indices and local field factors.

Even though the issue of SFG experimental geometry has been discussed to some extent in the SFG-VS literature [84, 85, 87], as also summarized by Buck and Himmelhaus in their recent review article [15], the dependence of the SFG-VS signal on the incident angles is yet to be clearly discussed in terms of effective polarization and orientational analysis.

Generally there are two basic geometries for doing a SFG-VS experiment in either reflection or transmission, namely, the co-propagating, and counter-propagating geometry. The basic difference between them is that in the former case, $\beta \simeq \beta_1$, while in the latter case β is significantly different from β_1. β is the outgoing angle of the SFG signal as defined in equation (4), while β_1 is the incident angle of the visible beam. Because the co-propagating, and counter-propagating experimental geometries in the reflection were widely used in the SFG-VS literature, we shall limit our discussions to them. Discussions on other geometries can follow suit.

From equations (6)–(9), it is easy to see that the value of $\chi^{(2)}_{\text{eff}}$ in different polarization configuration depends on the Fresnel factors given by equation (5). Equation (5) indicates that the Fresnel factors are functions of the incident angles, the dielectric constants (or the refractive indices, $n_i(\omega_i)$) of both bulk phases, as well as the local field factors in the interface layer ($n'(\omega_i)$). For a given molecular interface, $n_i(\omega_i)$ and

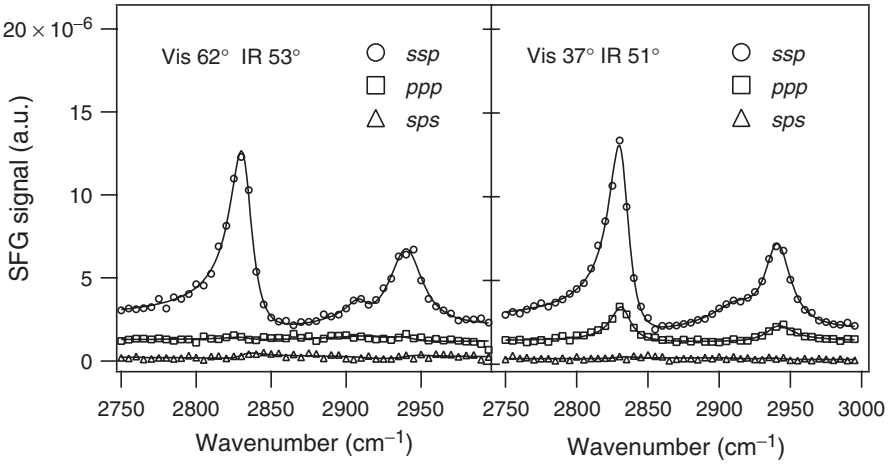

Figure 4. SFG-VS of vapour/methanol interface in two different experimental configurations. The *ppp* SFG spectrum shows clear features in the right, but no features in the left. The incident angle dependence can be fully quantified by the calculated $d^2R(\theta)$ values, with known parameters discussed later. Full results to be published elsewhere. The assignments of the peaks can be found in table 4.

$n'(\omega_i)$ values are fixed numbers, even though the $n'(\omega_i)$ values may not be exactly known. Therefore, the dependence of the SFG-VS signal in different polarization configurations on the IR and visible incident angles can be used to evaluate the $n'(\omega_i)$ values in some special cases [22, 40, 86].

One of the important aspects of the incident angle dependence is that the SFG-VS spectra in different polarization configurations, i.e. *ssp*, *sps*, *pss*, and *ppp* configurations, have different incident angle dependence. People have noticed spectral differences when they try to compare the SFG-VS spectra on the same molecular interface obtained in different research groups, where different incident angles of IR and visible beams were used [84, 85, 87]. But systematic analysis on this dependence has been generally overlooked. Here we shall show how intriguing this analysis is.

Figure 4 shows the SFG-VS spectra of the vapour/methanol interface with two sets of incident angles (Set I: $\beta_1 = 62^\circ$, $\beta_2 = 53^\circ$; Set II: $\beta_1 = 37^\circ$, $\beta_2 = 51^\circ$) in the reflective co-propagating geometry in ambient conditions. It is easy to see that the *ppp* spectrum with Set II exhibits clear spectral features. In the literature [65, 72–75, 77], SFG-VS spectra of the vapour/methanol interface obtained by different researchers are all similar to the spectra on the left side of figure 4, with featureless spectra in the *sps*, *pss*, as well as *ppp* polarizations. Therefore, polarization and orientational analysis of the vapour/methanol interface has been quite limited, until the PNA method was used recently [77].

Now with the SFG spectra in Set II, the peak intensity around 2928 cm^{-1} in the *ppp* spectrum is about one-quarter of that in the *ssp* spectrum. So the polarization and orientational analysis with the traditional PIR method can be performed. Fitting the spectra in Set II, we obtained $\chi_{ssp}/\chi_{ppp} = -2.0 \pm 0.3$ (the other value with the + sign is physically unreasonable, see [65]), and accordingly the order parameter is $D = 1.6^{+1.1}_{-0.6}$ [87]. The large error bar of this results comes mostly from the uncertainty

from fitting the weak *ppp* peak. This error bar of the D value from the PIR method is thus about one order of magnitude larger than that from the PNA measurement discussed in section 3.1.

Analysis of the incident angle dependence not only can help find proper incident angles to increase spectral intensity in certain polarizations, usually the *ppp* spectrum is the most sensitive, but also can be used to find proper incident angles for optimization of the accuracy and sensitivity of the PNA method. With Set I incident angles, the PNA method gives $D = 0.97 \pm 0.06$, while with Set II incident angles, the PNA gives $D = 0.96^{+0.18}_{-0.15}$. This difference of error bars with measurement in different incident angle sets is not accidental. Full incident angle analysis has indicated that with Set II, the error bar is about three times of that with Set I, when the accuracy for the Ω^{null} value measured in the PNA experiment is the same [87]. Analysis further indicated that the PNA sensitivity depends only very slightly on the IR incident angle β_2, but the dependence on the visible incident angle β_1 is quite significant. Analysis has also shown that the optimal incident angles are $\beta_1 \cong 60^\circ$ and β_2 between 50° and 70° in order to get the best PNA sensitivity and strong SFG-VS signal in the *ssp* polarization for the vapour/methanol interface [87].

Thus, we have shown that incident angle analysis is quite useful in terms of obtaining unseen spectra in certain polarizations, and it is also quite useful in terms of doing PNA analysis with optimal incident angles. Now we are going to discuss one of the crucial aspects from incident angle analysis in SFG-VS. It is the fact that the polarization and orientational analysis is essentially insensitive to the IR refractive indices in the co-propagating experimental configurations. This fact clearly makes the co-propagating experimental configurations the ideal choice for polarization and orientational analysis, and additional knowledge of the IR refractive indices can be obtained from counter-propagating geometries.

As discussed in the literature [22, 40, 83, 88–90] and indicated in equation (5), the determination of the molecular orientation with SFG-VS and SHG is quite sensitive to the values of $n'(\omega_i)$, which is usually not accurately known, especially for the IR wavelengths. Moreover, in some cases the value of $n'(\omega_2)$, as well as $n_2(\omega_2)$ in the IR wavelengths should vary significantly across the spectral region, because the dispersion of the refractive index in resonance with the IR wavelengths can be strong. Therefore, in order to make a quantitative analysis of $\chi^{(2)}_{\text{eff}}$, it is most difficult to assess the values of the $L_{ii}(\omega_2)$ terms in equation (3). In most SFG-VS studies, this issue of uncertainty on IR refractive indices was generally evaded and the treatment can only be considered qualitative and semi-quantitative, except for a few very careful studies by Zhuang, Wei and Shen *et al.* [22, 40].

However, detailed analysis of the terms in equations (6)–(9) provides a relatively easy solution for this problem. This comes from the fact that in equation (9), the second and third term nearly cancel each other in a co-propagating geometry. When both the SF frequency ω and the visible frequency ω_1 are not in resonance with the interfacial molecules, $\chi_{xzx} = \chi_{zxx}$ is generally valid. Therefore, the sum of the second and third terms in equation (9) is proportional to the term $\Delta = -\cos\beta \sin\beta_1 + \sin\beta \cos\beta_1 = \sin(\beta - \beta_1)$ for co-propagating geometry. For counter-propagating geometry, $\Delta = -\sin(\beta - \beta_1)$, as from the discussion above for equation (3). Table 1 lists calculated Δ values for incident angle Set I and Set II in both co-propagating and

Table 1. Comparison of Δ values for different incident angles in co-propagating and counter-propagating geometries. The wavelengths and frequency used are: visible (ω_1) 532 nm, IR (ω_2) 3000 cm^{-1}. In order to compare with the other two terms in equation (9), Δ/Δ_1 and Δ/Δ_2 are also calculated, where $\Delta_1 = \cos\beta\cos\beta_1$ and $\Delta_2 = \sin\beta\sin\beta_1$.

Geometry	β_1 (°)	β_2 (°)	β (°)	Δ	Δ/Δ_1	Δ/Δ_2
Co-propagating	62.0	53.0	60.6	−0.024	−0.10	−0.03
Counter-propagating	62.0	53.0	40.7	0.36	1.0	0.63
Co-propagating	37.0	51.0	38.8	0.031	0.050	0.082
Counter-propagating	37.0	51.0	24.3	0.22	0.30	0.89
Co-propagating	60.0	55.0	59.3	−0.012	−0.047	−0.016

counter-propagating geometries. The calculation indicates that in the co-propagating geometry, the second term and the third term in equation (9) contribute insignificantly to the total $\chi^{(2)}_{\text{eff},ppp}$, as discussed by Wei and Shen *et al.* [40]; while in the counter-propagating geometry, these two terms contribute quite significantly. For the SFG experiment in collinear geometry, where $\beta = \beta_1 = \beta_2$, one always has $\Delta = 0$. This indicates that in order to have better cancellation of the second and third terms in equation (9), it is better to arrange the IR and visible beams as close to collinear geometry as possible, for example, the $\beta_1 = 60^\circ$ and $\beta_2 = 55^\circ$ set is better than the Set I and II incident angles.

Now with the remaining two terms in equation (9) for $\chi^{(2)}_{\text{eff},ppp}$ in the co-propagating geometry, the ratio $\chi^{(2)}_{\text{eff},ppp}/\chi^{(2)}_{\text{eff},ssp}$ is very weakly dependent on the refractive indices across the IR wavelengths, since the term $L_{zz}(\omega_2)$ in $\chi^{(2)}_{\text{eff},ppp}/\chi^{(2)}_{\text{eff},ssp}$ can simply cancel each other. Because the $\chi^{(2)}_{\text{eff},ppp}/\chi^{(2)}_{\text{eff},ssp}$ value can be accurately determined from the PNA measurement as shown in equation (19), polarization analysis with co-propagating geometry should be generally immune from the uncertainty of the refractive indices and local field factors in the interface layer across the IR wavelengths.

It is interesting to note that even though $\chi^{(2)}_{\text{eff},sps}$, $\chi^{(2)}_{\text{eff},pss}$, and the second and third terms in $\chi^{(2)}_{\text{eff},ppp}$ themselves do not contain the $n'(\omega_2)$ term, they have to be avoided in order to make sure $\chi^{(2)}_{\text{eff},ppp}/\chi^{(2)}_{\text{eff},ssp}$ is free from the influence of $n'(\omega_2)$, as well as the $n_2(\omega_2)$, $n_2(\omega_1)$ values. Generally, $n'(\omega_2)$ cannot be exactly known for the IR wavelengths; while $n_2(\omega_2)$ and $n_1(\omega_2)$ ($n_1(\omega_2) \cong 1.00$ if medium 1 is air) can be measured but the data is generally not available. Even when they are available, different values at each wavelength near the resonant IR frequency greatly complicate the data processing. Therefore, in practice the analysis here simplifies a lot of things in SFG-VS quantitative analysis, and underlines the effectiveness and accuracy of the PNA methods in the co-propagating geometry. Actually, we did find that in the calculation of the D values with the PNA method, the resulted D value changed very insignificantly when the values of the IR refractive indices were varied in a fairly large range. In the mean time, D is much more sensitive to the values of the refractive indices of the SF and visible laser frequencies used.

Therefore, one can reach the following conclusions from equations (6)–(9) and the discussions above,

(a) The ratios $\chi^{(2)}_{\text{eff},sps}/\chi^{(2)}_{\text{eff},ssp}$ or $\chi^{(2)}_{\text{eff},sps}/\chi^{(2)}_{\text{eff},ppp}$ are not independent of the refractive indices across the IR wavelengths, even for the co-propagating geometry.

Therefore, determination of the orientational parameter D using these two ratios is subject to large errors and uncertainties. However, if the orientational parameter can be accurately determined with other measurement, e.g. from $\chi^{(2)}_{\mathrm{eff},ppp}/\chi^{(2)}_{\mathrm{eff},ssp}$, these two ratios can be used to calculate the IR local field factor in the interface layer.

(b) Polarization analysis in counter-propagating geometry has to deal with the strong dependence on the refractive indices across the IR wavelengths. Therefore, in order to have better quantitative polarization and orientational analysis, the counter-propagating geometry should be generally avoided in SFG-VS interface studies.

(c) If a series of SFG-VS measurements using both co-propagating and counter-propagating geometries with certain incident angles are conducted on the same molecular interface, the co-propagating geometry experiments should be able to give reliable information on the molecular orientation, and based on this information, the counter-propagating geometry experiments should be able to give information on the IR refractive indices. In general, combining measurements with different incident angle sets and using their different relative sensitivities on different parameters should directly benefit quantitative polarization and orientational analysis in SFG-VS.

The effectiveness of the co-propagating geometry discussed above may not hold for double resonance SFG-VS, in which the SF frequency is usually in resonance with the interfacial molecules. Therefore, $\chi^{(2)}_{xzx} = \chi^{(2)}_{zxx}$ generally does not hold due to the dispersion in the SF frequency, and the first two indices in $\chi^{(2)}_{ijk}$ cannot be interchanged. In these cases, the co-propagating geometry may not be advantageous over the counter-propagating geometry in quantitative polarization and orientational analysis.

Therefore, incident angle and incident geometry analysis is very important in terms of polarization and orientational analysis. It not only further exhibits the effectiveness of the PNA method, but also helps simplify parameter analysis in SFG-VS, especially in avoiding the influence of the refractive indices across the IR wavelengths in SFG-VS quantitative polarization and orientational analysis.

3.3. *Value of the local field factors in the interface layer*

Here the values of the local field factors and models to assess these values are discussed.

Determination of the molecular orientation in SFG-VS and SHG is subjected to the values of the local field factor $n'(\omega_i)$ in the interface layer [22, 40, 83, 88–90]. We would like to point to the classical papers by Shen and his co-workers for the definition of the effective indices $n'(\omega_i)$, or the effective dielectric constant $\epsilon'(\omega_i) = (n'(\omega_i))^2$, of the interface layer [22, 40, 91]. The physical meaning of $\epsilon'(\omega_i)$ is the ratio between the microscopic local-field correction factors, i.e. $\epsilon'(\omega_i) = l_\parallel/l_\perp$ [22, 40, 91]. Therefore, $\epsilon'(\omega_i)$ depends on the anisotropy of the dielectric properties in the molecular layer, and also depends on the orientational order of the molecular dipoles [91].

It is known that since the interface layer is only one or several molecules thick and with certain orientational order, its refractive index can be different from that of the bulk material formed with the same molecule [89, 92–99]. A theoretical treatment

of the local-field correction factor l_{ii} in the molecular layer for SHG was given by a classical point-dipole model by Ye and Shen [91]. In a molecular monolayer with rotational symmetry around the interface normal z, we generally have $l_{\parallel} = l_{xx} = l_{yy}$, $l_{\perp} = l_{zz}$. The point-dipole model expresses the l_{ii} in terms of molecular packing distances, the molecular polarizability α_{ii} at the optical frequencies in the parallel and perpendicular directions, as well as the distance of the molecule from the defined substrate surface. This model has been tested in some cases and can quantitatively describes the local-field correction factor l_{ii} in the molecular layers [92, 93, 95–99]. However, it is generally more difficult to determine the parameters with enough accuracy in this model. In particular, on one hand, accurate orientational angles and distributions of the molecular dipoles in the molecular layer have to be known to calculate the l_{ii} terms for obtaining $\epsilon'(\omega_i)$, and on the other hand, $\epsilon'(\omega_i)$ value have to be known to determine the orientational angles and distributions from the SHG or SFG-VS experimental measurements in different polarization combinations. Therefore, this problem has to be solved through a self-consistent approach, as suggested by Munn *et al.* [97–99]. Here we are not going to get into the detailed expressions and parameters of this point-dipole model. However, we would like to point out some facts from the calculations with the l_{ii} terms from the point-dipole model.

(a) Molecular polarizability α in the optical frequency for small molecules is typically in the range of a few Å^3, for example, a water molecule has $\alpha = 1.5$ Å^3 and a methanol molecule has $\alpha = 3.3$ Å^3 [100]. With the molecular distance calculated from their bulk densities, their l_{ii} are relatively small and close to unity. Therefore, according to the formula in Ye and Shen [91], the $n'(\omega_i)$ of the water interface changes from 1.14 to 1.21 when the molecular dipole of the water molecule at the pure water interface changes from completely flat to upright; while for the methanol interface, $n'(\omega_i)$ changes from 1.18 to 1.25. Because the molecular polarizability α is generally additive, the larger the molecule, the bigger the α, as well as the molecular distance. Since the molecular dipole is usually not completely flat or completely upright at the interfaces, therefore, for dielectric molecular layers far from electronic resonances, it is reasonable to say that for a simple liquid not in resonance or strong dispersion, $n'(\omega_i)$ is generally around 1.20 ± 0.05, which is very close to the $n'(\omega_i) = 1.18 \pm 0.04$ value used in recent quantitative analysis [22, 40, 86].

(b) For large chromophore, α is usually more than one order larger than for small molecules. For example, the chromophores of 5CT and 8CB molecules have their $\alpha > 50$ Å^3 at 800 nm [97–99, 101]. Simulation of an 8CB monolayer with the formulation in Ye and Shen [91] shows that its $n'(\omega)$ changes from about 1.4 to 1.9 as the orientation angle changes for about 10° in the molecular monolayer and its average interface density changes from 52 to 40 Å^2 [101]. Therefore, $n'(\omega)$ of such molecular layers changes significantly with the interface molecular density as well as molecular orientation. We have recently developed a self-consistent approach to calculate the molecular orientation and $n'(\omega)$ values from the SHG data using the classical point-dipole model of the 8CB Langmuir monolayer at the air/water interface [23, 101].

Both molecular orientation and the local field factors can be obtained at different surface densities, and they agrees quantitatively with the simulation results above.

As summarized by Shen *et al.* [22], in the SFG-VS and SHG literature, the values of $n'(\omega_i)$ were used either equal to the refractive index of one of the bulk phases, or equal to the bulk refractive index of molecules in the interface layer, or equal to values from certain experimental estimations. According to the discussions above, these approaches were not on solid foundations. However, in the past two decades or so, Shen and his co-workers have built the foundations for a quantitative treatment of this problem [22, 40, 91]. In practice, the polarization and experimental configuration analysis of SFG-VS and SHG we have demonstrated in the previous sections can also be helpful on this problem.

There are three $n'(\omega_i)$s, namely, $n'(\omega)$ for the SF frequency, $n'(\omega_1)$ for the visible frequency, and $n'(\omega_2)$ for the IR frequencies, one has to deal with in SFG-VS analysis. In single resonant SFG-VS studies, $n'(\omega) = n'(\omega_1)$ is generally valid within 0.03 units, because the dispersion effect is small between the SF and visible frequencies. In section 3.2, we demonstrated that by choosing co-propagating geometry for polarization and orientational analysis, the value for $n'(\omega_2)$ of the IR frequency is insensitive in the analysis. Therefore, the problem can be generally simplified by letting $n'(\omega) = n'(\omega_1) = n'(\omega_2)$ in quantitative analysis with co-propagating SFG-VS measurement. Thus, only one value for the effective refractive index in the interface layer, i.e. $n'(\omega)$, needs to be determined or modelled. However, for SFG-VS in counter-propagating geometry, this assumption is generally not valid.

In a recent study, Shen and co-workers used $n'(\omega_i) = 1.18 \pm 0.04$ for all the molecular moieties in the 5CT Langmuir monolayer at the air/water interface [22]. So far this work is one of the benchmark analyses of molecular orientation and conformation with both SFG-VS and SHG [22, 40]. By doing so, consistent orientation angles and conformation for the CH_3, terphenyl and CN groups of the 5CT molecule were obtained. However, they also pointed out that using the $n'(\omega_i) = 1.18 \pm 0.04$ value for the terphenyl and CN groups is less justifiable, and the use of the proper values for $n'(\omega_i)$ in SFG-VS and SHG has to be determined with care [22].

From what we have discussed of this analysis, we can now provide some new perspectives on these results.

Firstly, since the co-propagating geometry was employed for SFG-VS measurement in this work [22], it is justifiable that $n'(\omega_i) = 1.18 \pm 0.04$ worked quite well with the CH_3 groups. This value was also supported by calculation with the Lorentz model treatment [22]. This Lorentz model implies a sharp interface with only randomly oriented dipoles. Therefore, it can be used to estimate the lower middle point, with the lower limit for the molecular dipole lying completely flat and with the upper limit completely upright at the interface of the $n'(\omega_i)$ at the dielectric interfaces with molecules of small molecular polarizability α. As in the above discussions, the error with this estimation is expected to be less than 0.05 units for such interfaces.

Secondly, for the CN group, since the SFG-VS peak intensity of the *ppp* and *sps* are very small [22], the calculation with the ratios $\chi^{(2)}_{\text{eff},sps}/\chi^{(2)}_{\text{eff},ssp}$ and $\chi^{(2)}_{\text{eff},ppp}/\chi^{(2)}_{\text{eff},ssp}$ using the PIR method is subject to significant errors. Furthermore, from the

discussion in section 3.2, these two ratios has very different dependence on the IR refractive indices and local field factors. Therefore, the $n'(\omega_i) = 1.18 \pm 0.04$ calculated from these data might be subject to these errors. We have recently investigated the same system with the PNA method and conducted polarization analysis; the results indicated that the $n'(\omega_i)$ value for calculating the CN orientation is larger than 1.18 ± 0.04 [101].

Thirdly, in calculating the terphenyl group orientation angle with SHG using the fundamental wavelength at 532 nm, $n'(\omega_\omega)$ has to be significantly different from $n'(\omega_{2\omega})$ because of dispersion. Moreover, the $|n'(\omega_{2\omega})/n'(\omega_\omega)|$ ratio can be directly determined from the SHG experiment, and it is usually significantly different from unity [23, 83]. Therefore, the treatment of SHG data of the terphenyl group with the assumption of $n'(\omega_{2\omega}) = n'(\omega_\omega)$, as well as $n'(\omega_i) = 1.18 \pm 0.04$, is generally not justifiable. The same conclusion goes for the treatment of the SHG study of the biphenyl chromophore in 8CB molecules at a rubbed polymer surface [23, 40]. A self-consistent calculation of the local field factors and the chromophore orientation in the 8CB Langmuir monolayer has been conducted, which indicates that it is possible to address the problems on changing $n'(\omega_i)$ values at different surface densities and orientations in such molecular layers [23, 101].

Therefore, it is still an open problem whether the layers with the CH_3, CN and terphenyl groups should use different or the same $n'(\omega_i)$ values in their orientation calculation, since they are within the same molecule layer. If different $n'(\omega_i)$ values have to be used for each of them, this implies three dielectric layers at this interface, which can be probed with different IR or visible frequencies. Further investigation with more accuracy is certainly warranted. Even with these flaws, the basic conclusion, the problem discussed and the procedure presented on molecular orientation and conformation analysis with SFG-VS and SHG in Zhuang and Shen's work [22] are extremely useful and illuminating. This work along with others has inarguably demonstrated how SFG-VS and SHG can certainly 'allow us to completely map out the orientation and conformation of a fairly complicated molecule at an interface' [22].

In summary, the $n'(\omega_i)$ values for dielectric molecular layers not in resonance with the SF or visible frequencies is about 1.20 ± 0.05. For such interfaces, experiments with SFG-VS found that $n'(\omega_i) = 1.18 \pm 0.04$ can be used for the CH_3 groups at liquid and polymer film interfaces [22, 86], without being subject to significant errors. The Lorentz model described by Shen *et al.* may be used to estimate the lower middle point of the $n'(\omega_i)$ values at simple dielectric interfaces, with an error smaller than 0.05 units. The D values in sections 3.1, 3.2 and 3.5 were calculated with the $n'(\omega_2)$ values from this Lorentz model. Since the $n'(\omega_2)$ can be made insensitive in the SFG-VS treatment with experiment in the co-propagating geometry, $n'(\omega) = n'(\omega_1) = n'(\omega_2)$ can be generally used in the calculation. However, this does not suggest that the values of the IR refractive indices and local field factors are trivial. On the contrary, this suggests a clear approach to address the issues regarding the values of the IR refractive indices and local field factors in the ordered interface layers. For molecules with large chromophores at the interface, $n'(\omega_i)$ changes significantly with the surface density and chromophore orientation. Further investigation is certainly needed for such interfaces, and the use of the proper values for $n'(\omega_i)$ in SFG-VS and SHG has to be determined with care. Generally speaking, knowledge

of the $n'(\omega_i)$ values is still not as certain as one expects. Therefore, it should be noted that the orientational parameter values calculated from SFG and SHG experiment data are generally subject to this uncertainty. This certainly calls for detailed molecular theory for dielectric interfaces.

3.4. *Raman depolarization ratio and hyperpolarizability tensor ratios*

Here the use of the Raman depolarization ratio and the bond polarizability derivative model on obtaining hyperpolarizability tensor ratios in SFG-VS analysis is discussed.

Since the very beginning of SFG-VS studies of molecular interfaces, there was a need to simplify the quantitative analysis of the polarization SFG-VS data through seeking for proper hyperpolarizability tensor ratios combining with symmetry analysis of the molecular vibrational modes so as to reduce the problem to a single unknown non-zero molecular polarizability tensor element $\beta_{i'j'k'}$ [34]. The Raman depolarization ratio and bond polarizability derivative model has been used to obtain a quantitative description of the hyperpolarizability tensor ratios in SFG-VS quantitative analysis [22, 34, 36–40, 66, 102]. (See Appendices A and B for details.) Even though there are many applications in the literature, these two approaches should still be used with general caution [22, 39], because the quantitative agreement of these approaches with SFG-VS spectral analysis has not been systematically tested. In order to have such a test, clearly defined parameters and SFG-VS data from reliable model molecular interfaces have to be used. We shall discuss these problems from our recent attempts on quantitative polarization and orientational analysis on simple vapour/liquid interfaces. So far, our general conclusion is that the hyperpolarizability tensor ratios obtained from the Raman depolarization ratio and the bond polarizability model can fairly well quantitatively, if not 100% accurately, reproduce and explain SFG-VS spectra for stretching vibrational modes of the CH_3, CH_2 and CH groups obtained in different polarization configurations. However, the single CH bond polarizability derivative ratio value is not simply transferable among all CH_n groups as initially expected, but their relative values can be quantitatively compared with SFG-VS studies [36, 37].

Now we briefly show how the value of the hyperpolarizability tensor ratio R for the C_{3v} groups can be determined from the Raman depolarization ratio ρ, which can be fairly accurately measured with polarized Raman techniques [103, 104]. The connection between the Raman depolarization ratio ρ and the hyperpolarizability tensor ratio is from equation (12). The Raman tensor $\alpha'_{i'j'}$ of the C_{3v} group has three symmetric tensor elements, i.e. $\alpha'_{aa} = \alpha'_{bb}, \alpha'_{cc}$ [36, 104]. Thus $\beta_{i'j'k'} = \alpha'_{i'j'} \cdot \mu'_{k'}$ (in order to simplify the expressions, the common constant in equation (12) can be omitted), and for C_{3v} group there are three corresponding symmetric hyperpolarizability tensors, i.e. $\beta_{aac} = \beta_{bbc}$, β_{ccc}. So if we define $R = \beta_{aac}/\beta_{ccc} = \alpha'_{aa}/\alpha'_{cc}$, according to the expressions for the Raman depolarization ratio ρ [36, 104], we have

$$\rho = \frac{3\gamma^2}{45\alpha^2 + 4\gamma^2} = \frac{3}{4 + 5[(1+2R)/(R-1)]^2} \tag{20}$$

with

$$\alpha = \frac{1}{3}(\alpha'_{aa} + \alpha'_{bb} + \alpha'_{cc}) = \frac{1}{3}\frac{(\beta_{aac} + \beta_{bbc} + \beta_{ccc})}{\mu'_c}$$

$$\gamma^2 = \frac{1}{2}\left[(\alpha'_{aa} - \alpha'_{bb})^2 + (\alpha'_{aa} - \alpha'_{cc})^2 + (\alpha'_{bb} - \alpha'_{cc})^2\right]$$

$$= \frac{1}{2}\frac{\left[(\beta_{aac} - \beta_{bbc})^2 + (\beta_{aac} - \beta_{ccc})^2 + (\beta_{bbc} - \beta_{ccc})^2\right]}{\mu'^2_c}.$$

If we let $Q = \sqrt{(3/5)((1/\rho) - (4/3))}$, then equation (20) gives $\pm Q = (1 + 2R)/(R - 1)$. So from a single ρ value, there are two corresponding R values as shown below. However, in reality only one R is physically correct. Eisenthal *et al.* demonstrated a method with polarized SFG-VS measurements to determine which R value is the correct one [38]

$$R = \frac{Q+1}{Q-2} \quad (\text{for } +Q) \qquad \text{or} \qquad R = \frac{Q-1}{Q+2} \quad (\text{for } -Q). \tag{21}$$

Generally, one can show with the bond polarizability derivative model that with $0 \le r < 1$ for the single XH bond, C_{3v} groups, such as CH_3, NH_3, and SiH_3, have $1 < R \le 4$ [22]. However, in the SFG-VS literature, there was some confusion on choosing the correct R values [1, 39, 105–107]. (In [39], it was stated that R and R^{-1} correspond to the same ρ value without supporting information. In [105], a R value <1 appeared, being chosen for analysing SFG-VS data for the CH_3 groups at the DMSO aqueous solution interface. In [1, 107], $R < 1$ were used for SFG-VS analysis of the NH_3 aqueous solution interface. This latter case was simply caused by using the Raman polarizability tensor data from reference [106], which misplaced the α_{xx} and α_{zz} values.) It is clear from equation (21) that the product of these two R values is $(Q^2 - 1)/(Q^2 - 4)$. Of course, when Q is large, this value approaches to unity, as indicated in some SFG-VS literature [39]. The reason that the Raman polarization ratio along cannot determine these two R value is easy to understand. The relationship of $\alpha'_{aa} = \alpha'_{bb} \neq \alpha'_{cc}$ indicates that the molecular group is a symmetric top. If $R < 1$, it is a prolate symmetric top; while $R > 1$ is an oblate symmetric top. The ρ value measured in an isotropic phase is the rotational average over all possible randomly distributed molecular orientations. Therefore, it is natural that ρ is not able to tell the difference between a prolate symmetric top from a oblate symmetric top when their Raman tensor ratio R_{prolate} and R_{oblate} satisfy $R_{\text{prolate}} R_{\text{oblate}} = (Q^2 - 1)/(Q^2 - 4)$. However, when the molecule is oriented, as in the interface layer, polarization spectroscopy can easily tell whether it is a prolate top or an oblate top [59]. This is why the polarization method demonstrated by Eisenthal *et al.* works with SFG-VS polarization measurements [38].

The effectiveness of the Raman depolarization ratio ρ for determining the hyperpolarizability tensor ratio R for the C_{3v} groups relies on the following three factors: (a) the validity of equation (12); (b) the accuracy of the ρ values; (c) the R value measured in one environment, e.g. the bulk liquid, can be used for another, e.g. the interface.

The validity of equation (12) has been fairly well established [33, 36, 67]. Experiments with ordinary Raman or coherent Raman techniques have shown that the depolarization ratio ρ can be measured as accurately as 0.001 [103, 108]. Experiments have shown that the Raman polarization ratio of the –CN and –C–C– stretching vibrations in a series of cyano-biphenyl liquid crystals did not change when temperature (338 to 368 K) and pressure (0 to 150 MPa) are changed in a broad range [109–111]. For example, under different temperature and pressure, the R value of the –CN group from these measurements all fell into the range 0.26–0.27. Therefore, there is good reason to believe that the Raman depolarization ratio ρ essentially does not change from the bulk liquid to liquid interfaces, unless specific interactions greatly alter related chemical bonds.

Even though there was discussion on whether the local mode treatment of the CH_3 and CH_2 groups with C_{3v} and C_{2v} symmetries, respectively, is valid, [39, 49] it has been generally accepted in molecular spectroscopy textbook that '... in the case of C–H stretches, the high frequency of the local vibration of the C–H bond tends to uncouple that motion from that of the rest of the molecule' [112]. In addition, slight deviation from the exact C_{3v} symmetry of the CH_3 group in actual molecules can be treated with perturbations, as discussed by Hirose *et al.* [36].

With above considerations, the Raman depolarization ratio ρ obtained from experiment ought to be reliable for calculation of the R values, especially for the CH_3 group. There is no reason to attribute big uncertainties to the R values if it is obtained from the Raman depolarization measurement data, even though it is clear that the R values for different CH_3 groups cannot be transferable. For example, R for the CH_3 group in methanol is 1.7, in ethanol is 3.4, and in ethane is 1.4 [39]. These are values directly obtained from ρ values measured in Raman experiments, and can be used to quantitatively address the different SFG-VS spectral features observed from these molecules, as we shall demonstrate in section 4 [26, 43].

For the symmetric stretching modes of C_{2v} groups, such as CH_2, because generally $\beta_{aac} \neq \beta_{bbc} \neq \beta_{ccc}$, besides ρ, an additional parameter has to be employed to get the values for the two hyperpolarizability tensors: $R_a = \beta_{aac}/\beta_{ccc}$ and $R_b = \beta_{bbc}/\beta_{ccc}$. This is partly responsible for why polarization and orientational analysis of SFG-VS spectra of the CH_2 group has been scarce in the literature [26, 36, 37, 40, 41, 113]. All these works were based on the calculation of the ratio R_a and R_b with the bond polarizability derivative model.

Hirose *et al.* formulated the SFG-VS bond polarizability derivative model for calculating the hyperpolarizability tensors of the CH_3 and CH_2 groups [36, 37, 114]. (See details in Appendix B.) In this formulation, the hyperpolarizability tensor elements $\beta_{l'j'k'}$ of CH_3 group with C_{3v} symmetry or CH_2 group with C_{2v} symmetry are expressed into quantities proportional to the bond polarization derivative ratio r of a single CH bond, as defined in Appendix B [37]. Therefore, the Raman depolarization ratio ρ, the hyperpolarizability ratio R for CH_3 group, and the R_a and R_b ratios for CH_2 can be expressed as a simple function of r. With the experimentally determined ρ values, R, or R_a and R_b, can be uniquely determined for quantitative polarization analysis in SFG-VS. Therefore, in this approach by Hirose *et al.*, the value of the single bond polarizability derivative ratio r is the only parameter needed to calculate the polarization and orientational dependence in SFG-VS. All the derivation assumed

C_{3v} symmetry for the CH_3 group, and C_{2v} symmetry for the CH_2 group. Hirose *et al*. also pointed out that distortions from C_{3v} and C_{2v} symmetry can be treated with small perturbations, and the relationships should generally hold, with slightly different r values [36].

However, the formulation derived by Hirose *et al*. has not been quantitatively tested for its effectiveness in SFG-VS analysis, and its application in SFG-VS analysis has been scarce. The general validity of the bond polarizability derivative model in SFG-VS analysis has been questioned with concerns about the transferability of the r and R values [39]. We recently reevaluated the expressions given by Hirose *et al*. for the hyperpolarizability tensors. We found that they are not consistent with themselves in different publications [36, 37, 114]. Therefore, attempts to test them cannot be done without completely re-deriving the equations (see details in Appendix B). Since the R value for the CH_3 group can be directly derived from the ρ value without using the Hirose formulation, and CH_3 has been the major focus in SFG-VS studies [15], Hirose's formulation were often mentioned but not practiced in the SFG-VS literature.

On the other hand, Shen *et al*. used the bond additivity model which is essentially the same as Hirose's formulation and performed detailed quantitative SFG-VS analysis on CH_2 at a polyvinyl alcohol surface [40, 41]. In this work, Shen *et al*. used the single bond polarizability derivative ratio $r = 0.14$, which was obtained for the CH single bond in the CH_3 group in alkanes [115]. (The $r = 0.14$ value for the CH single bond in SFG-VS references [40, 41, 113] was cited in this paper. However, suggestions of this value cannot be found here.) The success of this work seems to suggest the validity of the bond polarizability derivative treatment. But since r can have different values for different CH bonds, the question of whether the bond polarizability derivative model is valid, and whether such r values can be used, needs to be addressed.

The bond polarizability derivative theory was first formulated and tested with relatively satisfactory results by D. A. Long in the 1950s to explain the relative intensities in Raman spectroscopy [116–120]. This theory was based on the simple assumption that a bond between two atoms 'has the same polarizability irrespective of environment, provided, of course, that it remains a correct representation of the bond in the molecule in question' [116]. The bond polarizability derivative, which is proportional to the square root of the Raman intensity, of a certain bond, e.g. C–H, can be empirically fitted from the observed Raman intensities. If this property is transferable between molecules, then relative Raman intensities can be predicted in another molecule [116–121]. However, later detailed experimental and theoretical studies have shown that the transferability of the bond polarizability derivative values is actually limited [115, 122–127]. Theoretical calculation have shown that the bond polarizability derivative of individual CH bond in a molecule with different positions can vary by up to 40% [127]. Therefore, the bond polarizability derivative may not be as transferable as initially hoped [116, 127]. However, it has been shown that bond polarizability derivative with similar molecular structure features may cluster at certain values, and since assignment of individual Raman peaks to particular bonds is generally out of the question, 'it is not inappropriate to use an average value for the total (Raman) intensity in the CH region' [127]. In SFG-VS, with narrower peaks, it is possible to distinguish modes belonging to the same kind of groups connected to different atoms in the molecule (see figure 10).

Therefore, it seems that the formulation by Hirose *et al*. can be valid in principle, even though the r values cannot be transferable between different molecules. Here we provide two direct examples with SFG-VS spectra from simple liquid interfaces to demonstrate that the Hirose formulation is far more effective and valid than previously thought, of course, using the re-derived expressions in Appendix B. As we shall discuss in section 4 [26, 43], SFG-VS as a vibrational spectroscopic technique is probably a more suitable technique for studying molecular group symmetry and detail vibrational spectral splitting in the condensed phase. SFG-VS spectra from liquid interfaces are generally narrower than IR and Raman spectra in the liquid phase. Molecules at the interfaces are naturally ordered, and since the interface is only molecularly thin, such a molecular path length does not disperse or rotate the SFG signal as with ordered bulk samples in the IR and Raman experiment where the light travels for a much longer optical path inside the sample. With SFG-VS as an intrinsically coherent polarization spectroscopy, these features allow SFG-VS to be truly sensitive to symmetry and spectral details, in comparison with other polarized spectroscopy techniques [59]. Therefore, SFG-VS from the interface layer should be a good ground to test the effectiveness of the bond polarizability derivative model.

The vapour/methanol interface was the first neat liquid interface to be studied with SFG [65]. The total lack of *ppp* and *sps* spectral features from the vapour/methanol interface has been well reported in the literature [65, 72–75, 77]. In figure 4, it is shown that with $\beta_1 = 37^\circ$ and $\beta_2 = 51^\circ$ co-propagating geometry, the *ppp* spectral features at $2828\,\mathrm{cm}^{-1}$ and $2940\,\mathrm{cm}^{-1}$ can be observed. Because the intensity changes between these two spectra agree well with the $R = 1.7$ value, as well as the bond polarizability derivative model with $r = 0.27$, this result quantitatively validates the $R = 1.7$ value obtained directly with the ρ and the bond polarizability calculation. The lack of features in the 2965–$2980\,\mathrm{cm}^{-1}$ region for the asymmetric stretching (*as*) mode of the CH_3 in both experimental configurations can also be fairly well explained by the small β_{aca}/β_{ccc} ratio calculated from the bond polarizability model in Appendix B.

Figure 5 presents SFG-VS spectra taken in the $\beta_1 = 60^\circ$ and $\beta_2 = 55^\circ$ co-propagating geometry on vapour/methanol and vapour/ethanol interfaces [43]. On the *ppp* and *sps* spectra, the CH_3 asymmetric stretching around $2965\,\mathrm{cm}^{-1}$ for methanol is more than an order weaker than that for ethanol. These cannot be explained by the different orientations of the CH_3 groups at the two interfaces. However, it can be explained with the bond polarizability derivative model, with the different r values calculated from the different experimental ρ values. Using the expressions in Appendix B, for methanol, $\beta_{aca}/\beta_{ccc} = 1.0$, while for ethanol $\beta_{aca}/\beta_{ccc} = 3.4$. Therefore, with the same orientation of CH_3 and with close β_{ccc} values, the *as* SFG-VS peak intensities for methanol on *ppp* and *sps* have to be $(3.4)^2 = 12$ times weaker than those for the vapour/ethanol interface, where the *as* peaks at $2965\,\mathrm{cm}^{-1}$ are pronounced features on both *ppp* and *sps* spectra. The interference features around $2965\,\mathrm{cm}^{-1}$ on *ssp* spectra for the ethanol interface is also observed. These effects can all be quantitatively analysed with the known R values and with the bond polarizability derivative formulation [101]. These results clearly indicate that the bond polarizability model is fairly effective and valid in quantitative analysis of SFG-VS spectra. It also indicates that the r values for the single CH bond cannot be directly transferred between different molecules

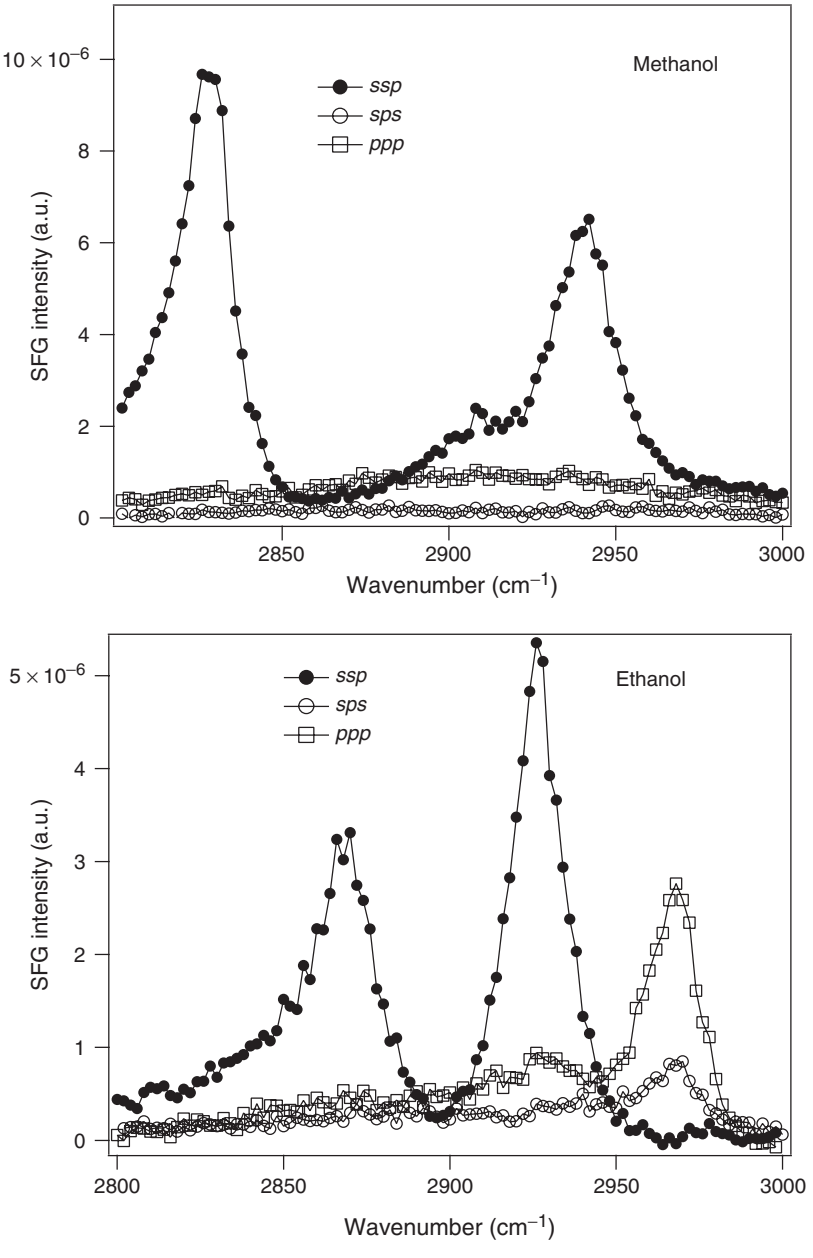

Figure 5. SFG-VS spectra of the vapour/methanol and vapour/ethanol interface with $\beta_1 = 60^\circ$ and $\beta_2 = 55^\circ$ in co-propagating geometry. Assignments of the peaks can be found in table 4 [43].

in SFG-VS studies. This latter point suggests that one can use SFG-VS spectra to distinguish CH bonds with different bond polarizability derivative values.

The relative intensity of the 2828 cm^{-1} peak for vapour/methanol and the 2870 cm^{-1} peak for the vapour/ethanol interface belongs to the CH_3 group in methanol and

ethanol, respectively [43]. The single bond CH has $r = 0.27$, and the CH_3 group has $R = 1.7$ for the methanol molecule; while for the ethanol molecule, $r = 0.025$ and $R = 3.4$. Since their relative intensity is about 2.8, calculation of their intensity, group orientation angle, and comparison with equation (39) show that $\beta_{ccc}^{\mathrm{CH,\,methanol}}/\beta_{ccc}^{\mathrm{CH,\,ethanol}} = 0.70$ [101], if their transition dipole moments are held with close values. This quantitatively explains the difference of the CH bond between methanol and ethanol CH_3 groups. With larger $\alpha'_{\xi\xi}$ values perpendicular to the CH bond in methanol, its $\alpha'_{\zeta\zeta}$ is smaller, therefore its $\beta_{ccc}^{\mathrm{CH,\,methanol}}$ value is also smaller than those for ethanol. The results indicate that quantitative comparison of the bond polarizability derivative values in different molecules is possible, and most importantly, such detailed comparison of the different CH bonds in methanol and ethanol can be used as one of the examples for the success of the bond polarizability derivative model.

In section 4.2, comparison of SFG-VS spectra of vapour/ethylene glycol (EG) interfaces in different incident angle sets will also help demonstrate the effectiveness of the bond polarizability derivative model for SFG-VS.

In practice, r can sometimes be used as a fitting parameter when there are enough independently measured SFG-VS intensities in different polarizations. Shen *et al.* demonstrated that the r value thus obtained was generally consistent with the r value obtained from the Raman polarization ratio measurement [22].

In summary, the bond polarizability derivative model formulated by Hirose *et al.* is generally effective and valid in quantitatively describing major aspects of SFG-VS spectra in detail. The bond polarizability derivative ratio r and hyperpolarizability ratio R obtained from the Raman depolarization ratio can be used in SFG-VS spectral analysis. Even though these ratios cannot be simply transferred to different molecules, a CH bond with similar structure properties can have similar r values. On these grounds, the same r value can be used for interpretation of SFG-VS spectra of groups with similar CH bonds in different molecules.

With better understanding of the problems associated with the local field factors and bond polarization model in the above sections, better quantitative polarization and orientational analyses can be achieved with SFG-VS studies. In the following sections we shall discuss problems on the application of quantitative orientational analysis and spectral analysis of SFG-VS for more complex molecular interfaces.

3.5. *Approach to complex molecular interfaces with the accurately measured orientational parameter D*

Here we try to provide an approach to use the accurately measured D values for orientational analysis of complex molecular interfaces.

With the ability to accurately measure the orientational parameter $D = \langle\cos\theta\rangle/\langle\cos^3\theta\rangle$ in SFG-VS, the orientational order of the molecular interfaces can be further illustrated. In section 3.1 we have discussed how to used the PNA method to measure small changes in D for molecular interfaces. Now we shall discuss the basic properties of D and its implications for understanding orientational order of complex molecular interfaces.

Simpson and Rowlen's elegant work discussed the properties of the orientational parameter D in SHG studies [56, 57]. By associating D with the first and third

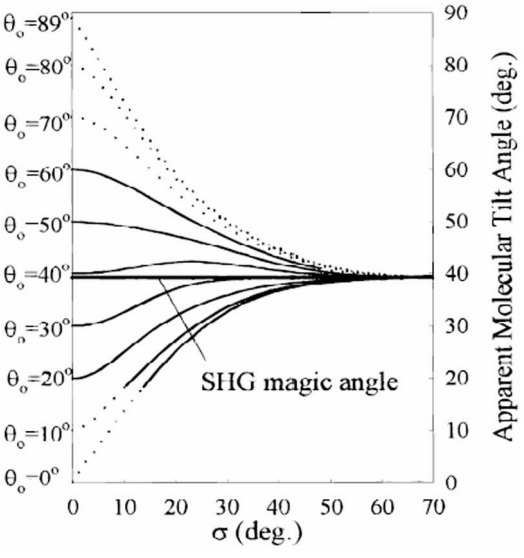

Figure 6. The apparent molecular tilt angle (calculated by assuming a δ-function distribution) as a distribution function of the root-mean-square width σ of a Gaussian distribution function. Each curve corresponds to a centre orientational angle θ_0. The straight line at 39.2 is the magic angle. Reproduced with permission from J. Am. Chem. Soc. 1999, **121**, 2635–2636. Copyright 1999 Am. Chem. Soc. [56].

orientational order parameters of molecular films, they raised awareness of the molecular orientational distribution for the SHG with the concept of the 'magic angle' in calculating molecular orientation angles with the D values (figure 6) [56]. To put it simply, a single value of D can be determined from a SHG or SFG experiment, but it cannot be used to uniquely determine both the orientational angle and its distribution width, even if the distribution function is known.

To address these problems, our laboratory recently developed the concept of a *general orientational parameter c* and formulated the *orientational functional* $R(\theta)$ in SHG and SFG-VS to determine both the orientation and orientational distribution width in the Langmuir monolayer with polarized SHG measurements [23]. This formulation, briefly presented in section 2.2.2, was applied to formulate the PNA method in SHG [23] and SFG-VS [24, 25], and was applied to develop the polarization selection rules for SFG-VS vibrational spectral assignment [26].

As discussed by Simpson and Rowlen [56] in figure 6, if one assumes a δ-distribution function for the orientational angle θ, then the value $D = 5/3$ gives a 'magic angle' at 39.2°. The apparent tilt angle θ is the *theta* value directly calculated from $D = 1/\cos^2\theta$, i.e. assuming a δ-distribution function of θ. However, this 'magic angle' corresponds to a broad range of $[\theta_0, \sigma]$ pairs as shown in figure 6. The existence of such a 'magic angle' does not imply that the D value alone can never give narrow distributions of the tilt angle θ. From figure 6 one can easily find that when the apparent θ is close to 0° (upright orientation) or 90° (lying flat at the interface), the distribution width σ can only have a small upper limit value, indicating that only a narrow distribution can be allowed for these D values.

It is to be noted that in our formulation, in order to be in line with the definition of the *general orientational parameter c*, the definition of D is the inversion of the D defined by Simpson and Rowlen [23, 56]. This difference does not affect any of the analysis.

With the basic understanding of the behaviour of D from Simpson and Rowlen's work, now we can discuss more interesting properties of the orientational parameter D, and its implications in understanding the orientational order of complex molecular interfaces.

From the definition of the orientational average denoted by $\langle\ \rangle$, the ensemble average $\langle\cos\theta\rangle$ and $\langle\cos^3\theta\rangle$ are equivalent to the summation of $\cos\theta$ and $\cos^3\theta$ for each individual molecular group divided by the total number of molecular groups, respectively. Therefore, we have

$$D = \frac{\langle\cos\theta\rangle}{\langle\cos^3\theta\rangle} = \frac{(1/N_s)\sum_i \cos\theta_i}{(1/N_s)\sum_i \cos^3\theta_i}. \tag{22}$$

The summation i is over each molecular group at the interface under study. Therefore, $\sum_i = N_s$. If the same kind of molecular groups have two distinct orientations in the interface layer, then we can let $N_s = N_1 + N_2$; the mole fraction of one of the two groups is $x = N_1/N_s$ $(0 \le x \le 1)$, and θ_1 and θ_2 as the tilt angles from the interface normal of the two groups, respectively, in equation (22). We have

$$D = \frac{x\langle\cos\theta_1\rangle + (1-x)\langle\cos\theta_2\rangle}{x\langle\cos^3\theta_1\rangle + (1-x)\langle\cos^3\theta_2\rangle}. \tag{23}$$

As shown in figure 7, left, equation (23) can be used to investigate the situation when the same molecular group at the interface can assume two distinct orientations. We came upon this formulation when we could not explain $D < 1$ values with the single orientation picture, no matter what distribution width is assumed. For the CH_3 groups at the vapour/acetone interface, PNA measurement gives $D = 0.83 \pm 0.05$ [80]. If a single distribution function for the tilting angle θ is assumed, $D < 1$ would be impossible. If there are two distinct oriented CH_3 groups, then a broad orientational distribution of the interfacial acetone molecules is not possible. So we have to reach for the picture of two distinct orientations with a relatively narrow distribution width for the CH_3 groups at the vapour/acetone interface.

Analysis of equation (23) indicates that since generally $|\langle\cos\theta\rangle| > |\langle\cos^3\theta\rangle|$, in order to have $D < 1$ from equation (23), $\langle\cos\theta_1\rangle/\langle\cos^3\theta_1\rangle$ has to be close to unity, and $\langle\cos\theta_2\rangle$ has to have opposite sign for $\langle\cos\theta_1\rangle$, so as to make $|x\langle\cos\theta_1\rangle + (1-x)\langle\cos\theta_2\rangle|$ smaller than $|x\langle\cos^3\theta_1\rangle + (1-x)\langle\cos^3\theta_2\rangle|$. Thus, for the two CH_3 groups in acetone, one has to point up close to the interface normal, while the other has to point into the bulk liquid phase. With a narrow orientational distribution, if the value of Δ can be determined in $\theta_2 = \theta_1 + \Delta$, equation (23) gives a unique set of $[\theta_1, \theta_2]$ values. For the vapour/acetone interface, MD simulation suggests the molecular plane is perpendicular to the interface [70]. Therefore, one can have $\Delta = 117.2^\circ$ as the C–C–C bond angle, and the calculation

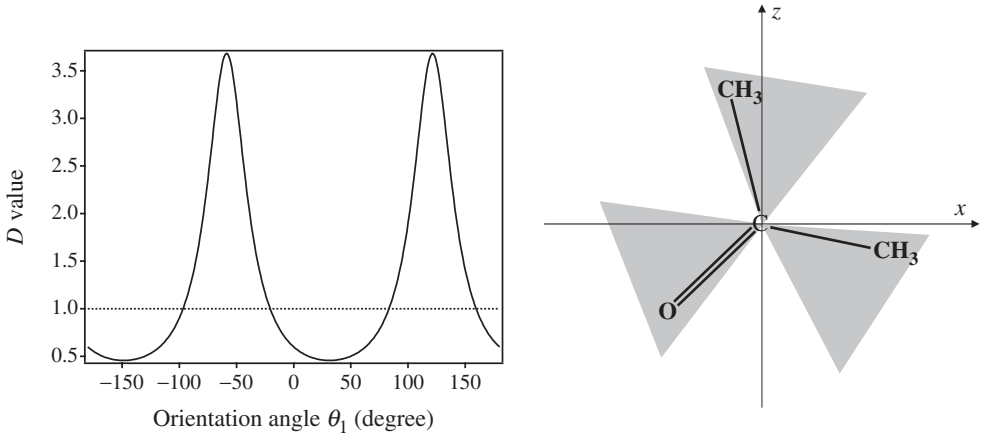

Figure 7. Left: When $\theta_2 = \theta_1 + \Delta$ and both θ_1 and θ_2 have a δ-distribution, D values in equation (23) can be smaller than unity. This feature for D has not been discussed before. If there is only one unique orientational distribution, D should always be larger than unity. In this plot, we put $x = 0.5$ and $\Delta = 117.2^\circ$, which is the angle between the two methyl groups in the acetone molecule. Right: Angular distribution of acetone at the vapour/acetone interface. The molecule illustrates the orientation with a δ-distribution function of θ_1 and θ_2, while the shadowed part represents the mathematically allowed range by simulation with a Gaussian distribution function [78, 79].

from equation (23) gives $\theta_1 = -14.4^\circ \pm 1.9^\circ$ and $\theta_2 = 102.8^\circ \pm 1.9^\circ$, if the δ-distribution function is assumed (figure 7, right).

Then what about some D value slightly larger than unity?

For CH_3 at the vapour/DMSO interface, we measured $D = 1.14 \pm 0.04$ [101]. From figure 6, we know that the distribution width σ of the tilt angle θ cannot be more than 17° in order to satisfy this D value, if a single distribution is assumed. Because the angle between the two CH_3 groups in a DMSO molecule is 97.4°, like the vapour/acetone interface, the two CH_3 groups in DMSO have to have two distinct orientations with a certain distribution width σ close to 17°. These two orientations together have to satisfy the value $D = 1.14 \pm 0.04$ through equation (23). Since one cannot make simple assumptions about the Δ value for DMSO without additional information, no values of θ_1 and θ_2 can be uniquely determined for the moment. But from equation (23), in order to satisfy $D = 1.14 \pm 0.04$, θ_1 has to be closer to the interface normal, while θ_2 is somewhere close to the interface, possibly but not necessarily to point into the bulk liquid DMSO phase. On the other hand, the CH_3 symmetric stretching vibrational peak is unusually strong in the *ssp* spectrum [105, 128]; this also indicates that the CH_3 orientation distribution at the vapour/DMSO interface has to be quite narrow.

The two uniquely oriented CH_3 groups at the vapour/acetone and vapour/DMSO interfaces cannot be differentiated from their SFG-VS spectra. Even though they may be in different chemical environments and experience different interactions at the interfaces due to their unique orientation, the splitting is not big enough to be observed from their SFG-VS spectra. However, the accurately measured D values from the PNA method with SFG-VS revealed their unique orientation conformations.

Similarly, the orientational order of the vapour/tert-butanol interface can be analysed. SFG-VS measurement gives $D = 1.32 \pm 0.06$ [101], which also indicates a well ordered interface, since a randomly ordered interface should give a much larger D value. Since each tert-butanol molecule has three CH_3 groups, equation (22) has to be formulated for three distinct oriented CH_3 groups. However, analysis suggests that no matter how we place the molecule, two of the three CH_3 groups have to have close orientation angles. Therefore, to have $x = 1/3$ or $2/3$ in equation (23) might be a good approximation to describe the orientational order of the vapour/tert-butanol interface. This fact implies that for complex molecular interfaces, treatment with more than two or three distinct orientation distributions may not be necessary, even though the assumption for a single orientation distribution seems to be too simple.

If the D values of two or more different groups in an interface layer can be measured, more information on the interface orientational and conformational order can be determined, because with D value of one group can already provide so much information. Mapping the order parameters of different molecular groups in the molecular layer may lead to discoveries of novel physics and chemistry at complex interfaces.

SFG-VS investigation on polymer interfaces has been a growing field because of their importance in material sciences and implications to biological membrane studies [17]. With the general formulation of D in equations (22) and (23), information on the orientational order of more complex molecular interfaces can be similarly extracted. Clearly, the terms in equation (22) can be grouped into more than two distinct orientated groups, but it seems that to have more than two or three distinct oriented groups is indeed not necessary. Analysis of such complex interfaces certainly requires other independently obtainable information or statistically theoretical treatment. Nevertheless, accurately measured D values of different molecular groups at such an interface are very important. For example, now we could measure D values for both CH_3 and –C=O groups at PMMA and PMA polymer interfaces [101]. More effort is certainly needed to explain these data. However, it is certain that the formulation and analysis discussed here will help shed new light on our understanding of the orientational order at complex molecular interfaces.

Finally, it is to be noted that the D value obtained from PNA and PIR methods depends on the values of the local field factors in the interface layer. Knowledge of these values for a particular interface has to be obtained as discussed in section 3.3.

4. SFG-VS: a unique vibrational spectroscopy

It is important to realize that SFG-VS is not simply a vibrational spectroscopy method for interface studies, but also a vibrational spectroscopy technique with many advantages for the study of molecular vibrational spectroscopy in the condensed phases. SFG-VS can provide detailed information on molecular vibrational spectroscopy in general.

Since the SFG-VS spectral intensity depends on many parameters, as we have discussed in previous sections, interpretation of the congested SFG-VS spectra from complex molecular interfaces has been difficult. Along with technical difficulties

in handling complex laser systems in the research laboratory, interface studies with SFG-VS have been mainly conducted on relatively simple molecular interfaces of fundamental and technological importance until most recently [15, 19]. These parameters determining the SFG-VS spectral intensity include polarization configuration, geometry of optical arrangement, the local field factors in the interface layer, symmetry properties of the molecular groups under investigation, and the hyperpolarizability tensor ratios. The discussions above show that these parameters can be fairly well understood, and quantitative analysis of SFG-VS can be well established for the simple interfaces. On these bases, more complex SFG-VS spectra can be better understood.

The first step to understanding SFG-VS spectra is to have an accurate assignment of the spectral peaks. The common practice for spectral assignment in SFG-VS studies has been to compare the spectrum with the IR and Raman results in the bulk media [13, 48, 129–132], and sometimes assisted with *ab initio* calculations of the IR or Raman band positions of free molecules in the gas phase [13, 39]. This is the natural approach because the selection rules of SFG dictate that any sum frequency active molecular vibrational mode has to be both IR and Raman active as dictated by equation (12) [33]. The above practice has been able to address major SFG-VS spectral features and has been reasonably successful in SFG-VS studies. Thus, the general consensus has been that '... there is no simple relationship between observed peak positions and intensities (in the SFG spectrum) and the properties of the underline modes, and the parameters can be extracted by curve fitting' [13]. This situation has lasted and has left the assignment of complex SFG-VS spectra subject to the difficulties and errors of the common IR and Raman studies.

If one looks into this matter closely, however, it is not hard to find the logical flaw in the spectral fitting approach in SFG-VS, because almost all SFG-VS spectra in the CH stretching vibration region, i.e. around 2800–3000 cm^{-1}, show narrower peaks and have more separated features than these of the same molecule measured with IR and Raman spectroscopy in the condensed phase [7, 26, 43]. This is due to the relatively much more ordered interfacial structure and the less dynamic nature of the interactions of the molecules at the interface than that in the condensed phase under the same ambient conditions [7, 30, 133, 134]. Consequently, some of these features could not be accounted for by the existing IR and Raman assignments [7, 26, 43]. For example, even though we generally know that the 2800–3000 cm^{-1} region belongs to the CH stretching vibrational modes in IR and Raman spectroscopy, the features in SFG-VS spectra of vapour/1-heptanol and vapour/1-octanol interfaces in figure 12 cannot be clearly assigned with knowledge only from IR and Raman assignments [43]. The difficulty in the practice of SFG-VS with knowledge only from IR and Raman spectroscopy calls for methods which can provide effective and '*in situ*' assignment on SFG-VS spectrum.

In IR and Raman spectroscopy, knowledge of the symmetry property, i.e. polarization property, of each vibrational peak is crucial for determination of its symmetry category, leading to explicit assignment of the spectra [135]. The ability to perform polarization measurements on oriented molecular samples is the key to success in spectral assignment [59]. However, it is generally difficult to prepare a well ordered molecular sample for such spectroscopic measurement. In previous IR or Raman studies, because of the inhomogeneous broadening effect in liquid or solid samples,

many vibrational spectral details can only emerge well below liquid hydrogen temperature with crystalline samples where the spectral line broadening is greatly suppressed [136–139]. Another disadvantage for an ordered crystalline sample is that it may add optical rotation to the polarization of the optical beam, making it difficult for accurate polarization measurement of the weak spectra. Therefore, the symmetry properties of many weaker peaks and overlapping peaks have not been well characterized in IR and Raman spectroscopy.

Since SFG-VS is by nature a polarization spectroscopic technique, and the molecules at the liquid interface are naturally ordered due to the anisotropic forces across the interfacial region, the polarization dependence in SFG-VS spectra may also be used to determine the symmetry property of each SFG-VS spectral peak. Additionally, since the interface layer is just molecularly thin, the refractive SFG-VS signal is not subject to optical rotation once we leave the interface. SFG-VS also has a stronger polarization dependence than IR and Raman spectroscopy, because as a second-order non-linear process, SFG-VS, whose $|\chi^{(2)}_{\text{eff}}|^2$ is a function of higher orders of $\cos\theta$ function than the linear absorption and Raman processes, has to be more sensitive to molecular orientation [23, 53, 59]. Because of these unique properties of SFG-VS, assignment from IR and Raman spectroscopy may not be enough to assign SFG-VS spectra. In order to avoid such limitations, it is better to have a set of selection rules for SFG-VS spectral assignment, and they can be used along with knowledge from IR and Raman studies.

The review of the practices in SFG-VS above indicated that polarization dependence has not been generally considered in assigning SFG-VS spectra. There has been work using SFG-VS intensities [22, 40] and orientation analysis [107] for deducing the orientational angle or the hyperpolarizability ratio of certain functional groups. But it is rare to use the spectral intensity relationship between different polarization configurations to help spectral assignments [86]. Only very recently, polarization selection rules in SFG-VS have been systematically attempted to help SFG-VS spectral assignment on CH_3, CH_2 and CH groups in the 2800–3000 cm^{-1} region [26, 43]. These studies demonstrate the importance and usefulness of SFG-VS polarization selection rules. Not only can many ambiguous assignments in SFG-VS spectra be addressed, but also some new spectral features and some incorrectly or ambiguously assigned peaks in the IR and Raman regime can be clarified. One such example is that of the 2940 cm^{-1} peak for the ethylene glycol (EG) molecule, which has long been considered an asymmetric C–H stretching mode in the literature [5, 26, 35, 140, 141]; it has been unambiguously identified as the Fermi resonance peak of the EG methylene symmetric stretching mode through SFG-VS polarization selection rules, and in addition, through measurement and analysis with four different sets of incident angles, as shown in figure 9 and the discussions in section 4.2.

It has been shown that SFG-VS polarization selection rules can help assignments on complex SFG-VS spectra [43]. This is one important step for its application to complex interfaces such as polymeric and bio-membrane surfaces. Using these selection rules, IR and Raman assignments can also be validated or corrected. These aspects make SFG-VS a unique vibrational spectroscopy not only for interface studies, but also for general vibrational spectral assignment purposes.

In this section, the polarization selection rules for SFG-VS are presented based on the formulation in section 2.2.3. Using these selection rules, SFG-VS spectra

of a series of vapour/liquid interfaces in the 2800–3000 cm^{-1} region are assigned, and some general considerations on related problems in IR and Raman assignments are also discussed.

4.1. *SFG-VS: molecular symmetry and polarization selection rules*

Polarization selection rules or guidelines in SFG-VS spectral analysis can be derived for molecular groups with different symmetry properties. This is based on the simple idea that vibrational peaks belonging to different symmetry types do not have the same polarization dependence in SFG-VS spectra. These rules help greatly to determine the symmetry types of vibrational modes with SFG-VS spectra in different polarizations. These rules allow the assignment of SFG-VS spectra *in situ*, i.e. with their own selection rules directly applied to SFG data, instead of *ex situ*, i.e. depending only on transferable knowledge from the IR and Raman assignments.

Even though the SFG-VS spectral intensity depends on many parameters, there are some generally held polarization dependence relationships, and they can be abstracted as rules or guidelines for SFG-VS spectral assignment. Since the function $d^2R(\theta)$ in equation (14) is responsible for the molecular contribution to the SFG-VS intensity, the d and c values for each vibrational modes of CH_3, CH_2 and CH groups in different polarization configurations can be evaluated, and the function $d^2R(\theta)$ can be evaluated against different orientational angles θ. Table 3 lists all the corresponding d and c values calculated using the parameters in table 2. In order to see the polarization selection rules for these three groups, each $d^2R(\theta)$ function is plotted against θ with a δ-distribution function in figure 8.

From table 3 and figure 8, some general relationship can be abstracted, and the following polarization selection rules (guidelines) can be reached.

For CH_3 groups, the polarization selection rules are:

(a) For the *ss* mode, the *ssp* intensity is always many times that for *ppp*, as well as for *sps* and *pss*.
(b) For the *as* mode, the *ppp* intensity is always many times that for *ssp*, and both of them would be largest when $\theta = 54.7^\circ$.
(c) For small θ, the *sps* and *pss* intensity is the largest for the *as* mode, and the smallest for the *ss* mode.
(d) In *ssp* spectra, the *as* mode would negatively interfere with the *ss* mode when their frequencies overlap.

Table 2. Refractive indices used in calculating d and c values plotted in figure 8. The refractive indices used for CH_3 and CH are intended for the *n*-normal alcohols; while the refractive indices used for CH_2 are intended for the diols. $n'(\omega)$ is calculated with the Lorentz model given by Shen *et al.* [22].

	CH_3 or CH			CH_2		
Group	ω	ω_1	ω_2	ω	ω_1	ω_2
$n_1(\omega_i)$	1.0	1.0	1.0	1.0	1.0	1.0
$n_2(\omega_i)$	1.36	1.36	1.36	1.44	1.44	1.44
$n'(\omega_i)$	1.16	1.16	1.16	1.18	1.18	1.18

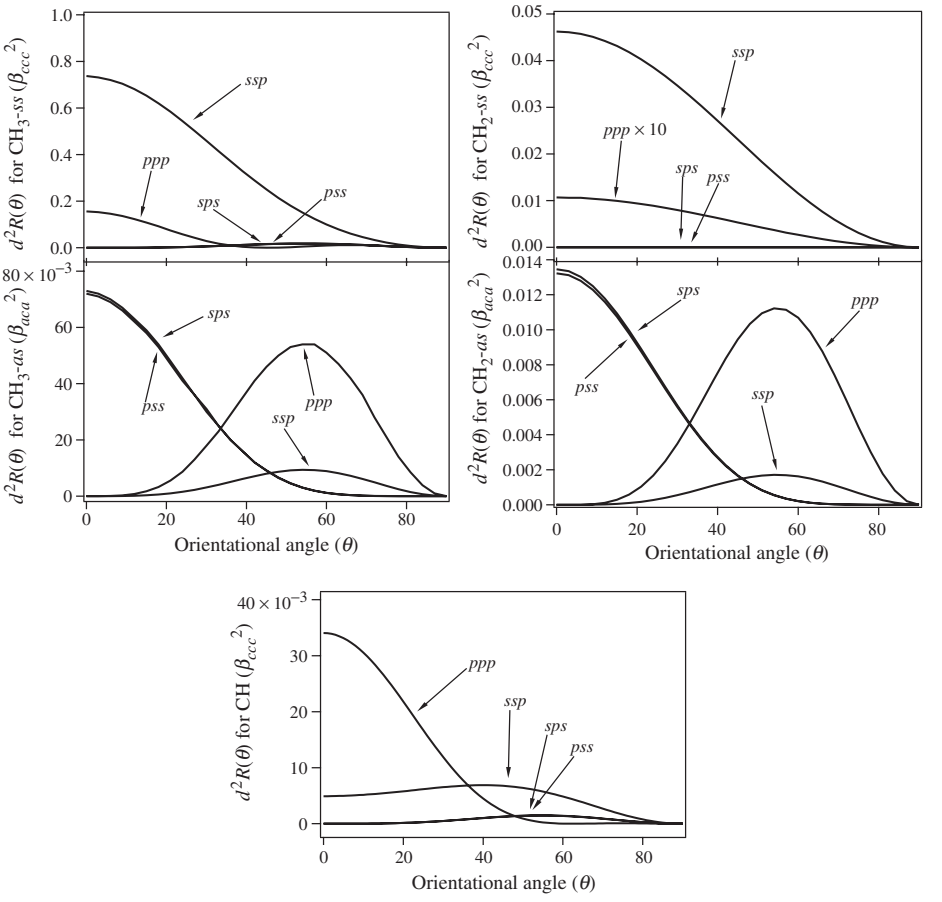

Figure 8. Polarization and symmetry dependence of symmetric and asymmetric stretching vibrational modes of CH_3, CH_2 and CH groups [26, 43]. $R = 3.4$ was used for CH_3 group, $r = 0.27$ for CH group. For CH_2, all r give the same plot in figure 8. All calculations are with $\beta_1 = 60^\circ$ and $\beta_2 = 55^\circ$ in the co-propagating geometry. Each curve is plotted against the orientational angle θ of the symmetry axis of the group. The units of SFG intensities are in $(\beta_{ccc})^2$ or $(\beta_{aca})^2$ of each individual group. Their relative intensity can be compared with the bond polarizability derivative calculations in Appendix B, and they are consistent with the experimental intensities [26, 43].

For the CH_2 group, the polarization selection rules are:

(e) No *ss* peak appears in *sps* and *pss* spectra.
(f) The *ssp-ss* intensity is always many times that of *ppp-ss*.
(g) Peaks in the *sps* and *pss* spectra generally come from the *as* mode with a relatively small tilt angle θ.
(h) For the *as* mode, the *ppp* intensity is always several times that of *ssp*. That is to say, if there is any peak which is stronger in the *ssp* than *ppp* spectra, it cannot be from the *as* mode.
(i) In the *ssp* spectra, the *ss* and *as* modes of the CH_2 groups with similar orientation negatively interfere with each other.

Table 3. d and c values for stretching vibrational modes for CH_3, CH_2 and CH groups. The units for d values are β_{ccc} or β_{aca} of each group for the symmetric stretching (*ss*) or asymmetric stretching (*as*) modes, respectively. The CH group does not have an *as* vibrational mode.

Modes		*ss*				*as*			
Group		*ssp*	*ppp*	*sps*	*pss*	*ssp*	*ppp*	*sps*	*pss*
CH_3	d	0.56	0.37	−0.33	−0.32	−0.13	0.31	−0.14*	−0.14*
	c	−0.55	2.0	1	1	1	1.0	∞	∞
CH_2	d	0.22	0.033	0.0	0.0	−0.11	0.28	−0.12*	−0.12*
	c	0	0	1	1	1	1.0	∞	∞
CH	d	0.16	−0.050	0.10	0.10				
	c	0.58	4.7	1	1				

The values listed with * are d*c values for $c = \infty$, in order to keep the general form for $R(\theta)$ in equation (15). $c = \infty$ means there is only $\langle \cos^3 \theta \rangle$ terms. All d and c values are calculated with the corresponding refractive index values listed in table 2 with $\beta_1 = 60^\circ$ and $\beta_2 = 55^\circ$ in co-propagating geometry. From [26, 43].

For CH group, the polarization selection rules are:

(j) The *ppp* intensity is strongest when θ is at smaller angles.
(k) The *ssp* intensity is strongest when θ is at large angles.
(l) The *sps* (*pss*) intensities are comparable to the *ssp* intensity when the R value is small.

These rules are simple, but useful when try to assign SFG-VS spectra. Even though these rules are drawn with the assumption of a δ-distribution function for θ, they generally hold for cases with a broad orientational distribution. The average over a distribution width is equivalent to taking a portion of each curve in figure 8 and making a normalized integration; it is easy to show that the general relationship between the curves does not change significantly. Therefore, similar polarization dependent relationships remain. The same goes for the change of incident angle geometry in the calculation. Because the ratio of the Fresnel factors in different directions does not change that much when incident angles are changed, the basic relationship between the curves does not change significantly, either. These facts underline the robustness of the polarization selection relationships, which can be generally used as rules or guidelines for assignment of SFG-VS spectra.

The rules are similar for the CH_3 and CH_2 groups except for some minor differences [26, 43]. The calculation for the CH_3 group used parameters for ethanol and longer chain *n*-alcohols. It is important to note that for methanol, those parameter are different, i.e. $R = 1.7$ with $r = 0.27$, $n_2(\omega_i) = 1.33$ and $n'(\omega_i) = 1.15$. Calculation shows that as long as $R > 1$, the differences of these parameters lead to different d and c values, but they do not alter the polarization selection rules listed above for CH_3 groups. The validity of the polarization selection rules with different experimental configurations, different parameters, and non-δ orientational distribution functions have been discussed in detail [26]. The conclusion with a similar treatment is that the polarization selection rules do hold for the CH_3, CH_2 and CH groups in varying experimental configurations and the parameters within broad physically allowed ranges. This further supports the qualitative assessments in the previous paragraph.

Dielectric constants and local field factors of metal or electrochemical interfaces are very different from those for dielectric interfaces discussed in this report. Polarization dependence of SFG and SHG for adsorbates at metal or electrochemical interfaces is usually dominated with *ppp* signals [142–144], even though sometimes the *ssp* signal can be comparable and significant [85]. The SFG spectrum is also complicated by the interference between the substrate and molecular contributions. Certainly the polarization selection rules derived for dielectric interfaces are not generally applicable to these interfaces without specific adjustments and modifications.

Even though the basic selections rules are similar for CH_3 and CH_2, it has not hard to distinguish these group frequencies in IR and Raman spectra [145–147]. Therefore, to distinguish CH_3 and CH_2 group peaks is generally not so difficult. However, there are many Fermi resonances in the CH stretching vibration region, especially for the CH_2 groups [136]. The position and intensity of the Fermi resonance modes and the asymmetric stretching modes are usually complex, and they usually overlap with each other and cannot be simply distinguished [136]. The polarization selection rules are most useful for identifying these CH_3 and CH_2 modes, since the symmetric Fermi modes follow completely different polarization selection rules from the asymmetric modes.

It is to be noted that rules (e)–(i) for CH_2 group have more twist. Unlike CH_3 and CH groups which have a freedom of rotation around their symmetrical axis, the CH_2 group cannot rotate around its C_2 symmetrical axis if the bone structure of the molecule assumes a particular orientation. Therefore, the rotational average over the ψ angle with the Euler transformation in equation (10) cannot be treated as ψ rotationally isotropic. This certainly modifies some of the selection rules for the CH_2 group. For example, the *ss* mode might appear in the *sps* and *pss* spectra with small intensities. Therefore, even though the effect is very weak, and the *sps* and *pss* spectra are usually very small, rule (a) and rule (c) are certainly weakened. Nevertheless, the selection rules frequently used in the determination of the *ss* mode and *as* mode in *ssp* and *ppp* polarization, i.e. rules (b) and (d), remain unaffected. We shall return to this point in section 4.2 with SFG-VS spectra for the vapour/ethelene glycol interfaces, and show how quantitative information can be abstracted.

4.2. *Assignment of SFG-VS spectrum for vapour/liquid interfaces*

Here detailed examples applying the polarization selection rules on SFG-VS spectra of a series of vapour/neat liquid interfaces are presented.

It is well known that in IR and Raman studies that the CH stretching spectra in the 2800–3000 cm^{-1} region are notoriously complex due to the congestion of the symmetric, asymmetric and Fermi resonance modes, which are quite sensitive to the specific couplings of conformational and environmental influences [136–138, 148, 149]. Snyder and Strauss *et al*. have carefully studied these modes in alkanes and polymethanes, and their results have been generally used in SFG-VS spectral assignments [136–138, 148, 149]. These practice have been generally successful, but difficulties come for many features which do not generally exhibit clear features (buried in broad peaks) in IR and Raman spectra as the reasons discussed above. We listed more than 40 such examples in SFG-VS assignment in the supporting information in a recent publication [26]. Among them, there are many ambiguities and probably mistakes

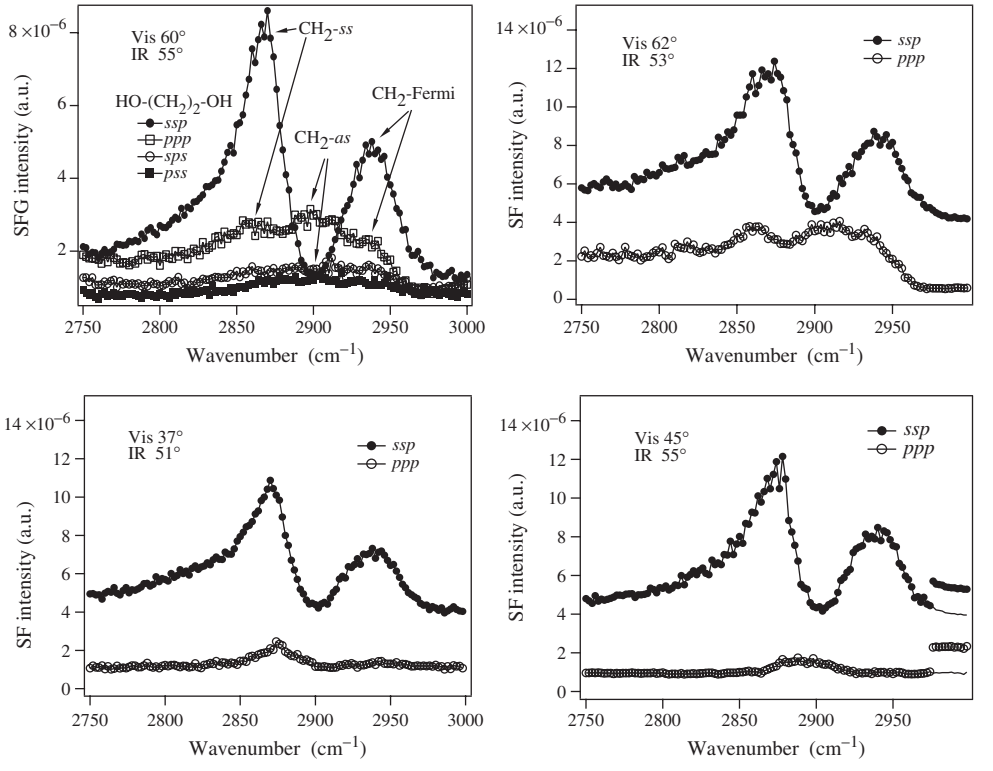

Figure 9. SFG-VS spectra of the vapour/ethylene glycol interface at four incident angle sets in co-propagating geometry [26, 81].

on assigning the related SFG-VS spectral peaks, especially for the Fermi resonance and *as* modes for the CH_2 groups. The CH_2 modes have been most troublesome in terms of spectral assignment, and we have to deal with them with CH_2-only model molecules such as diols.

The polarization selection rules for CH_2 help greatly in understanding the SFG-VS spectrum of the CH_2 group vibrational modes. Figures 9 and 10 show SFG-VS for a few CH_2-only interfaces. SFG-VS spectra of ethylene glycol (EG) at vapour/liquid and liquid/solid interfaces were reported before [5, 35, 140, 141]. In these studies, the $2940\,cm^{-1}$ peak in the *ssp* spectra was assigned to the CH_2-*as* mode as usual. However, assignments of SFG-VS spectra of vapour/EG and two other vapour/diol interfaces according to the polarization selection rules are in figures 9 and 10. According to rule (f), this $2940\,cm^{-1}$ peak on the *ssp* spectrum must belong to a *ss* mode as identified as the CH_2-Fermi-*ss* mode; while the CH_2-*as* mode is about $2900\,cm^{-1}$, which appears clearly on the *ppp* spectrum, and it is in opposite phase to the CH_2-*ss* peaks at $2870\,cm^{-1}$ and $2940\,cm^{-1}$ on the *ssp* spectrum, as predicted exactly by rule (i) [26].

Here we can see the usefulness of the formulation of $R(\theta)$ with the d and c parameters in section 2.2 [23, 53]. Table 3 lists the $d = -0.11$, $c = 1.0$ for the CH_2-*as* mode,

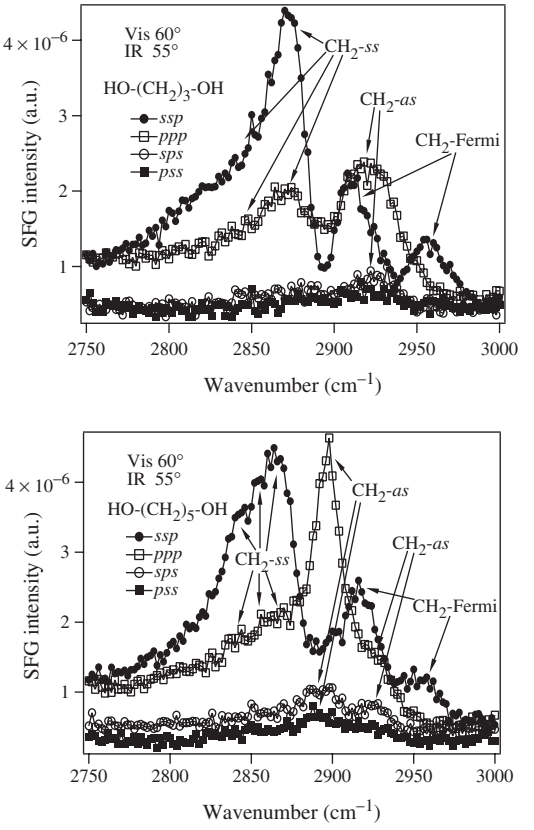

Figure 10. SFG-VS spectra of vapour/1,3-propanediol and vapour/1,5-pentanediol interfaces, with $\beta_1 = 60^\circ$ and $\beta_2 = 55^\circ$ in co-propagating geometry [26].

and $d = 0.22$, $c = 0$ for the CH_2-*ss* mode in *ssp* polarization. Therefore, these two modes should have their $dr(\theta)$ field factors in opposite phase throughout all θ values. In the mean time, in the *ppp* polarization, we have $d = 0.28$, $c = 1.0$ for the CH_2-*as* mode, and $d = 0.033$, $c = 0$ for the CH_2-*ss* mode. Therefore, these two modes have the same phase for their $dr(\theta)$ field factors. In fitting SFG-VS *ssp* spectra of the vapour/EG interface, a small peak at about 2900 cm^{-1} in opposite phase with the 2870 cm^{-1} and 2940 cm^{-1} peaks has to be included. Therefore, the detailed interference in the SFG-VS spectrum is correctly predicted by the calculated d and c values. It is important to realize that both d and $r(\theta)$, i.e. c, contribute to the sign of the phase. If $c > 1$, $r(\theta)$ changes sign when θ crosses the value $\theta = \arccos\left(c^{-1/2}\right)$. This is a very useful concept when the interference effects in complex spectra, especially in the *ppp* polarization, need to be analysed. Given the importance of the interference effect in SFG-VS spectrum analysis [150, 151], the detailed analysis with this formulation will find more applications in SFG-VS studies. Such spectral detail can be very difficult to discern without such tools. For example, from table 3, the negative interference between the CH_3-*as* mode around 2960 cm^{-1} and the tail of the CH_2 or CH_3-Fermi-*ss* in that vicinity

on the *ssp* spectrum is predicted and observed in SFG-VS spectra of the vapour/ethanol interface as in figure 5.

To further validate the assignments for the spectrum of the vapour/EG interface, SFG-VS spectra in four sets of incident angles in the co-propagating geometry were obtained in figure 9. The quantitative aspects of these spectra can be fairly well addressed with the bond polarizability derivative mode with a $r \simeq 0.3$ and a twist angle ψ around 50° [101]. This relatively large r value is consistent with the fact that the CH_2 groups are directly connected to the OH group, which increases the perpendicular polarizability derivatives of the single CH bond. The same effect was observed in the CH_3 group in the methanol molecule, which has $r = 0.27$. It seems that generally when CH_2 or CH_3 are connected to the OH group, their single bond r value should increase quite significantly.

In figure 9, in the *ppp* spectrum with $\beta_1 = 62°$ and $\beta_2 = 53°$, three peaks are clearly present; on the *ppp* spectrum with $\beta_1 = 37°$ and $\beta_2 = 51°$, only the CH_2-*ss* peak at 2870 cm^{-1} is present; while on the *ppp* spectra with $\beta_1 = 45°$ and $\beta_2 = 55°$, a small 2870 cm^{-1} overlaps with a small 2900 cm^{-1} peak. Simulation with the incident angle dependence quantitatively predicts the polarization dependence of all the peaks in figure 9. This is clear confirmation that there is essentially negligible contribution to the 2940 cm^{-1} peak on the *ssp* spectrum from the CH_2-*as* mode [101, 141].

In the four sets of SFG-VS spectra in figure 9, the polarization selection rules for CH_2 are all valid. This fact clearly indicates the robustness of these selection rules for different experimental configurations. As we mentioned above, one thing that does not fit the selection rule is that small intensities on *sps* and *pss* persist in all the spectral sets (only shown with $\beta_1 = 60°$ and $\beta_2 = 55°$ set). Usually such a small signal can be treated as noise. However, careful examination indicates that this is evidence that the twist angle ψ is not randomly distributed as discussed below.

From Appendix B, we can see that the relationship $\beta_{aac} + \beta_{bbc} - 2\beta_{ccc} = 0$ holds generally for all r values in the CH_2 group. This will make all the terms in equation (32) with $\beta_{aac} + \beta_{bbc} - 2\beta_{ccc}$ disappear. Therefore, no *sps-ss* and *pss-ss* are allowed as stated by the selection rule (e). However, with the twist angle ψ, equation (30) has to be used for CH_2-*ss* modes. The $\beta_{aac} + \beta_{bbc} - 2\beta_{ccc} = 0$ in equation (32) now becomes $2\langle\cos^2\psi\rangle\beta_{aac} + 2\langle\sin^2\psi\rangle\beta_{bbc} - 2\beta_{ccc} \neq 0$, as long as $\langle\cos^2\psi\rangle \neq \langle\sin^2\psi\rangle \neq 1/2$. However, because $\beta_{aac} + \beta_{bbc} - 2\beta_{ccc} = 0$ is still true, the value of $2\langle\cos^2\psi\rangle\beta_{aac} + 2\langle\sin^2\psi\rangle\beta_{bbc} - 2\beta_{ccc}$ has to remain small. Thus, the *sps-ss* and *pss-ss* intensity at 2870 cm^{-1} and 2940 cm^{-1} can only be very small compared to the *ssp-ss* and *ppp-ss* intensities. Therefore, the polarization selection rules regarding the *ssp* and *ppp* intensities are generally valid even if the twist angle ψ cannot be averaged out as with random rotation.

Quantitative analysis of the spectra in figures 9 and 10 can further reveal the effectiveness of the bond polarizability derivative model. One striking fact is the very strong peak around 2900 cm^{-1} in the *ppp* SFG-VS spectra for the vapour/1,5-pentanediol interface in figure 10. This peak clearly belong to the CH_2-*as* mode [26]. In each 1,5-pentanediol molecule, there are three kinds of CH_2 groups, two directly connected to the end OH groups at the α position, two on the β position, one in the centre at the γ position. Therefore, their r value should decrease as the CH_2 is further from the OH group. From the bond polarizability derivative model for CH_2 in equation (40), one has

$\beta_{aca}^{CH_2}/\beta_{ccc}^{CH_2} = 2.1(1-r)/(1+2r)$. Therefore, the bigger the r, the smaller the ratio, and vice versa. For $r=0$, the ratio is 2; for $r=0.3$, the ratio is 7/8. Since their ratios differ by 2.3 times, their SFG-VS intensities can differ by 5.3 times. Therefore, this strong peak can be quantitatively explained by bond polarizability differences between different CH_2 groups.

Using polarization selection rules, new peaks can be identified on the SFG-VS spectra. Figure 10 clearly shows that the 2920 cm^{-1} and 2955 cm^{-1} belong to the CH_2-Fermi-*ss* peaks, which was not identified previously [26]. These peaks clearly do not belong to the CH_2-*as* modes because they do not have strong peak in the *ppp* spectrum at the same wavelength. The 2920 cm^{-1} peak on the *ssp* spectra has often been assigned to the CH_2-*as* in IR and Raman, as well as SFG-VS studies [26]. Polarization selection rules for the CH_2 group clearly indicate that it is a CH_2-Fermi-*ss* in the *ssp* spectrum; while in the *ppp* spectrum there is a CH_2-*as* peak a few cm^{-1} to its left [26]. In IR and Raman spectra, these two modes generally overlap with each other, since the peaks are generally broader and the polarization dependence not as strong as in SFG-VS. It has been shown in [26] that reevaluation of SFG-VS spectral assignments for CH_2 stretching modes is warranted. Plenty of examples have shown what surprises in vibrational spectral assignment these polarization selection rules can bring us [26].

With the success of the polarization selection rules for the CH_2 vibrational stretching modes, one can move to SFG-VS spectra congested with more CH_3 and CH_2 modes. The SFG-VS spectra in *ssp* of the vapour/*n*-normal alcohol interfaces ($n = 1 \sim 8$) were reported by Stanners *et al*. [74]. Spectral assignment for the major features and orientational order of these interfaces were discussed. However, with polarization orientational analysis and the polarization selection rules, SFG-VS spectra of these interfaces in different polarizations indicate that much more detailed information can be learned from these interfaces. Figure 11 shows SFG-VS spectra of vapour/*n*-normal alcohol interfaces ($n = 1 \sim 8$) in *ssp*, *ppp*, and *sps* polarizations. All the spectral features can be identified with the selection rules. The detailed spectral assignment of the vapour/1-heptanol and vapour/1-octanol interfaces using the selection rules are presented here in figure 12 [43]. The assigned peak positions for all eight vapour/alcohol interfaces are listed in table 4 [43]. Detail discussions of these assignments can be found elsewhere [26, 43].

One thing that needs to be specially mentioned is the assignment of the spectrum for the vapour/ethanol interface in figure 5 and table 4 [43]. Its *ssp* SFG-VS spectrum was reported by Stanners *et al*. [74], and the assignments based on previous assignments from IR and Raman measurement on deuterated ethanol liquids [152, 153] are the following: the 2868, 2926 and 2970 cm^{-1} peaks were assigned to the CH_2-*ss*, CH_3-*ss* and CH_3-*as* mode, respectively [74, 154]. One big difference between ours and their assignments is whether the 2868 cm^{-1} peak belongs to CH_2-*ss* or CH_3-*ss*. Using the PIR measurement of the 2926 cm^{-1} peak, Stanners *et al*. concluded that the CH_3 group of the ethanol molecule at the interface has an orientation angle $\theta_0 < 30^\circ$. However, since the intensities of this 2926 cm^{-1} peak on *sps* and *ppp* spectra are week, PIR cannot give an accurate determination of the orientational angle, as we discussed in section 4.

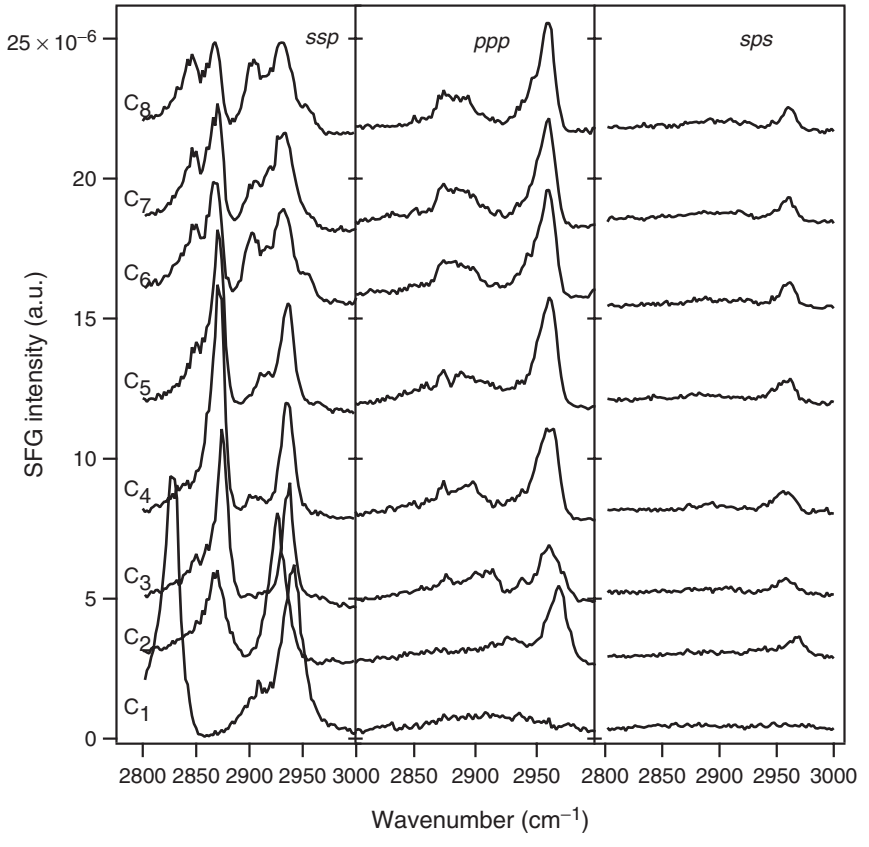

Figure 11. SFG-VS spectra of vapour/*n*-normal alcohols ($n = 1 \sim 8$) interfaces, with $\beta_1 = 60^\circ$ and $\beta_2 = 55^\circ$ in co-propagating geometry. The baselines of the spectra were offset for viewing [43].

Since the CH_3 spectra for the vapour/ethanol interface exhibit the following simple relationships (figure 5): $I_{ppp,CH_3-as} > I_{sps,CH_3-as} > I_{ssp,CH_3-as}$, simple orientational analysis using figure 8 would give a tilt angle around $40 \pm 5^\circ$ for the CH_3 group. Using the PNA method for the same peak, we obtained $\theta \simeq 40^\circ$. Since the angle between the bisectional axis of the CH_2 group and the C_3 axis is about 125°, this CH_3 angle indicates that the CH_2 group lies nearly flat ($\theta \simeq 85^\circ$) at the interface. Therefore, if $2868\,cm^{-1}$ is assigned to the CH_2-*ss* mode, it cannot have such a strong intensity in the *ssp* spectrum with such an orientation. Therefore, with our assignment in table 4, 2868 and $2926\,cm^{-1}$ are CH_3-*ss* and CH_3-Fermi-*ss*, respectively, and PNA measurement of these two peaks both give $\theta_0 \simeq 40^\circ$. We went further to conduct SFG-VS measurement on both vapour/CH_3CD_2OH and vapour/CD_3CH_2OH interfaces (figure 13). The three peaks at 2868, 2926 and $2970\,cm^{-1}$ disappeared for the vapour/CD_3CH_2OH interface, and remained almost the same for the vapour/CH_3CD_2OH interface. This completely confirms our assignment and the measurement on the CH_3 and CH_2 orientations. (Recently Professor Y.R. Shen indicated to H.F.W. that his group also realized inconsistencies for the ethanol spectral assignment in a previous paper [74]. He told H.F.W. that his group had measured the SFG-VS spectra

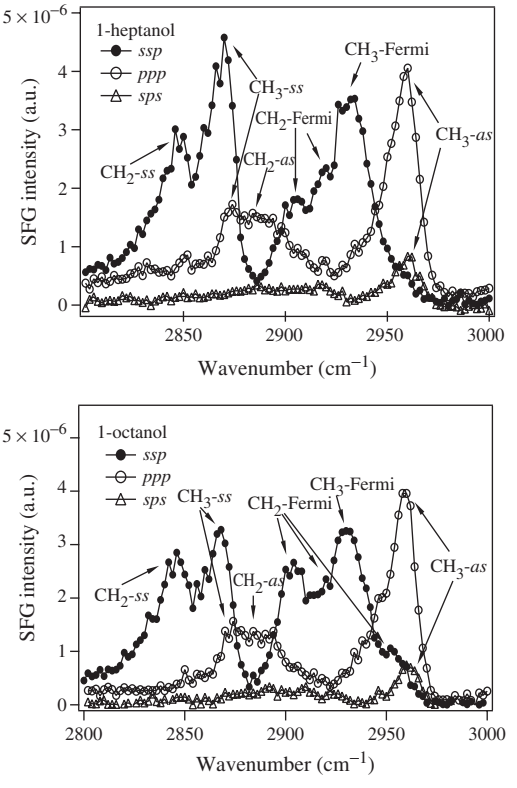

Figure 12. SFG-VS spectra and assignments of CH vibrational modes of vapour/1-heptanol and vapour/1-octanol interfaces, with $\beta_1 = 60^\circ$ and $\beta_2 = 55^\circ$ in co-propagating geometry [43].

Table 4. Assignment of SFG-VS spectra of vapour/1-alcohol ($n = 1 \sim 8$) interfaces. From [43].

Assignment (notation[137, 138]) polarization	CH_2-*ss* (d^+) *ssp*	CH_3-*ss* (r^+) *ssp*	CH_2-*as* (d^-) *ppp* & *sps*	CH_2-FR (d^+)-FR *ssp*	CH_2-FR (d^+)-FR *ssp*	CH_3-FR (r^+)-FR *ssp*	CH_3-*as* (r^-) *ppp* & *sps*
Methanol	–	2828	–	–	–	2910, 2940	–
Ethanol	–	2868	–	–	–	2926	2970
1-Propanol	2850	2874	2908 (br)	–	–	2938	2960
1-Butanol	2850	2872	2898 (br)	2904	–	2938	2960
1-Pentanol	2850	2870	2890 (br)	–	2918	2934	2960
1-Hexanol	2848	2868	2884 (br)	2904	2918, 2954	2932	2960
1-Heptanol	2848	2870	2884 (br)	2906	2918	2932	2960
1-Octanol	2846	2868	2884 (br)	2904	2918, 2954	2930	2960

br = broad peak.

of the vapor/1-alcohol interfaces in different polarizations since 2002. But his group had not done deuterated ethanol experiments, and full analysis of these data has yet to be finished.) This result indicates how polarization analysis along with the polarization selection rules can help make correct assignment on the vibrational spectrum. In section 4.3, we shall discuss the ethanol vibrational spectrum further.

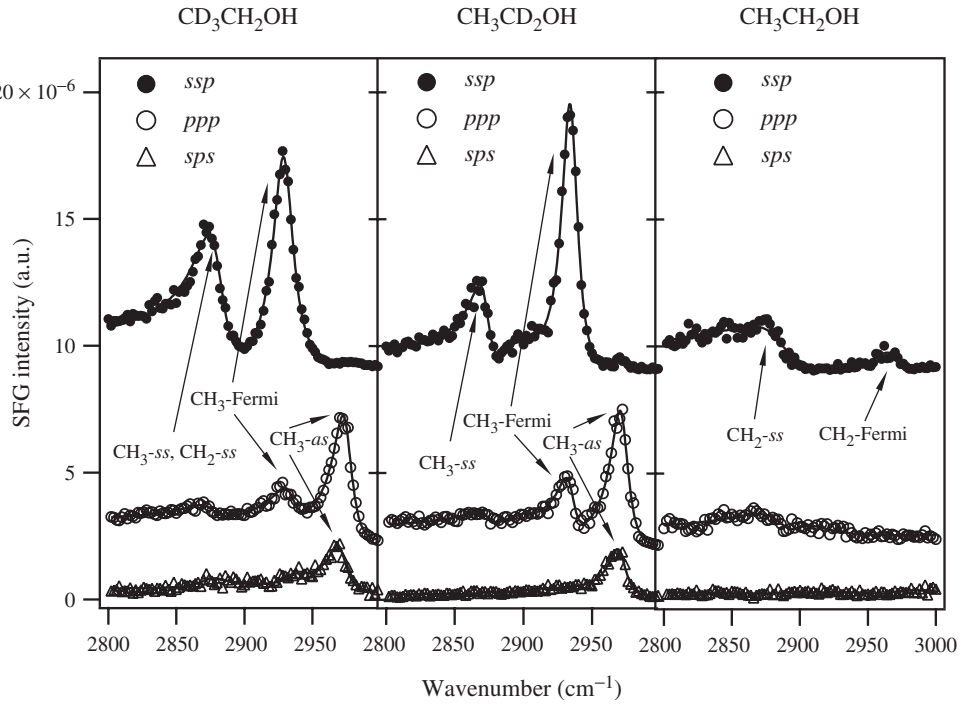

Figure 13. SFG-VS spectra of vapour/ethanol interfaces, with $\beta_1 = 62^\circ$ and $\beta_2 = 52^\circ$ in co-propagating geometry. Solid lines are fitting curves. The baselines of *ssp* and *ppp* spectra are offset for viewing purpose.

The selection rules for the single CH stretching vibration can be useful in assignment of SFG-VS spectra of protein interfaces, because all natural amino acid molecules, except for glycine, have a CH group. The CH group stretching mode is generally hard to identify in IR and Raman spectroscopy [155, 156]. Extremely low temperature [137] and gaseous [148] Raman experiments with hydrocarbons containing –CHD– and $–CHD_2$ groups have shown that the methine stretching is around $2900\,cm^{-1}$. To our knowledge, there is only one recent SFG-VS study on L-leucine at the air/water interface that presented a slight feature at $2902\,cm^{-1}$ on the *ssp* spectra for the methine group [15, 157]. Using the polarization selection rules, a feature on the *ssp* and *ppp* SFG-VS spectra of the vapour/2-propanol at $2914\,cm^{-1}$ has been identified as the CH stretching vibration in the 2-propanol molecule [43]. We expect that with the polarization selection rules and the ability to observe narrower peaks at the molecular interfaces in SFG-VS, more observations of the CH stretching vibration will be reported on protein and bio-membrane interfaces.

It is worth noting that to apply the polarization selection rules, SFG-VS spectra in more than one or two polarization combinations need to be measured for comparison. In the SFG-VS literature, systematic comparison of SFG-VS spectra in different polarization configurations has not been the norm for spectral assignment. The importance of obtaining SFG-VS spectra with different incident angle sets has not been discussed and done. The analysis and examples with vapour/liquid interfaces illustrated here

demonstrate that it is crucial to have SFG-VS measurement in different polarization configurations for spectral assignment purpose. In some cases, spectra from different incident angle sets also need to be compared. However, assignment of SFG-VS spectrum of complex molecular interface may still be difficult. It is hoped that more knowledge can be gained through the polarization selection rules and detailed polarization analysis and simulation.

We have shown in this section that with polarization selection rules, SFG-VS spectra obtained in different polarizations can be used to identify new spectral features, which are not identified in IR and Raman studies. However, great caution has to be taken for the new spectral features in SFG-VS spectra. Because SFG-VS is a sensitive interface probe, spectral features can easily be detected from surface enrichment of the very diluted surface active impurities or contaminates in the solution. Therefore, impurity and contamination may cause SFG-VS big problems. Bulk probes, such as IR and Raman spectroscopy, would not have this problem for small amounts of impurities. However, since the polarization selection rules provide a tool for *in situ* SFG-VS spectral assignment and analysis, together with knowledge from IR and Raman studies, these selection rules can provide direct symmetry properties analysis of the observed spectral features, and help identify whether these new spectral features are from the impurity or are from the interfacial molecules under investigation.

Recently, a polarization mapping procedure based on the polarization analysis method was proposed to mathematically reconstruct the small hidden features from SFG-VS spectra in different polarizations [69]. Demonstration of differentiation of small hidden non-electronically resonant chiral contributions to SFG-VS spectra in different polarizations of adsorbed fibrinogen molecules was also reported [158]. These applications of polarization analysis to such high accuracy would certainly be exciting if confirmed by further examinations. Of course, the key to accurate polarization analysis nevertheless relies on the ability for effective polarization control in SFG-VS experiment [24, 25, 77, 80, 87].

4.3. *SFG-VS and its implications on IR and Raman vibrational spectroscopy*

There are some general issues raised from SFG-VS spectral assignment on vibrational spectroscopy in the condensed phase.

Vibrational spectral assignment is the first step for identification of molecular structural and conformational properties, and also the starting point for dynamics studies on vibrational energy transfer (VET) as well as redistribution, and solute–solvent coupling [159]. From discussions in section 4.2, we have seen examples of the ambiguity and confusion in IR and Raman assignments. As vibrational spectroscopy developed purely for interface studies, SFG-VS has shown its ability and possibility to discern complex vibrational spectrum through the polarization selection rules based on molecular symmetry properties, and through more careful polarization spectral analysis. The vibrational spectral assignment of the ethylene glycol, ethanol molecules are such examples.

These developments may bring important consequences and broad implications in vibrational spectroscopy and dynamics. For example, based on the assignment of the 2968 cm^{-1} peak for the CH_2-*ss* mode in ethanol [152, 153], the vibrational energy transfer

dynamics of liquid ethanol was studied with the ultrafast IR-Raman pump-probe experiment [160]. The vibrational energy on the OH bond excited with 3500 cm^{-1} was observed flowing sequentially first to the 2868 cm^{-1} CH_2 band in less than 1 ps, and then to the 2930 cm^{-1} band CH_3 band in another 0.4 ps [160]. Because this assignment of spectrum is incorrect, this sequential VET process cannot be established with the reported ultrafast dynamics measurements [160]. The conclusion for sequential through-bond VET was certainly a victim of previously unclear assignments from IR and Raman studies [152, 153]. In the same work, data on 1-propanol and 1-butanol also went to the same through-bond VET dynamics [160]. Because the ultrafast probe pulse used in this work has a 25 cm^{-1} bandwidth [160], the CH_2-*ss* band at 2850 cm^{-1} and the CH_3-*ss* band at 2870 cm^{-1} as listed in table 4 cannot be resolved. Therefore, this is also not valid. In conclusion, the surprising sequential through-bond dynamics in this report cannot be supported from spectroscopic evidences.

On these grounds, the IR and Raman measurements on deuterated ethanol liquids [152, 153] reported previously need to be closely checked. Because of the inhomogeneous broadening in the liquid phase, the IR and Raman spectra are broad, and they cannot resolve the overlapping CH_2-*ss* and CH_3-*ss* peaks around 2870 cm^{-1}. Photoacoustic stimulated Raman (PASR) measurement of CH_3CH_2OH, CH_3CD_2OH, and CD_3CH_2OH with a resolution of 1 cm^{-1} indicate that both CH_2-*ss* and CH_3-*ss* peaks with much narrower resolution (less than 10 cm^{-1} FWHM) than that in bulk Raman measurement are present at 2870 cm^{-1} [161]. SFG spectra (figure 13) obtained for the vapour/deuterated ethanol interfaces indicate that the 2870 cm^{-1} peak is clearly dominated by the CH_3 group. Due to the nearly lying flat orientation of the CH_2 group at the vapour/ethanol interface, the CH_2-*ss* spectra at 2870 cm^{-1} almost disappeared on SFG-VS spectra of the vapour/CD_3CH_2OH interface.

This example on the CH stretching vibrational spectral assignment for ethanol indicates how the knowledge learned from SFG-VS can be used to address general vibrational spectroscopy problems in the condensed phase. It also indicates the limitations of our knowledge on vibrational spectrum of simple molecules.

Another example is with the methanol molecule. The vapour/methanol interface was the first liquid interface studies with SFG-VS [65], and it has been extensively studied in the literature [24, 25, 43, 65, 72, 75]. It has been accepted that the 2828, 2910 and 2940 cm^{-1} belong to CH_3 symmetric stretching and Fermi resonance modes. Since these SFG-VS spectral positions for vapour/methanol interface are at the same positions as the IR and Raman spectra of liquid methanol, the assignment for the liquid methanol IR and Raman spectra should be attributed to the same modes as at the vapour/methanol interface. However, in many literature and standard databases, the 2940 cm^{-1} peak was assigned to the asymmetric stretching mode of CH_3 [162]. Recently, this incorrect assignment has led to self-contradictory interpretations for ultrafast dynamics studies on liquid methanol [159, 163].

SFG-VS not only can shed new light on spectral assignment in IR and Raman spectroscopy and dynamics studies, but it can also help quantitatively address the molecular detail of the different chemical bonds in the molecule. As we have demonstrated in sections 3.4 and 4.2, the bond polarizability derivative model in Raman spectroscopy can be used to quantitatively interpret SFG-VS spectra in different polarizations. Reciprocally, because SFG-VS has the advantage to study spectral details, it can be

used to obtain detailed information on the bond polarizability of the same chemical bond in different molecules or in different places in the same molecule. Because the vibrational spectra obtained with SFG-VS are usually narrower, and some of the peaks may be suppressed in different polarizations, it has certain power to help resolve uncertain vibrational modes in IR and Raman spectroscopies in the condensed phase. We have shown here even with relatively very simple molecules, such as ethylene glycol and ethanol, there is ambiguity and confusion in their vibrational spectroscopy, which can be discerned with SFG-VS polarization analysis. In the meantime, with the abilities for detailed spectral assignment and quantitative polarization analysis of SFG-VS spectrum as presented in this review, it is possible to employ it to investigate spectroscopy, structure, and dynamics at the complex molecular interfaces at the molecular and chemical bond level.

5. Summary

In summary, the ability to use SFG-VS for understanding of molecular interfaces depends on the abilities to make detailed interpretation of SFG vibrational spectrum, and depends on our ability to analyse the polarization data in SFG-VS measurements for the orientational order parameters of the molecular interface. Through examples of a series of vapour/neat liquid interfaces, this review focuses on the recent developments regarding the aspects on the ability of SFG-VS for quantitative polarization and orientational analysis, and polarization spectral analysis. The intensity of SFG-VS spectral peaks depends on many parameters and factors, such as the experimental polarization configuration, geometry of optical arrangements, the local field factors in the interface layer, symmetry properties of the molecular groups under investigation, and the hyperpolarizability tensor ratios. Therefore, depending on so many parameters, quantitative analysis of SFG-VS data used to be a somewhat dreadful exercise. Detailed discussion on these parameters and factors helps us to develop optimized experimental arrangements to assess the influences of each parameter and factor, to test the validity of models for local field factors in molecular layers and model for bond polarizability derivative, and to analyse the molecular symmetry through polarization data. With better understanding of the determining parameters and factors on SFG-VS intensities, spectroscopic, structural, conformational information of the molecules in the interface layer can be quantitatively investigated.

We have discussed in detail the PNA method and the incident angle geometry for accurate determination of the molecular orientational parameters in the molecular layer. It is shown that the PNA method can be much more accurate than the PIR method. We have also shown that in doing PNA measurements in co-propagating geometry, the D value obtained is independent of the refractive indices and local field factors in the molecular layer in IR wavelengths, which are usually not available. We then discussed the issues related to the local field factors in the molecular layer.

In order to examine and test the bond polarizability derivative model, general expressions of non-zero molecular hyperpolarizability tensors are given for C_{3v}, C_{2v} and $C_{\infty v}$ molecular groups in Appendix B. The effectiveness and validity of the model in quantitative SFG-VS analysis are tested with SFG-VS measurement

on vapour/neat liquid interfaces. It is demonstrated that with the bond polarizability derivative model, detailed information on molecular bonds can be explained. Even though the r or R values of a molecular group cannot be generally transferable, clues can be found for similar r values of a certain C–H bond in similar chemical environment, and the differences of r values can be generally compared.

Polarization analysis of SFG-VS intensities from molecular groups with different symmetries leads to a set of polarization selection rules or guidelines for assignment of complex SFG-VS vibrational spectra. These selection rules enabled the spectral assignment in SFG-VS to be *in situ*, i.e. with its own abilities, instead of being *ex situ*, i.e. depending only on indirect knowledge from IR and Raman assignments. Of course, knowledge from IR and Raman studies is nevertheless very helpful. The selection rules developed here may need to be modified to some extent, but the concept to make *in situ* SFG-VS spectral assignment will certainly advance the ability in SFG-VS for investigation of complex molecular interfaces. With these selection rules, explicit assignments of SFG-VS spectra are achieved for a series of vapour/diol and vapour/normal alcohol interfaces. Some ambiguity and confusion in the assignments of IR and Raman spectrum in liquid phase is also addressed. Polarization selection rules and polarization analysis in SFG-VS are essential steps for understanding of the vibrational spectroscopy of complex molecular interfaces. Moreover, SFG-VS may also be used to elucidate spectral ambiguity and confusion on spectral assignment where IR and Raman may not work.

In order to make effective quantitative orientational and spectral analysis, SFG-VS experiments need to be performed in different polarizations, and some times with different incident angle geometries. In these measurement, accurate control of polarization and incident angle is required [24, 25, 77, 80, 87]. The effectiveness of such polarization analysis can only be tested with reliable experimental data on well defined model interfaces. Vapour/neat liquid interfaces are ideal model interfaces for such purposes.

Even though SFG-VS measurements on different polarizations has been generally practiced and the PIR method has been commonly used to study molecular orientation at interfaces, systematic comparison of the polarization dependence of SFG-VS spectrum has not been employed for SFG-VS spectral assignment until recently. The incident angle geometry dependence of SFG-VS intensities has not been effectively discussed in previous SFG-VS studies. We have shown that co-propagating incident angle geometry can greatly simplify the quantitative analysis of SFG-VS data. And the incident angle analysis can be used to resolve overlapped spectral peaks.

As Shen *et al*. pointed out recently, SFG-VS is the only technique that can yield a vibrational spectrum for molecules at a free liquid or liquid mixture interface [7]. With the development of quantitative orientational and spectral analysis in SFG-VS, molecular interfaces, especially liquid interfaces, can be studied in great detail. Recently, with accurate determination of the orientational parameters at the vapour/methanol–water mixture and vapour/acetone–water mixture interfaces, a double layered structure at these liquid interfaces was determined, and adsorption free energies for the first and second layers were also determined [77, 78, 80]. The ideas, concepts, and knowledge learned on the liquid interfaces at such detailed molecular level can be used for understanding of other kinds of molecular interfaces, and it is equally

important that the techniques and methodologies developed can find broad applications to other molecular interfaces as well.

Acknowledgments

H.F.W. acknowledges support from the Chinese Academy of Sciences (the Hundred Talent Program starting fund, 1999–2002), the Natural Science Foundation of China (NSFC No. 20274055, No. 20425309), and the Chinese Ministry of Science and Technology (MOST No. G1999075305). We thank Wen-kai Zhang and Hui Wu for help with some derivations of the relationships in Appendix B. All SFG spectra were obtained with the SFG spectrometer built by EKSPLA, Co. We thank the fine services provided by the EKAPLA engineers. As neophytes in SFG-VS interface studies, we have been trying to learn the ropes of the complicated SFG-VS technique. We are greatly indebted to those who have laid the foundations and developed the key concepts on which advancements were made possible. H.F.W. thanks Kopin Liu for his suggestion to prepare this work. H.F.W. also thanks K.B. Eisenthal, Hai-lung Dai, Ron Y. R. Shen, and Na Ji for their valuable discussions and encouragement.

Appendix

Appendix A: susceptibility tensors for molecular groups with C_{3v}, C_{2v}, and $C_{\infty v}$ symmetry

According to Goldstein [47], there are 12, i.e. $2 \times 3!$, ways to make the Euler transformation between the molecular coordinates frame $x'y'z'$, or abc, and the laboratory coordinates frame xyz. Here we use the Euler transformation defined in figure 14, one of the two popular definitions in describing problems in molecular spectroscopy [16, 33, 59, 67], and it has to be noted that inconsistencies should generally arise with the ψ and ϕ terms if these different ways of Euler transformations are not carefully distinguished and kept self-consistent. In our work, the Euler transformation matrix $\Re$ is,

$$\Re = \begin{pmatrix} \cos\psi\cos\phi - \cos\theta\sin\phi\sin\psi & -\sin\psi\cos\phi - \cos\theta\sin\phi\cos\psi & \sin\theta\sin\phi \\ \cos\psi\sin\phi + \cos\theta\cos\phi\sin\psi & -\sin\psi\sin\phi + \cos\theta\cos\phi\cos\psi & -\sin\theta\cos\phi \\ \sin\theta\sin\psi & \sin\theta\cos\psi & \cos\theta \end{pmatrix} \tag{24}$$

as defined in

$$\begin{pmatrix} x \\ y \\ z \end{pmatrix} = \Re \times \begin{pmatrix} x' \\ y' \\ z' \end{pmatrix} = \begin{pmatrix} R_{xx'} & R_{xy'} & R_{xz'} \\ R_{yx'} & R_{yy'} & R_{yz'} \\ R_{zx'} & R_{zy'} & R_{zz'} \end{pmatrix} \begin{pmatrix} x' \\ y' \\ z' \end{pmatrix}. \tag{25}$$

The molecular fixed coordinates abc for the CH_3 and CH_2 are defined in figure 15. The expressions of the susceptibility tensors for C_{3v}, C_{2v}, and $C_{\infty v}$ symmetry groups

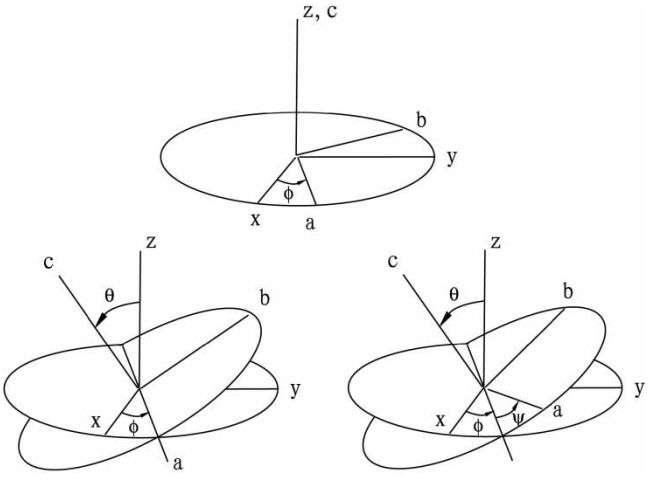

Figure 14. The Euler transformation between the laboratory coordinates xyz and the molecular coordinate abc (or $x'y'z'$) through three Euler angles (ϕ, θ, ψ).

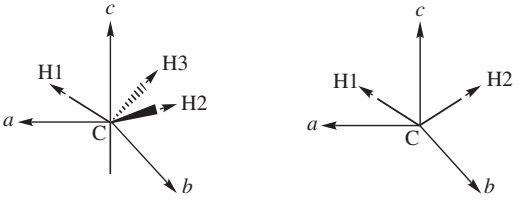

Figure 15. The definition of molecular fixed coordinates of CH_3 and CH_2.

have been scattered in the literature, and in slightly different forms from each other. Here we try to put them together in a consistent form for convenience in future applications.

***C_{3v}* symmetry group.** There are 11 non-zero microscopic hyperpolarizability elements for C_{3v} symmetry group, such as CH_3, NH_3, and SiH_3 groups, etc. [36, 37, 68]. The first three terms are symmetric terms, and the last eight terms are asymmetric terms, corresponding to the symmetric stretching and asymmetric stretching modes, respectively:

$$\begin{aligned} &\beta_{aac} = \beta_{bbc}, \qquad \beta_{ccc} \\ &\beta_{aca} = \beta_{bcb}, \qquad \beta_{caa} = \beta_{cbb} \\ &\beta_{aaa} = -\beta_{bba} = -\beta_{abb} = -\beta_{bab}. \end{aligned} \tag{26}$$

When both the SF and visible frequencies are off resonance, one has $\beta_{aca} = \beta_{bcb} = \beta_{caa} = \beta_{cbb}$. Then for a rotationally isotropic interface, the seven non-zero macroscopic elements of $\chi^{(2)}_{ijk}$ are obtained through integration over the two Euler angles (ϕ and ψ) as in the following [164, 165].

For the symmetric stretching (*ss*) vibrational mode,

$$\begin{aligned} \chi^{(2),ss}_{xxz} = \chi^{(2),ss}_{yyz} &= \frac{1}{2}N_s\beta_{ccc}\left[(1+R)\langle\cos\theta\rangle - (1-R)\langle\cos^3\theta\rangle\right] \\ \chi^{(2),ss}_{xzx} = \chi^{(2),ss}_{zxx} = \chi^{(2),ss}_{yzy} = \chi^{(2),ss}_{zyy} &= \frac{1}{2}N_s\beta_{ccc}(1-R)\left[\langle\cos\theta\rangle - \langle\cos^3\theta\rangle\right] \\ \chi^{(2),ss}_{zzz} &= N_s\beta_{ccc}\left[R\langle\cos\theta\rangle + (1-R)\langle\cos^3\theta\rangle\right]. \end{aligned} \tag{27}$$

For the asymmetric stretching (*as*) vibrational mode,

$$\begin{aligned} \chi^{(2),as}_{xxz} = \chi^{(2),as}_{yyz} &= -N_s\beta_{aca}\left(\langle\cos\theta\rangle - \langle\cos^3\theta\rangle\right) \\ \chi^{(2),as}_{xzx} = \chi^{(2),as}_{zxx} = \chi^{(2),as}_{yzy} = \chi^{(2),as}_{zyy} &= N_s\beta_{aca}\langle\cos^3\theta\rangle \\ \chi^{(2),as}_{zzz} &= 2N_s\beta_{aca}\left(\langle\cos\theta\rangle - \langle\cos^3\theta\rangle\right). \end{aligned} \tag{28}$$

Here the hyperpolarizability ratio is $R = \beta_{aac}/\beta_{ccc} = \beta_{bbc}/\beta_{ccc}$. R is different for the methyl group in different molecules, which can be explicitly determined from the independently measured Raman depolarization ratio [22, 38]. It has been indicated that R has to be in the range of about 1.66–4.0 for the methyl group [22, 36, 37, 72, 103], with $R = 1.7$ for methanol, $R = 3.4$ for ethanol and longer chain 1-alcohols, $R = 1.9$ for acetone, and $R = 2.3$ for DMSO [70, 72, 103, 105]. Actually, R can be smaller than 1.66 in some cases, but it should be generally larger than 1 for C_{3v} groups, as discussed in Appendix B. θ is the tilt angle of the C_3 axis from the surface normal, and the operator $\langle\ \rangle$ denotes orientational ensemble average over different molecular orientations. It is noted that the last four of the 11 non-zero hyperpolarizability elements for methyl group vanishes in equation (27) and equation (28) due to the orientational ensemble average. It is also noted that the asymmetric susceptibility tensor terms for the methyl group are different from the corresponding terms for the asymmetric terms of the methylene group by a factor of 2 [26, 164, 165], instead of bearing the exact same forms [86], unless the two fold degeneracy of the CH_3-*as* mode is lifted.

It is to be noted that in some work, $\cos 3\theta$, instead of $\cos^3\theta$, is used in the above expressions [131]. They are equivalent through the trigonometrical relationship $\cos 3\theta = 4\cos^3\theta - 3\cos\theta$.

C_{2v} symmetry group. For C_{2v} symmetry groups, such as the CH_2 group, there are seven non-vanishing molecular hyperpolarizability tensor elements [36, 37, 40, 68]. The first three terms are symmetric (a_1), and the last four terms are asymmetric (b_1 and b_2), corresponding to the symmetric stretching and asymmetric stretching modes of the CH_2 group, respectively:

$$\beta_{aac}, \quad \beta_{bbc}, \quad \beta_{ccc}, \quad \beta_{aca} = \beta_{caa}, \quad \beta_{bcb} = \beta_{cbb}. \tag{29}$$

Averaging over the Euler angle ϕ for the rotationally isotropic interface, the seven non-zero macroscopic $\chi^{(2)}_{ijk}$ elements are the following.

For the symmetric stretching (ss, a_1) vibrational modes,

$$\begin{aligned}
\chi^{(2),ss}_{xxz} = \chi^{(2),ss}_{yyz} &= \frac{1}{2}N_s\left[\langle\cos^2\psi\rangle\beta_{aac} + \langle\sin^2\psi\rangle\beta_{bbc} + \beta_{ccc}\right]\langle\cos\theta\rangle \\
&\quad + \frac{1}{2}N_s\left[\langle\sin^2\psi\rangle\beta_{aac} + \langle\cos^2\psi\rangle\beta_{bbc} - \beta_{ccc}\right]\langle\cos^3\theta\rangle \\
\chi^{(2),ss}_{xzx} = \chi^{(2),ss}_{zxx} &= \chi^{(2),ss}_{yzy} = \chi^{(2),ss}_{zyy} \\
&= -\frac{1}{2}N_s\left[\langle\sin^2\psi\rangle\beta_{aac} + \langle\cos^2\psi\rangle\beta_{bbc} - \beta_{ccc}\right]\left[\langle\cos\theta\rangle - \langle\cos^3\theta\rangle\right] \\
\chi^{(2),ss}_{zzz} &= N_s\left[\langle\sin^2\psi\rangle\beta_{aac} + \langle\cos^2\psi\rangle\beta_{bbc}\right]\langle\cos\theta\rangle \\
&\quad - N_s\left[\langle\sin^2\psi\rangle\beta_{aac} + \langle\cos^2\psi\rangle\beta_{bbc} - \beta_{ccc}\right]\langle\cos^3\theta\rangle.
\end{aligned} \tag{30}$$

For the asymmetric stretching (as, b_1) vibrational mode,

$$\begin{aligned}
\chi^{(2),as}_{xxz} = \chi^{(2),as}_{yyz} &= -N_s\beta_{aca}\langle\sin^2\psi\rangle\left[\langle\cos\theta\rangle - \langle\cos^3\theta\rangle\right] \\
\chi^{(2),as}_{xzx} = \chi^{(2),as}_{zxx} = \chi^{(2),as}_{yzy} &= \chi^{(2),as}_{zyy} \\
&= \frac{1}{2}N_s\beta_{aca}\left[\langle\cos^2\psi\rangle - \langle\sin^2\psi\rangle\right]\langle\cos\theta\rangle + N_s\beta_{aca}\langle\sin^2\psi\rangle\langle\cos^3\theta\rangle \\
\chi^{(2),as}_{zzz} &= 2N_s\beta_{aca}\langle\sin^2\psi\rangle\left[\langle\cos\theta\rangle - \langle\cos^3\theta\rangle\right].
\end{aligned} \tag{31}$$

The b_2 asymmetric mode bears the same expressions as the b_1 mode. The only difference is that each $\chi^{(2),as}_{ijk}$ term in b_2 symmetry is proportional to β_{bcb} instead of β_{aca}. β_{bcb} is zero if the molecule is placed in the molecular coordinates system *abc* as in figure 15.

The Euler angle ψ can be integrated if the H–X–H plane of the XH_2 group can freely rotate along its *c* axis. This is usually hindered if there are other groups attached to the X atom. So generally the polyethylene, i.e. $-(CH_2{-}CH_2)_n-$, chain cannot rotate freely. However, for those XH_2 groups that can freely rotate, the Euler angle can be averaged out by letting $\langle\cos^2\psi\rangle = \langle\sin^2\psi\rangle = 1/2$ in equations (32) and (33). So, we have the following:

$$\begin{aligned}
\chi^{(2),ss}_{xxz} = \chi^{(2),ss}_{yyz} &= \frac{1}{4}N_s(\beta_{aac} + \beta_{bbc} + 2\beta_{ccc})\langle\cos\theta\rangle \\
&\quad + \frac{1}{4}N_s(\beta_{aac} + \beta_{bbc} - 2\beta_{ccc})\langle\cos^3\theta\rangle \\
\chi^{(2),ss}_{xzx} = \chi^{(2),ss}_{zxx} &= \chi^{(2),ss}_{yzy} = \chi^{(2),ss}_{zyy} \\
&= -\frac{1}{4}N_s(\beta_{aac} + \beta_{bbc} - 2\beta_{ccc})\left(\langle\cos\theta\rangle - \langle\cos^3\theta\rangle\right) \\
\chi^{(2),ss}_{zzz} &= \frac{1}{2}N_s(\beta_{aac} + \beta_{bbc})\langle\cos\theta\rangle - \frac{1}{2}N_s(\beta_{aac} + \beta_{bbc} - 2\beta_{ccc})\langle\cos^3\theta\rangle
\end{aligned} \tag{32}$$

and the non-vanishing tensor elements for methylene asymmetric-stretching mode (*as*),

$$\begin{aligned}
\chi^{(2),as}_{xxz} &= \chi^{(2),as}_{yyz} = -\frac{1}{2}N_s\beta_{aca}\left(\langle\cos\theta\rangle - \langle\cos^3\theta\rangle\right)\\
\chi^{(2),as}_{xzx} &= \chi^{(2),as}_{zxx} = \chi^{(2),as}_{yzy} = \chi^{(2),as}_{zyy} = \frac{1}{2}N_s\beta_{aca}\langle\cos^3\theta\rangle\\
\chi^{(2),as}_{zzz} &= N_s\beta_{aca}\left(\langle\cos\theta\rangle - \langle\cos^3\theta\rangle\right)
\end{aligned} \tag{33}$$

For the CH_2 group, there is a general relationship $\beta_{aac} + \beta_{bbc} - 2\beta_{ccc} = 0$, as shown in Appendix B. Therefore, equation (32) can be greatly simplified for polarization spectral analysis [26]. Especially, this relationship makes $\chi^{(2),ss}_{xzx} = \chi^{(2),ss}_{zxx} = \chi^{(2),ss}_{yzy} = \chi^{(2),ss}_{zyy} = 0$, which means no *ss* vibrational mode spectra must be observed in the *sps* and *pss* polarizations according to equation (32). However, if *ss* vibrational mode spectra for CH_2 group can be observed in the *sps* and *pss* polarizations, the conclusion is that the twist angle ψ cannot be rotationally averaged, and the analysis has to used equations (30) and (31).

$C_{\infty v}$ symmetry group. The XH groups, such as single OH and CH bond, would have $C_{\infty v}$ symmetry. The non-zero hyperpolarizability terms for a $C_{\infty v}$ group are all symmetric [66, 102], i.e. $\beta_{aac} = \beta_{bbc} = R\beta_{ccc}$, with the R value falling into the range 0–0.28 for C–H, equal to its bond polarizability derivative ratio r [22, 37, 103]. Generally, $0 \le r < 1$ is for a single chemical bond. It is easy to show that the non-zero elements for $C_{\infty v}$ symmetry susceptibility tensors follow the same expressions as those for the *ss* mode of the CH_3 group in equation (27). However, as we have shown in section 4, the different R values for the CH_3 and CH groups should lead to quite different polarization selection rules for the two groups. The r value for the single O–H group is about 0.32 or less [102, 166], the treatment for the methine group here can be applied to the analysis to stretching mode of the O–H group, the C=O group, and other molecular groups with $C_{\infty v}$ symmetry.

Appendix B: hyperpolarizability and Raman depolarization ratio

As we pointed out above, knowledge of the hyperpolarization ratios between different $\beta_{i'j'k'}$ tensor elements is crucial for quantitative interpretation and polarization analysis of SFG-VS spectrum. Hirose and co-workers used a bond polarizability derivative model to derive expressions for non-zero hyperpolarizability tensor elements of the CH_3 and CH_2 groups from the single CH bond polarizability derivative with a $C_{\infty v}$ symmetry, and the single bond polarizability derivative ratio $r = \alpha'_{\xi\xi}/\alpha'_{\zeta\zeta} = \alpha'_{\eta\eta}/\alpha'_{\zeta\zeta}$, in which $\xi\eta\zeta$ is the molecular coordinates of the single CH bond with ζ as the CH bond axis. The r value can be empirically obtained from the measured Raman depolarization ratio ρ through the bond polarizability derivative ratio [36, 37, 114].

In Hirose's initial formulation of the bond polarizability derivative model [36], $r = 0$ was assumed. However, the inadequacy of this assumption is apparent, because the CH single bond does have a polarizability and polarizability derivative perpendicular to the

bond axis direction [115]. Therefore, revisions [37, 114] were made by Hirose *et al*. [36], to incorporate the case for $0 \leq r < 1$. This revision should have been able to be reduced back to the initial expressions [36] if we let $r = 0$. However, careful examination indicated that the expressions given in both cases are not fully consistent with themselves [36, 37, 114]. This might be the reason that even though these seminal works by Hirose *et al*. have been very popularly cited in the SFG-VS literature, concrete test of validity of the model cannot be found. We have carefully reexamined the derivations, checked the consistency, and tried to test its quantitative validity on interpretation of SFG-VS spectral intensities with some cases as reviewed here.

A detailed bond polarizability derivative calculation has been conducted by Dr. Xing Wei in Prof. Y. R. Shen's group for CH_2 group with $r = 0.14$, and applied to SFG-VS study on the CH_2 groups at a rubbed polyvinyl alcohol polymer surface [40, 41]. Our expressions for CH_2 give exactly the same R_a and R_b ratios as them for the CH_2 group when $r = 0.14$ is plugged in. This is one indication that the expressions we derived should be in the correct form. So we list these expressions of the hyperpolarizability tensors in terms of the bond polarizability derivative ratio below. The expressions are all based on the seminal papers by Hirose *et al*. [36, 37, 114]. Even though the expressions are derived for CH_n groups, they can be readily used for groups with the same molecular groups respectively.

It is to be noted that even though this approach has been called the bond polarizability derivative model, in order to derive the hyperpolarizability tensors, both the bond polarizability derivative model (for Raman tensors) and bond moment derivative model (for IR bond moment) are actually used. The effectiveness of Hirose's model actually depends on the effectiveness of both models. Even though we have presented some good examples supporting the validity of Hirose's model for quantitative analysis of SFG-VS spectra, further detailed examinations are still warranted.

CH group with $C_{\infty v}$ symmetry. For a single CH bond with $C_{\infty v}$ symmetry, $r = \alpha'_{\xi\xi}/\alpha'_{\zeta\zeta} = \alpha'_{\eta\eta}/\alpha'_{\zeta\zeta}$. Its three non-zero elements for the symmetric stretching mode are

$$\begin{aligned} \beta_{aac} &= \beta_{bbc} = r\beta_{ccc} \\ \beta_{ccc} &= -\frac{1}{2\epsilon_0\omega_{\mathrm{CH}}} G_{\mathrm{CH}} \left(\frac{\partial\alpha_{\zeta\zeta}}{\partial\zeta}\right)_0 \left(\frac{\partial\mu_\zeta}{\partial\zeta}\right)_0 = \frac{G_{\mathrm{CH}}}{\omega_{\mathrm{CH}}}\beta^0_{\mathrm{CH}}. \end{aligned} \tag{34}$$

Here ω_{CH} is the stretching frequency of the CH single bond; $G_{\mathrm{CH}} = 1/M_{\mathrm{C}} + 1/M_{\mathrm{H}}$ is the inverse effective mass of the CH bond; and $\beta_{ccc} = G_{\mathrm{CH}}\beta^0_{\mathrm{CH}}/\omega_{\mathrm{CH}}$ is the hyperpolarizability constant for a single CH bond, as defined by Shen *et al*. [40, 41]. For the CH group, the molecular fixed coordinates (*abc*) are equivalent to the single bond fixed coordinates ($\xi\eta\zeta$). The single CH bond polarizability derivative ratio r can be obtained from the Raman depolarization ratio ρ. Of course, only one of the two solutions in equation (35) which satisfies $0 \leq r < 1$ is physically acceptable for the single CH bond.

$$\rho = \frac{3\gamma^2}{45\alpha^2 + 4\gamma^2} = \frac{3}{4 + 5[(1+2r)/(1-r)]^2}. \tag{35}$$

CH_3 group with C_{3v} symmetry. The definition of the molecule fixed coordinates for CH_3 is shown in figure 15. With r as the single bond polarizability derivative ratio, the 11 non-zero molecular hyperpolarizability tensor elements for CH_3 with a C_{3v} symmetry are listed as follows:

$$\begin{aligned}
\beta_{aac} &= \beta_{bbc} = -\frac{3}{2}\frac{G_{\mathrm{sym}}\beta^0_{\mathrm{CH}}}{\omega_s}\left[(1+r)-(1-r)\cos^2\tau\right]\cos\tau \\
\beta_{ccc} &= -3\frac{G_{\mathrm{sym}}\beta^0_{\mathrm{CH}}}{\omega_s}\left[r+(1-r)\cos^2\tau\right]\cos\tau \\
\beta_{bcb} &= \beta_{cbb} = \beta_{caa} = \beta_{aca} = -\frac{3}{2}\frac{G_{\mathrm{deg}}\beta^0_{\mathrm{CH}}}{\omega_d}(1-r)\sin^2\tau\cos\tau \\
\beta_{aaa} &= -\beta_{bba} = -\beta_{abb} = -\beta_{bab} = \frac{3}{4}\frac{G_{\mathrm{deg}}\beta^0_{\mathrm{CH}}}{\omega_d}(1-r)\sin^3\tau
\end{aligned} \tag{36}$$

where τ is the $\angle$H–C–H bond angle for the CH_3 group; $G_{\mathrm{sym}} = (1+2\cos\tau)/M_{\mathrm{C}} + 1/M_{\mathrm{H}}$ and $G_{\mathrm{deg}} = (1-\cos\tau)/M_{\mathrm{C}} + 1/M_{\mathrm{H}}$ are the inverse effective mass for the symmetric and asymmetric normal modes, with M_{C} and M_{H} as the atomic masses of C and H atoms, respectively. ω_s and ω_d are the vibrational frequency of the symmetric and asymmetric vibrational modes for CH_3. These definitions are the same as given by Hirose *et al.* [36, 37]. Then, one can have

$$R = \frac{\beta_{aac}}{\beta_{ccc}} = \frac{1+r-(1-r)\cos^2\tau}{2[r+(1-r)\cos^2\tau]} \tag{37}$$

and then with equation (20), it is easy to show that

$$\rho = \frac{3\gamma^2}{45\alpha^2+4\gamma^2} = \frac{3}{4+20\left[\frac{1+2r}{(1-r)(1-3\cos^2\tau)}\right]^2}. \tag{38}$$

With equation (37), one can only get one solution for $0 \le r < 1$. Therefore, the value for R calculated from equation (37) is unique. Because for CH_3 the bond angle $\tau \cong 109.5^\circ$ and $\cos\tau \cong -1/3$, with $0 \le r < 1$ one can show that $4 \ge R > 1$ [22].

For example, $\rho = 0.014$ [103] for the CH_3 group in methanol, and so $r = 0.28$ and $R = 1.67$; while $\rho = 0.053$ [103] for the CH_3 group in ethanol, so $r = 0.026$ and $R = 3.4$. It is clear that the r and R values for the CH_3 group cannot be transferred between methanol and ethanol molecules.

It is interesting to note that β_{aca} is proportional to $1-r$. Therefore, the larger the r, the smaller the asymmetric intensity. Therefore, from equation (36), calculation using the $r = 0.28$ gives $\beta_{aca}/\beta_{ccc} = 1.0$ and $r = 0.026$ gives $\beta_{aca}/\beta_{ccc} = 3.4$. Since the SFG-VS intensity is proportional to $(\beta)^2$, this fact explains quantitatively why the SFG-VS peak of the asymmetric modes of CH_3 group in interfacial methanol is more than 10 times weaker than that of ethanol, as well as other long chain normal alcohols [43].

The ratio $\beta_{ccc}^{CH_3}/\beta_{ccc}^{CH}$ can be derived to compare the CH_3 and CH SFG-VS spectral intensities,

$$\frac{\beta_{ccc}^{CH_3}}{\beta_{ccc}^{CH}} = -3\frac{G_{sym}\omega_{CH}}{\omega_s G_{CH}}\left[r + (1-r)\cos^2\tau\right]\cos\tau. \tag{39}$$

Given $M_C = 12$, $M_H = 1$, $\tau = 109.5^\circ$, $\omega_{CH} = 2920\,cm^{-1}$, $\omega_{CH_3-ss} = 2870\,cm^{-1}$, we have $\cos\tau \cong -1/3$, and $\beta_{ccc}^{CH_3}/\beta_{ccc}^{CH} = 0.107(1+8r)$.

CH_2 with C_{2v} symmetry. Definition of the molecule fixed coordinates for CH_2 is shown in figure 15. Then the seven non-zero hyperpolarizability tensor elements of CH_2 with C_{2v} symmetry are as follows:

$$\begin{aligned}
\beta_{aac} &= \frac{G_a\beta_{CH}^0}{\omega_{a1}}[(1+r)-(1-r)\cos\tau]\cos\left(\frac{\tau}{2}\right)\\
\beta_{bbc} &= \frac{2G_a\beta_{CH}^0}{\omega_{a1}}r\cos\left(\frac{\tau}{2}\right)\\
\beta_{ccc} &= \frac{G_a\beta_{CH}^0}{\omega_{a1}}[(1+r)+(1-r)\cos\tau]\cos\left(\frac{\tau}{2}\right)\\
\beta_{aca} &= \beta_{caa} = \frac{G_b\beta_{CH}^0}{\omega_{b1}}[(1-r)\sin\tau]\sin\left(\frac{\tau}{2}\right)\\
\beta_{bcb} &= \beta_{cbb} = 0
\end{aligned} \tag{40}$$

where τ is the $\angle$H–C–H bond angle for the CH_2 group; $G_a = (1+\cos\tau)/M_C + 1/M_H$ and $G_b = (1-\cos\tau)/M_C + 1/M_H$ are the inverse effective mass for the symmetric (a_1) and asymmetric (b_1) normal modes, with M_C and M_H as the atomic mass of C and H atoms, respectively. ω_{a1} and ω_{b1} are the vibrational frequencies of the respective modes. Then one has

$$\begin{aligned}
R_a &= \frac{\beta_{aac}}{\beta_{ccc}} = \frac{1+r-(1-r)\cos\tau}{1+r+(1-r)\cos\tau}\\
R_b &= \frac{\beta_{bbc}}{\beta_{ccc}} = \frac{2r}{1+r+(1-r)\cos\tau}\\
R &= \frac{R_a+R_b}{2} = \frac{\beta_{aac}+\beta_{bbc}}{2\beta_{ccc}} = \frac{1+3r-(1-r)\cos\tau}{2[1+r+(1-r)\cos\tau]}.
\end{aligned} \tag{41}$$

Therefore, the Raman depolarization ratio can also be derived from equation (20) as follows:

$$\rho = \frac{3}{4+20[(1+2r)^2/(1-r)^2(1+3\cos^2\tau)]}. \tag{42}$$

Because for CH_2 the bond angle $\tau \cong 109.5^\circ$ and $\cos\tau \cong -1/3$, with $0 \le r < 1$, one has $2 \ge R_a = (2+r)/(1+2r) > 1$, $1 > R_b = 3r/(1+2r) \ge 0$, and $R = 1$. Therefore, with $r = 0.14$, $R_a = 1.67$ and $R_b = 0.33$. These are just the same ratios obtained by Shen *et al*. [40, 41].

Another very important relationship is that $R = 1$ is generally true for CH_2 group no matter what r value is for the single bond. This relationship is determined by the fact that $\tau = 109.5^\circ$. This indicates that $\beta_{aac} + \beta_{bbc} - 2\beta_{ccc} = 0$ is generally true for the CH_2 group. In the meantime, since for the water molecule $\tau = 104.5^\circ$, one can show that the $\beta_{aac} + \beta_{bbc} - 2\beta_{ccc}$ value for the C_{2v} water molecule has to be very small. This fact can be very useful in quantitative analysis of SFG-VS spectra of the interface water molecules.

It is interesting to note that β_{aca} of C_{2v} group is also proportional to $1 - r$. Therefore, the larger the r, the smaller the asymmetric SFG-VS intensity. This fact can be used to compare SFG-VS spectral intensity of different CH_2 groups in the molecular interface layer. A very good example is presented in section 3.4 for vapour/1,5-pentanediol interface [26].

Finally, the ratio $\beta_{ccc}^{CH_2}/\beta_{ccc}^{CH}$ can be derived to compare the CH_2 and CH SFG-VS spectral intensities,

$$\frac{\beta_{ccc}^{CH_3}}{\beta_{ccc}^{CH}} = \frac{G_a\omega_{CH}}{\omega_{a1}G_{CH}}[(1+r)+(1-r)\cos\tau]\cos\left(\frac{\tau}{2}\right). \tag{43}$$

Given $M_C = 12$, $M_H = 1$, $\tau = 109.5^\circ$, $\omega_{CH} = 2920\,cm^{-1}$, $\omega_{CH_3-ss} = 2850\,cm^{-1}$, we have $\cos\tau \cong -1/3$, and $\beta_{ccc}^{CH_2}/\beta_{ccc}^{CH} = 0.384(1+2r)$.

References

[1] M. J. Shultz, C. Schnitzer, and S. Baldelli, Int. Rev. Phys. Chem. **19,** 123 (2000).
[2] V. Vogel and Y. R. Shen, Annu. Rev. Mater. Sci. **21,** 515 (1991).
[3] K. B. Eisenthal, Annu. Rev. Phys. Chem. **43,** 627 (1992).
[4] K. B. Eisenthal, Acc. Chem. Res. **26,** 636 (1993).
[5] Y. R. Shen, Nature **337,** 519 (1989).
[6] K. B. Eisenthal, Chem. Rev. **96,** 1343 (1996).
[7] P. B. Miranda and Y. R. Shen, J. Phys. Chem. B **103**(17), 3292 (1999).
[8] M. J. Shultz, S. Baldelli, C. Schnitzer, and D. Simonelli, J. Phys. Chem. B **106,** 5313 (2002).
[9] G. L. Richmond, Chem. Rev. **102,** 2693 (2002).
[10] Y. R. Shen, Annu. Rev. Phys. Chem. **40,** 327 (1989).
[11] T. F. Heinz, *Nonlinear Surface Electromagnetic Phenomena* edited by H. E. Ponath and G. I. Stegman (North-Holland, New York, 1994), pp. 353.
[12] R. M. Corn and D. A. Higgins, Chem. Rev. **94,** 107 (1994).
[13] C. D. Bain, J. Chem. Soc. Faraday Trans. **91,** 1281 (1995).
[14] C. D. Bain and P. R. Greene, Curr. Opin. Coll. Int. Sci. **6,** 313 (2001).
[15] M. Buck and M. Himmelhaus, J. Vac. Sci. Technol. A **19,** 2717 (2001).
[16] J. I. Dadap and T. F. Heinz, Nonlinear optical spectroscopy of surfaces and interfaces, in *Encyclopedia of Chemical Physics and Physical Chemistry*, edited by J. H. Morre and D. D. Spencer (Institute of Physics, Bristal, 2001), pp. 1089–1125.
[17] Z. Chen, Y. R. Shen, and G. A. Somorjai, Annu. Rev. Phys. Chem. **53,** 437 (2002).
[18] F. Vidal and A. Tadjeddine, Rep. Prog. Phys. **68,** 1095 (2005).
[19] X. Chen, M. L. Clarke, J. Wang, and Z. Chen, Int. J. Mod. Phys. B **19**(4), 691 (2005).
[20] G. A. Somorjai and G. Rupprechter, J. Phys. Chem. B **103,** 1623 (1999).
[21] G. A. Somorjai and Rupprechter, J. Chem. Educ. **75,** 162 (1998).

[22] X. Zhuang, P. B. Miranda, D. Kim, and Y. R. Shen, Phys. Rev. B **59,** 12632 (1999).
[23] Y. Rao, Y. S. Tao, and H. F. Wang, J. Chem. Phys. **119,** 5226 (2003).
[24] R. Lu, W. Gan, and H. F. Wang, Chin. Sci. Bull. **48**(20), 2183 (2003).
[25] R. Lu, W. Gan, and H. F. Wang, Chin. Sci. Bull. **49**(9), 899 (2004).
[26] R. Lu, W. Gan, B. H. Wu, H. Chen, and H. F. Wang, J. Phys. Chem. B **108,** 7297 (2004).
[27] Ekspla Co., Vilnius, Lithuania. http://www.ekspla.com
[28] L. J. Richter, T. P. Petralli-Mallow, and J. C. Stephenson, Opt. Lett. **23,** 1594 (1998).
[29] E. L. Hommel, G. Ma, and H. C. Allen, Ana. Sci. **17,** 1 (2001).
[30] A. W. Adamson, *Physical Chemistry of Surfaces*, 6th ed. (Wiley-Interscience, New York, 1991).
[31] *The Dynamics and Structure of the Liquid–Liquid Interface*, Faraday Discussion Vol. 129 (2004).
[32] Y. R. Shen, IEEE Journal on Selected Topics in Quantum Electronics **6,** 1375 (2000).
[33] Y. R. Shen, *The Principles of Nonlinear Optics* (Wiley-Interscience, New York, 1984).
[34] P. Guyot-Sionnest, J. H. Hunt, and Y. R. Shen, Phys. Rev. Lett. **59,** 1597 (1987).
[35] J. H. Hunt, P. Guyot-Sionnest, and Y. R. Shen, in *Laser Spectroscopy VIII*, edited by W. Persson and S. Svanberg (Springer, Berlin, 1987), pp. 253–266.
[36] C. Hirose, N. Akamatsu, and K. Domen, J. Chem. Phys. **96,** 997 (1992).
[37] C. Hirose, H. Yamamoto, H. N. Akamatsu, and K. Domen, J. Phys. Chem. **97,** 10064 (1993).
[38] D. Zhang, J. Gutow, and K. B. Eisenthal, J. Phys. Chem. **98,** 13729 (1994).
[39] G. R. Bell, Z. X. Li, C. D. Bain, P. Fischer, and D. C. Duffy, J. Phys. Chem. B **102,** 9461 (1998).
[40] X. Wei, S. C. Hong, X. W. Zhuang, T. Goto, and Y. R. Shen, Phys. Rev. E **62,** 5160 (2000).
[41] X. Wei, PhD Dissertation (Department of Physics, University of California, Berkeley, 2000).
[42] Y. R. Shen, private communication.
[43] R. Lu, W. Gan, B. H. Wu, Z. Zhang, Y. Guo, and H. F. Wang, J. Phys. Chem. B **109**, 14118 (2005).
[44] N. Bloembergen and P. S. Pershan, Phys. Rev. **128,** 606 (1962).
[45] M. B. Feller, W. Chen, and Y. R. Shen, Phys. Rev. A **43,** 6778 (1991).
[46] C. Hirose, N. Akamatsu, and K. Domen, Appl. Spectro. **46,** 1051 (1992).
[47] H. Goldstein, *Classical Mechanics* (Addison-Wesley Publishing Company, Inc., Reeding, Massachusetts, USA, 1980), p. 147.
[48] C. D. Bain, P. B. Davies, T. H. Ong, R. N. Ward, and M. A. Brown, Langmuir **7,** 1563 (1991).
[49] T. H. Ong, P. B. Davies and C. D. Bain, Langmuir **9,** 1836 (1993).
[50] M. G. Brown, E. A. Raymond, H. C. Allen, L. F. Scatena, and G. L. Richmond, J. Phys. Chem. A **104,** 10220 (2000).
[51] R. Superfine, J. Y. Huang, and Y. R. Shen, Chem. Phys. Lett. **172,** 303 (1990).
[52] K. A. Briggman, J. C. Stephenson, W. E. Wallace, and L. J. Richter, J. Phys. Chem. B **105,** 2785 (2001).
[53] H. F. Wang, Chin. J. Chem. Phys. **17**(3), 362 (2004).
[54] G. J. Simpson and K. L. Rowlen, Anal. Chem. **72,** 3399 (2000).
[55] G. J. Simpson and K. L. Rowlen, Anal. Chem. **72,** 3407 (2000).
[56] G. J. Simpson and K. L. Rowlen, J. Am. Chem. Soc. **121,** 2635 (1999).
[57] G. J. Simpson, S. G. Westerbuhr, and K. L. Rowlen, Anal. Chem. **72,** 887 (2000).
[58] J. Wang, Z. Paszti, M. A. Even, and Z. Chen, J. Am. Chem. Soc. **124,** 7016 (2002).
[59] J. Michl and E. W. Thulstrup, *Spectroscopy with Polarized Light* (VCH Publishers, Inc, New York, 1995).
[60] S. Jen, N. A. Clark, P. S. Pershan, and E. B. Priestley, J. Chem. Phys. **66,** 4635 (1977).
[61] A. Szabo, J. Chem. Phys. **72,** 4620 (1980).
[62] Y. R. Shen, Appl. Phys. B **68,** 295 (1999).
[63] X. Wei, S. C. Hong, A. I. Lvovsky, H. Hermann, and Y. R. Shen, J. Phys. Chem. B **104,** 3349 (2000).
[64] H. Hermann, A. I. Lvovsky, X. Wei, and Y. R. Shen, Phys. Rev. B **66,** 205110 (2002).
[65] R. Superfine, J. Y. Huang, and Y. R. Shen, Phys. Rev. Lett. **66**(8), 1066 (1991).
[66] R. P. Chin, J. Y. Huang, Y. R. Shen, T. J. Chuang, H. Seki, and M. Buck, Phys. Rev. B **45,** 1522 (1992).
[67] A. J. Moad, and G. J. Simpson, J. Phys. Chem. B **108,** 3548 (2004).
[68] P. Fischer and A. D. Buckingham, J. Opt. Soc. Am. B **15,** 2951 (1998).
[69] J. Wang, M. L. Clarke, and Z. Chen, Ana. Chem. **76,** 2159 (2004).
[70] Y. L. Yeh, C. Zhang, H. Held, A. M. Mebel, X. Wei, S. H. Lin, and Y. R. Shen, J. Chem. Phys. **114,** 1837 (2001).
[71] J. Kim, K. C. Chou, and G. A. Somorjai, J. Phys. Chem. B. **107,** 1592 (2003).
[72] K. Wolfrum, H. Graener, and A. Laubereau, Chem. Phys. Lett. **213,** 41 (1993).
[73] J. Y. Huang and M. H. Wu, Phys. Rev. E **50,** 3737 (1994).
[74] C. D. Stanners, Q. Du, R. P. Chin, P. Cremer, G. A. Somorjai, and Y. R. Shen, Chem. Phys. Letts. **232,** 407 (1995).
[75] G. Ma and H. C. Allen, J. Phys. Chem. B **107,** 6343 (2003).
[76] K. R. Wilson, R. D. Schaller, D. T. Co, R. J. Saykally, B. S. Rude, T. Catalano, and J. D. Bozek, J. Chem. Phys. **117,** 7738 (2002).

[77] H. Chen, W. Gan, R. Lu, Y. Guo, and H. F. Wang, J. Phys. Chem. B **109,** 8064 (2005).
[78] H. Chen, PhD dissertation, Structure and Adsorption of Acetone and Methanol at Vapor/ Liquid Interfaces by Sum Frequency Generation Vibrational Spectroscopy (Institute of Chemistry, the Chinese Academy of Sciences, 2004). No. 200118003202812, Defence date: June 24, 2004.
[79] H. Chen, W. Gan, B. H. Wu, D. Wu, Z. Zhang, and H. F. Wang, Chem. Phys. Lett. **408,** 284 (2005).
[80] H. Chen, W. Gan, B. H. Wu, D. Wu, Y. Guo, and H. F. Wang, J. Phys. Chem. B **109,** 8053 (2005).
[81] Unppublished data.
[82] T. F. Heinz, H. W. K. Tom, and Y. R. Shen, Phys. Rev. A **28,** 1883 (1983).
[83] T. G. Zhang, C. H. Zhang, and G. K. Wong, J. Opt. Soc. Am. B **7**(6), 902 (1990).
[84] Y. Tanaka, S. Lin, M. Aono, and T. Suzuki, Appl. Phys. B **68**, 713 (1999).
[85] S. Baldelli, N. Markovic, P. Ross, Y. R. Shen, and G. Somorjai, J. Phys. Chem. B **103,** 8920 (1999).
[86] J. Wang, C. Y. Chen, S. M. Buck, and Z. Chen, J. Phys. Chem. B **105,** 12118 (2001).
[87] W. Gan, B. H. Wu, H. Chen, Y. Guo, and H. F. Wang, Chem. Phys. Lett. **406,** 467 (2005).
[88] G. R. Bell, C. D. Bain, and R. N. Ward, J. Chem. Soc. Faraday Trans. **92,** 515 (1996).
[89] R. Braun, B. D. Casson, and C. D. Bain, Chem. Phys. Lett. **245,** 326 (1995).
[90] J. A. Ekhoff and K. L. Rowlen, Ana. Chem. **74,** 5954 (2002).
[91] P. X. Ye and Y. R. Shen, Phys. Rev. B **28,** 4288 (1983); with a small correction in, *ibid*, **30,** 6202 (1984).
[92] G. Cnossen, K. E. Drabe, and D. A. Wiersma, J. Phys. Chem. **97,** 4512 (1992).
[93] Z. Xu, W. Y. Lu, and P. W. Bohn, J. Phys. Chem. **99,** 7154 (1995).
[94] B. D. Casson and C. D. Bain, Langmuir **13,** 5465 (1997).
[95] D. Roy, Phys. Rev. B **61,** 13283 (2000).
[96] R. W. Munn, J. Chem. Phys. **97,** 4532 (1992).
[97] M. in het Panhuis and R. W. Munn, J. Chem. Phys. **112,** 6763 (2000).
[98] M. in het Panhuis and R. W. Munn, J. Chem. Phys. **113,** 10685 (2000).
[99] M. in het Panhuis and R. W. Munn, J. Chem. Phys. **113,** 10691 (2000).
[100] J. N. Israelachvili, *Intermolecular and Surface Forces*, 2nd ed. (Academic Press, London, 1991), p. 80.
[101] Unpublished data.
[102] Q. Du, R. Superfine, E. Freysz, and Y. R. Shen, Phys. Rev. Lett. **70,** 2313 (1993).
[103] M. J. Colles and J. E. Griffiths, J. Chem. Phys. **56,** 3384 (1972).
[104] D. A. Long, *The Raman Effect: A Unified Treatment of the Theory of Raman Scattering by Molecules* (John Wiley and Sons, Chichester, 2002).
[105] H. C. Allen, D. E. Gragson, and G. L. Richmond, J. Phys. Chem. B **103,** 660 (1999).
[106] V. Pouthier, C. Ramseyer, and C. Girardet, J. Chem. Phys. **108,** 6502 (1998).
[107] D. Simonelli and M. J. Shultz, J. Chem. Phys. **112,** 6804 (2000).
[108] Y. Saito, T. Ishibashi, and H. Hamaguchi, J. Raman. Spectrosc. **31,** 725 (2000).
[109] K. Miyano, J. Chem. Phys. **69,** 4807 (1978).
[110] L. G. P. Dalmolen and W. H. de Jeu, J. Chem. Phys. **78,** 7353 (1983).
[111] S. Y. Yakovenko, M. Maiwald, A. Würflinger, and J. Pelzl, Liq. Crys. **26,** 23 (1999).
[112] J. L. McHale, *Molecular Spectroscopy* (Prentice Hall, Inc., Upper Saddle River, NJ, USA, 1999), p. 280.
[113] M. Oh-e, H. Yokoyama, and S. Baldelli, Appl. Phys. Lett. **84,** 4965 (2004).
[114] Hirose, C., A manuscript in Japanese on SFG theory and detailed derivations of the bond polarizbility expressions. Some revisions were made from the published papers of the author [36, 37]. Full text available at http://comp.ims.ac.jp/hirose.html
[115] K. M. Gough, J. Chem. Phys. **91,** 2424 (1989).
[116] D. A. Long, Proc. Roy. Soc. London Ser. A **217,** 203 (1952).
[117] D. A. Long and A. G. Thomas, Proc. Roy. Soc. London Ser. A **223,** 130 (1954).
[118] D. A. Long, A. H. S. Matterson, and L. A. Woodward, Proc. Roy. Soc. London Ser. A **224,** 33 (1954).
[119] D. A. Long, D. C. Milner, and A. G. Thomas, Proc. Roy. Soc. London Ser. A **237,** 197 (1956).
[120] D. A. Long, T. V. Spencer, D. N. Waters, and L. A. Woodward, Proc. Roy. Soc. London Ser. A **240,** 499 (1957).
[121] M. Gussoni, in *Advances in Infrared and Raman Spectroscopy*, edited by R. J. H. Clark and R. E. Hester (Heyden and Son, London, 1980), Vol. 6, Chapter 2.
[122] R. G. Snyder, A. L. Aljibury, H. L. Strauss, H. L. Casal, K. M. Gough, and W. F. Murphy, J. Chem. Phys. **81,** 5352 (1984).
[123] K. M. Gough and W. F. Murphy, J. Chem. Phys. **85,** 4290 (1986).
[124] K. M. Gough and W. F. Murphy, J. Chem. Phys. **87,** 1509 (1987).
[125] K. M. Gough and W. F. Murphy, J. Chem. Phys. **87,** 3332 (1987).
[126] K. M. Gough and W. F. Murphy, J. Chem. Phys. **87,** 3341 (1987).
[127] K. M. Gough and J. R. Dwyer, J. Phys. Chem. A **102,** 2723 (1998).
[128] H. C. Allen, E. A. Raymond, and G. L. Richmond, Curr. Opin. Coll. Inter. Sci. **5,** 74 (2000).

[129] J. Y. Huang, R. Superfine, and Y. R. Shen, Phys. Rev. A **42,** 3660 (1990).
[130] M. R. Watry and G. L. Richmond, J. Phys. Chem. B **106,** 12517 (2002).
[131] S. R. Goates, D. A. Schofield, and C. D. Bain, Langmuir **15,** 1400 (1999).
[132] R. N. Ward, D. C. Duffy, P. B. Davies, and C. N. Bain, J. Phys. Chem. **98,** 8536 (1998).
[133] D. Zimdars, J. I. Dadap, K. B. Eisenthal, and T. F. Heinz, J. Phys. Chem. B **103,** 3425 (1999).
[134] D. Zimdars and K. B. Eisenthal, J. Phys. Chem. A **103,** 10567 (1999).
[135] G. Herzberg, *Molecular Spectra and Molecular Structure II: Infrared and Raman Spectra of Polyatomic Molecules* (D. Van Nostrand Company, Inc., Princeton, 1945), Chapter V.
[136] R. G. Snyder and J. R. Scherer, J. Chem. Phys. **71,** 3221 (1979).
[137] P. A. MacPhail, H. L. Strauss, R. G. Snyder, and C. A. Elliger, J. Phys. Chem. **88,** 334 (1984).
[138] R. G. Snyder, S. L. Hsu, and S. Krimm, Spectrochim. Acta A **34,** 395 (1978).
[139] R. A. MacPhail, R. G. Snyder, and H. L. Strauss, J. Chem. Phys. **77**(3), 1118 (1982).
[140] *Selected Raman Spectral Data*, edited by L. B. Beach (Thermodynamic Reseach Center Hydrocarbon Project Publications, College Station, Texas, 1983), Ser. No. 807, 653, 55.
[141] E. L. Hommel, J. K. Merle, G. Ma, C. M. Hadad, and H. C. Allen, J. Phys. Chem. B **109,** 811 (2005).
[142] M. Saß, M. Lettenberger, and A. Laubereau, Chem. Phys. Lett. **356,** 284 (2002).
[143] L. Dreesen, C. Humbert, Y. Sartenaer, Y. Caudano, C. Volcke, A. A. Mani, A. Peremans, and P. A. Thiry, Langmuir **20,** 7201 (2004).
[144] C. Bilger and B. Pettinger, Chem. Phys. Letts. **294,** 425 (1998).
[145] L. J. Bellamy, *The Infrared Spectra of Complex Molecules* (Chapman and Hall, London, 1975).
[146] A. Weber, *Raman Spectroscopy of Gases and Liquid* (Springer-Verlag, Berlin, 1979).
[147] N. B. Colthup, L. H. Daly, and S. E. Wiberley, *Introduction to Infrared and Raman spectroscopy* (Academic Press, Inc., San Diego, 1990).
[148] R. G. Snyder, A. L. Aljibury, H. L. Strauss, H. L. Casal, and W. F. Murphy, J. Chem. Phys. **81,** 5352 (1984).
[149] R. G. Snyder, H. L. Strauss, and C. A. Elliger, J. Phys. Chem. **86,** 5145 (1982).
[150] M. G. Brown, E. A. Raymond, H. C. Allen, L. F. Scatena, and G. L. Richmond, J. Phys. Chem. B **104,** 10220 (2000).
[151] A. G. Lambert, D. J. Neivandt, A. M. Briggs, E. W. Usadi, and P. B. Davies, J. Phys. Chem. B **106,** 5461 (2002).
[152] J. P. Perchard and M. L. Josien, J. Chim. Phys. **65,** 1834 (1968).
[153] J. P. Perchard and M. L. Josien, J. Chim. Phys. **65,** 1856 (1968).
[154] J. Sung, K. Park, and D. Kim, J. Korean Phys. Soc. **44**(6), 1394 (2004).
[155] J. J. Fox and A. E. Martin, Proc. Roy. Soc. A **175,** 208 (1940).
[156] A. Pozefsky and N. D. Coggeshall, Anal. Chem. **23**(11), 1611 (1951).
[157] N. Ji and Y. R. Shen, J. Chem. Phys. **120**(15), 7107 (2004).
[158] J. Wang, X. Y. Chen, M. L. Clarke, and Z. Chen, Proc. Nat. Acd. Sci. **102,** 4978 (2005).
[159] D. D. Dlott, Chem. Phys. **266,** 149 (2001).
[160] Z. H. Wang, A. Pakoulev, and D. D. Dlott, Science **296,** 2201 (2002).
[161] Unpublished data, in collaboration with Professor Shi-lin Liu at Department of Chemical Physics, University of Science and Technology of China.
[162] T. Shimanouchi, *Tables of Molecular Vibrational Frequencies Consolidated*, (National Bureau of Standards, 1972), Vol. I, pp. 1–160. Also in the NIST Chemistry Webbook Database at http://webbook.nist.gov
[163] L. K. Iwaki and D. D. Dlott, J. Phys. Chem. A **104,** 9101 (2000).
[164] N. Akamatsu, K. Domen, and C. Hirose, J. Phys. Chem. **97,** 10070 (1993).
[165] C. Y. Wang, H. Groenzin, and M. J. Shultz, J. Phys. Chem. B **108,** 265 (2004).
[166] W. F. Murphy, Mol. Phys. **36,** 727 (1978).